Physics – Uspekhi **50** (10) 985 – 1029 (2007)

REVIEWS OF TOPICAL PROBLEMS PACS numbers: 05.10.Ln, 33.20.Kf, **34.70.+e**, **71.35.–y**, 78.40.Me, **82.20.–w**

Theory of the J-band: from the Frenkel exciton to charge transfer

V V Egorov, M V Alfimov

DOI: 10.1070/PU2007v050n10ABEH006317

Contents

V V Egorov, M V Alfimov Photochemistry Center, Russian Academy of Sciences, ul. Novatorov 7a, 119421 Moscow, Russian Federation
Tel. (7-495) 936 77 53. Fax (7-495) 936 12 55
E-mail: egorov@photonics.ru, alfimov@photonics.ru

Received 15 December 2006, revised 24 April 2007
Uspekhi Fizicheskikh Nauk **177** (10) 1033 – 1081 (2007)
DOI: 10.3367/UFNr.0177.200710a.1033
Translated by Yu V Morozov; edited by A Radzig

Abstract. This review concerns the current status of the theory of formation of the so-called J-band (Jelley, Scheibe, 1936), an abnormally narrow, high-intensity, red-shifted optical absorption band arising from the aggregation of polymethine dyes. Two opposite approaches to explaining the physical nature of the J-band are given special attention. In the first of these, the old one based on Frenkel's statistical exciton model, the specific structure of the dye is considered irrelevant, and the J-band is

explained by assuming that the quickly moving Frenkel exciton acts to average out the quasistatic disorder in electronic transition energies of molecules in the linear J-aggregate (Knapp, 1984). In the second approach, on the contrary, the specific structure of the dye (the existence of a quasilinear polymethine chain) is supposed to be very important. This new approach is based on a new theory of charge transfer. The explanation of the J-band here is that an elementary charge transfer along the J-aggregate's chromophore is dynamically pumped by the chaotic reorganization of nuclei in the nearby environment at a resonance between electronic and nuclear movements — when the motion of nuclei being reorganized is only weakly chaotic (Egorov, 2001).

1. Introduction

Present-day scientific and technical progress is inconceivable without nanotechnologies based on the achievements of nanophysics or mesophysics — a new area of physicochemical knowledge dealing with 1 – 10 nm[1] objects intermediate between solids and individual molecules. Such objects include both inorganic and organic systems, e.g., semiconducting quantum dots [1 – 5] and organic molecular aggregates [6 – 8]. Mesophysics has begun to be as important for the further development of human society as nuclear physics was in the past (and still is at present). For this reason, mesophysics is part of the 'physical minimum' [9] covering the most essential aspects of theoretical physics of which every physicist is expected to have a proper idea.

The so-called J-aggregates of cyanine (polymethine) dyes are of special interest in the mesophysics of organic molecular aggregates (see, for instance, Refs [6 – 8, 10]). The shape of polymethine-dye optical bands and the related abnormally narrow high-intensity J-band has been a focus of extensive studies during the last half-century. The great interest shown in this problem is due to the unique spectral characteristics of these organic systems, accounting for their wide practical application for light energy transformation. By way of example, polymethine dyes and J-aggregates are used as optical sensitizers, laser active media, passive modulators of laser Q-quality, primers for polymerization reactions, organic photoconducting materials, highly polarizable systems for nonlinear optics, and fluorescent tags (see review [11] and references cited therein). Polymethine dye-based systems embedded in a polymer matrix [12] have begun to find application in the development of cost-effective light sources and flexible laptop displays [13]. Chromophores of polymethine dyes exhibit a relatively simple and easy-to-vary structure [11].

It should be noted that researchers have shown ever-increasing interest in the J-band problem during the last 20 years, the main reasons being the spectral width of the J-band is unprecedentally small for organic substances (only dozens of inverse centimeters at cryogenic temperatures [14 – 16]); the enormous oscillator strength due to the radiation lifetime reduced to a few dozen of picoseconds [14 – 16], and the giant cubic susceptibility of order $10^{-7} - 10^{-5}$ cm^3 erg^{-1} [17 – 19] (a record value not only for organic but also for inorganic compounds). Taken together, these unusual properties of J-aggregates and relatively simple methods of their preparation make them highly promising objects for optical technologies in the near future. Recently synthesized J-aggregates with cylindrical geometry [20 – 22] also open up the possibility of manufacturing artificial light-harvesting systems in which a controlled transfer of accumulated energy is realized.

The Frenkel molecular exciton concept [23] was made use of to explain the nature of the J-band almost as soon as it was discovered. This concept was increasingly more widely employed in further studies. Despite its simplicity, the Frenkel model proved applicable to the description not only of the shape of the J-band for the majority of presently synthesized aggregates of different geometry [24 – 27] but also of their nontrivial temperature and spectral dynamics [28 – 35] and nonlinear response [36 – 38]. The model has been used with equal success to describe the optical and transport properties of conjugated polymers [39 – 41].

In 1936, Jelley [42, 43] and Scheibe [44, 45] independently found that the width of the optical absorption band markedly decreased with a rise in the polymethine dye (pseudoisocyanine) concentration in an aqueous solution. This band, now usually referred to as the J-band (after Jelley) and occasionally the Scheibe band, is shifted to the long-wave region of the spectrum and has a higher intensity than that at a low dye concentration. The appearance of the J-band was ascribed to the formation of molecular aggregates, later called J-aggregates or Scheibe aggregates (see, for instance, Ref. [46]) in which electron transitions of individual molecules are tightly coupled by their excitonic interaction (see, for instance, Ref. [47]) as in the case of molecular crystals [48 – 51]. This interpretation of the optical band shape for J-aggregates, suggested by Franck and Teller [52] in 1938 and based on the notion of the Frenkel exciton [23], gained universal recognition (see, for example, Ref. [53]). The model describing the long-wave shift and enhanced band intensity had the form of a linear chain of two-level point molecules with dipole – dipole interaction, in which molecular dipoles of electron transitions exhibited a 'head-to-tail' orientation [54 – 57]. Optical transitions for such a structure are allowed only to the bottom of the exciton band where collective excitation of a large number of molecules accumulates the total oscillator strength into a single quantum transition.

The problem of quantitative interpretation of the small width and the entire shape of the J-band in the framework of the exciton theory was posed by Knapp, Scherer, and Fischer in 1984 (see Refs [58, 59] and references cited therein). The authors offered an explanation for the small J-band width based on the statistical analysis of environmental influence on the position of electronic levels of molecules in a chain linked by exciton interaction. Also, they used their vibron theory to explain the specific shape of the short-wave wing of the J-band produced by pseudoisocyanine, viz. a classical dye studied in the pioneering works of Jelley and Scheibe. A quickly moving Frenkel exciton averages the quasistatic disorder that decreases roughly $\sqrt{N_c}$-fold, where N_c is the number of coherently coupled molecules (exchange narrowing — that is, band narrowing due to exciton exchange or Knapp narrowing [58]). The vibron theory allows not only states close to the bottom of the exciton band but also states either inside this band or near its top, depending on the specific structure (helical or linear) of a concrete pseudoisocyanine J-aggregate [59].

In Ref. [58], the narrowing effect due to exciton exchange was obtained analytically in the framework of the perturba-

[1] This field of physics is referred to as 'mesoscopic physics' or 'interdisciplinary physics' in the Western scientific literature.

tion theory. However, the problem cannot be resolved with the help of this theory and requires numerical computation when the number of coherently coupled molecules is much smaller than the aggregate length. A series of numerical calculations of optical band shapes of molecular aggregates was performed at the Photochemistry Centre, Russian Academy of Sciences, in the framework of the statistical exciton approach based on an analytical method [60, 61, 63, 65] currently referred to in the Western scientific literature as the smoothing technique [67] or smoothening technique [30] and widely used to calculate concrete experimental systems. These works and their results will be briefly discussed in Section 5.

Unfortunately, the statistical exciton approach does not take into consideration the concrete structure of individual molecules of polymethine dyes (Sections 6–8) making up J-aggregates, namely, the extended distribution of π-electron density alternating along a quasilinear polymethine chain. It is the transition moment that is directed parallel to this chain [11]. There is no difficulty in understanding that such a spatial spread of the π-electron charge enables only its small part concentrated at the 'junction' between the chains of a 'head-to-tail' structure to be involved in exciton interaction. Clearly, the magnitude of exciton (dipole–dipole) interaction in the exciton theory is grossly overestimated. As may be inferred from the extended dipole model (Section 3.1.4), the real interaction in head-to-tail structures must be ten times smaller. It cannot ensure the J-band effect stated in the exciton theory and gives an optical band practically indistinguishable from a monomer band.

It is worthwhile to emphasize, however, the lack of reliable data on the package geometry of monomers in a linear J-aggregate. In all probability, it is something other than an unstable head-to-tail configuration. On the other hand, it can be assumed that the 'tilted card-pack' assembly ensures both the angle necessary for the J-type resonant dipole–dipole interaction and the small distance between monomers, which yields the desired magnitude of interaction. For this reason, the above arguments concerning the overestimated magnitude of interaction in the exciton approach appear to refer only to the head-to-tail dipole configuration deemed responsible for the J-effect in the pioneering work by Franck and Teller [52], classical works by Kasha and coworkers [54–57], and the work by Wiersma et al. [68] (see Sections 4.5.2 and 5.1, Fig. 11). Nor is this reasoning consistent with the results of a recent study reported by Knoester et al. [26] who modelled the absorption spectrum of double-wall cylindrical J-aggregates, using the extended dipole model and the 'brickwork' package of molecules. A good agreement between theoretical and experimental spectra was obtained in the framework of the exciton approach, the latter spectrum consisting of three bands: one broad, and two narrow ones. Unfortunately, such models comprise a very large number (over ten) fitting parameters, which substantially decreases their real value. Thus, we are still a long way from understanding the magnitude of exciton interaction in J-aggregates.

Anyway, there is a fundamental difficulty in applying the exciton approach to the explanation of the J-band effect, regardless of the solution to the exciton interaction problem in the future. Specifically, direct experimental justification is needed of the paradigm existing in the statistical exciton approach, according to which all characteristic features of the optical spectrum of monomer molecules in a J-aggregate

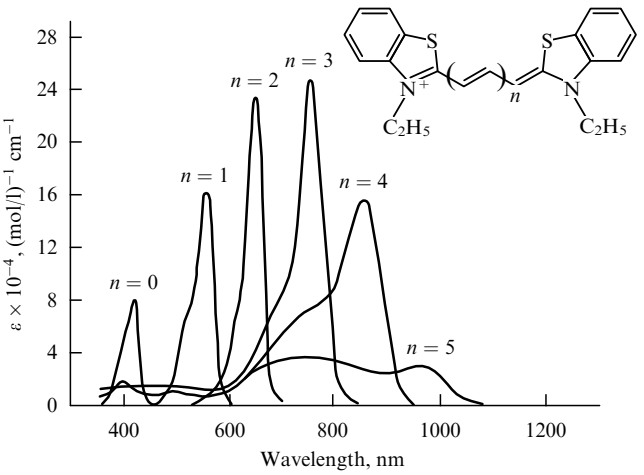

Figure 1. Experimental optical absorption data for the vinylogous series of thiapolymethinecyanine in methanol at room temperature (from Brooker et al. [74]).

practically degrade (as a result of averaging static disorder by the Frenkel exciton [58]). As mentioned above, the J-band effect is observed only for a certain type of molecules, viz. polymethine dyes having a linear extended π-electron system. Meanwhile, this effect should also be expected to occur with the molecules other than polymethines if it is really a common property of molecular aggregates with a certain structure (e.g., a popular brickwork structure or some other), which is unrelated to the structure of monomer molecules constituting J-aggregates, as postulated in the exciton approach. Therefore, at least one example of 'alternative' molecules forming J-aggregates is needed for the experimental justification of the above-said excitonic degradation paradigm for the optical properties of individual molecules in a J-aggregate; the optically active electronic structure of these molecules must be essentially different from the linear extended π-electron structure of polymethine dyes. To our knowledge, no such example has been found in experiment during the 70-year history of J-band studies; evidently, this fact testifies against the statistical exciton approach.

It is therefore natural to take a new, competing approach to the J-band problem, having the opposite sense and in accordance with which J-aggregation gives rise to the development of a certain characteristic feature of the monomer spectrum [69–73]. It was proposed in Refs [69–71] that such a characteristic feature is the most intense absorption band in a series of one dye (roughly in the midst of it) where the polymethine chain length varies in a broad range [74] (see also Ref. [75]) (Fig. 1). The new approach takes into consideration the aforementioned specific structure of polymethine dye monomers and ascribes the most intense band in the polymethine series to weak electron-nuclear resonance arising at an 'average' length of the polymethine chain and related to the peculiarities of quantum transition dynamics [69–73]. As shown in Section 13, this resonance band associated with the formation of J-aggregates intensifies so much as to transform into the J-band [71, 73]. We shall briefly consider below in this introductory section the physical substance of the novel approach to interpreting the nature of the J-band and the results obtained from its application.

Thus, this approach implies that an explanation of the band shape of J-aggregates should be linked to that of their

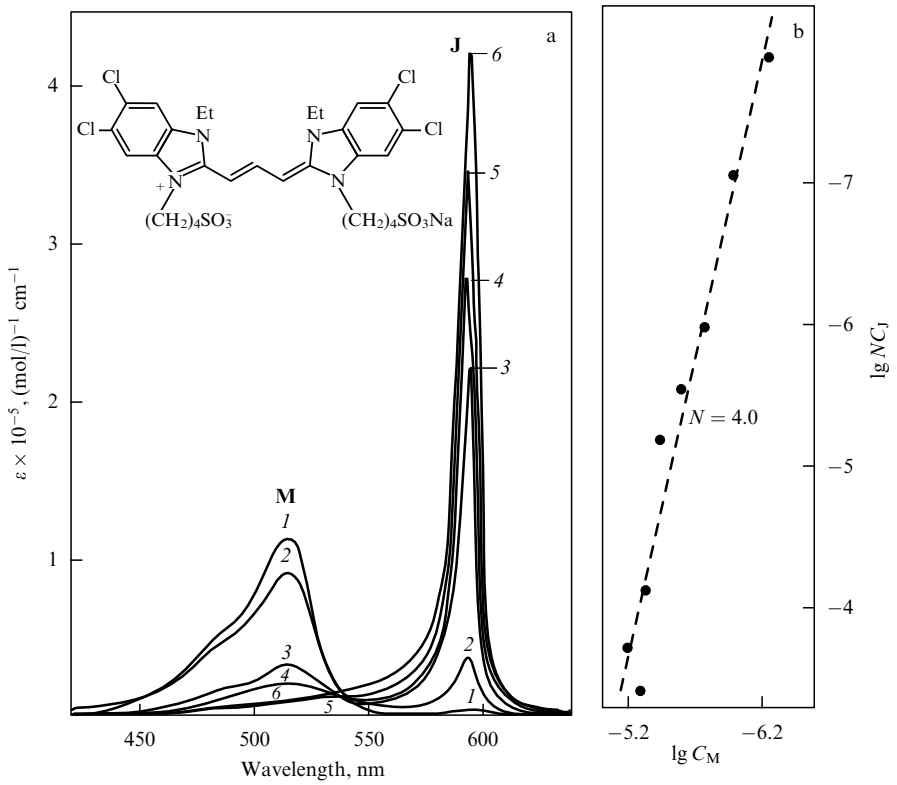

Figure 2. Herz's experimental data on the dye concentration dependence of optical absorption by benzimidacarbocyanine at 25 °C. (a) Dye concentration is given in units of micromole/liter of an aqueous NaOH solution (0.001 mol l^{-1}): 0.5 (*1*), 1.0 (*2*), 5.0 (*3*), 10 (*4*), 100 (*5*), and 400 (*6*). (b) Molar concentrations of the dye in monomeric (C_M) and aggregated (C_J) forms are borrowed from figure (a). The number of molecules N making up the J-aggregate is then determined based on the law of mass action.

constituent monomers [69 – 71, 73]. The first attempts at explaining the shape of optical bands of polymethine dye monomers date to the early 1950s, when the methods of the theory of multiphonon processes were developed (see Refs [76, 77] and references cited therein). However, the attempts were successful only in the case of low temperatures, when the spectrally resolved intramolecular vibrational structure could be approximated by the totality of Poisson distributions ([77] and references cited therein). At room temperature, spectra of polymethine dyes exhibit extremely poor resolution ([77] and references cited therein) and remain asymmetric as at low temperatures. Therefore, they cannot be interpreted in terms of the standard theory of multiphonon processes [76, 77] that in this case results in the Gaussian distribution for the optical band shape. This is not surprising, since the Gaussian distribution is known to have been used as early as the 1950s (see review [76] and references cited therein) to interpret optical bands for admixture centres in insulators and semiconductors whose local electronic structure is markedly different from the extended electronic structure of a polymethine chain, the principal dye chromophore (Section 8). Collectively, these facts point to two important circumstances [73]. First, the band shape of polymethine dyes at room temperature depends on the interaction of electron transition with the environment rather than with intramolecular vibrations. Second, the standard theory of multiphonon processes does not take into account the characteristic features of electron transitions in polymethine dyes, associated with their considerable extension.

Thus, the problem of the optical band shape of monomers in polymethine dyes has until lately remained unresolved, as confirmed by the absence of a theoretical explanation for well-known experimental data, such as obtained by Brooker and co-workers [74] (see also Ref. [75] and Fig. 1). One of the authors of this review has recently explained these classical experimental findings (Section 13.2) based on his newly proposed theory of elementary charge transfer processes [69 – 73] (Section 10).

The same theory was used successfully to account for the well-known experimental data of Herz [78, 79] (see also monograph [75]) concerning formation of J-aggregates of benzimidacarbocyanine (Fig. 2). These brilliant experimental findings obtained by A H Herz in 1974 are fairly well reproduced in modern experiments and cited as a pattern of confidence in the recent review by Shapiro [8]. They provide a classic example of describing the appearance of the J-band in the long-wave spectral region upon a rise in concentration of a polymethine dye in solution. Each concentration effects attaining an appropriate thermodynamically reversible equilibrium between monomeric and J-aggregated forms of the dye; this correspondence is manifested as the appearance of an isobestic point (see Fig. 2). It should be emphasized that these classic experiments on the formation of J-aggregates are not in principle amenable to theoretical interpretation in terms of the existing exciton model; they were explained for the first time in our works [69, 70]. Analysis of Herz's experimental data in the framework of the new charge transfer theory is presented in Section 13.3. It is worth noting that our theoretical interpretation allows both J-aggregate and monomer spectra to be reproduced for various dye concentrations (see Fig. 2, and Section 13.3 with its Fig. 21). The new theory also permits reproducing the isobestic point

and its location with a high degree of accuracy (3 – 4%). These results clearly demonstrate the advantages of explaining the nature of the J-band based on the novel theory of charge transfer as opposed to the exciton approach.

The new dynamic theory of elementary charge transfer processes has been built as a generalization of the standard multiphonon transition theory [76] to the case of their spatial extension; it is therefore referred to as *electrodynamics of extended multiphonon transitions* [70, 73]. The construction is based on the Green function method. The explanation of the J-band here is that electron charge transfer along a J-aggregate chromophore is dynamically pumped by the ordered constituent of nuclear reorganization in the nearby environment.

A generalization of the multiphonon transition theory (MTT) [76] to the case of spatially extended transitions implies inclusion of dissipative processes (quantum dynamics of medium relaxation), so that the MTT would represent a limiting case of the electron transfer theory corresponding to an extremely large dissipation. An essentially new and important result in the theory is the presence of inherent singularity in the probability of extended transitions, when the electron-nuclear system contains no dissipation; this singularity results from the huge difference between the masses of the electron and nuclei in its environment. The presence of such a singularity can be demonstrated by the simplest example of electron transition in the potential box with an absolutely movable wall, where its motion simulates reorganization of environmental nuclei (Section 11.1). Generally speaking, the problem of description of electron-nuclear movements lies beyond the scope of usual quantum mechanics. In order to eliminate singularity, dissipation is introduced in the electron-nuclear motion in the simplest possible way, i.e., by replacing the standard infinitely small imaginary quantity $i\gamma$ in the energy denominator of the Green function by any finite number [69, 70] (Sections 10.1 and 10.2). Evidently, the postulated procedure for damping electron-nuclear motion in the transient state assigns a certain 'direction of exit beyond quantum mechanics'.[2] Note that the dissipative transient electron-nuclear state (DTS) is similar to entangled quantum states[3] widely discussed today in a new branch of physics called quantum information (see, for instance, Refs [80, 81]). It is an example that exposes the limited resources of standard quantum mechanics and gives incentive to the development of a more comprehensive quantum theory in the future. Thus, our arguments about the nature of the J-band may 'pour oil on the flames' of discussions currently underway not only about quantum information but also about conceptual problems of quantum mechanics at large (see, for instance, Refs [80 – 86]) — the discussions first initiated by A Einstein.

In what follows, we briefly consider all the existing approaches to the J-band theory.

2. The Frenkel exciton. Elementary model of electron-excited states of aggregated molecules

Generally speaking, the molecules, atoms, ions, and electrons making up condensed systems do not perform independent individual movements. Strong interactions between particles in these systems account for the appearance of quasiparticles or quanta of collective motion of a condensed medium, playing a most important role in modern solid-state physics and related disciplines. Investigations into the physical properties of crystals have demonstrated a large number of quasiparticles in these structures. One of them is the exciton discovered in quantum-mechanical studies of collective motion of electrons [51]. The fundamental notion of the exciton as a currentless electron excitation was readily accepted by modern solid-state physics and is now widely applied in considering optical, photoelectric, photochemical, and other phenomena.

Interpretation of many experimental data related to crystals with different types of bonds is based on different exciton models, the most popular being Frenkel excitons and Wannier – Mott excitons. These excitations can be conveniently illustrated as an excited molecular state passing from one site to another (Frenkel exciton) or a moving electron – hole pair encompassing several molecules (Wannier – Mott exciton) [51]. Frenkel and Wannier – Mott excitons correspond to two limiting situations arising from electron – hole coupling, because in the former case the electron and the hole become tightly bound and localized on a single molecule. For this reason, the Frenkel exciton is frequently regarded as a strong coupling case or small-radius exciton, and the Wannier – Mott exciton as a weak coupling case or large-radius exciton [49, 51].

The Frenkel model fairly well describes excitons in organic systems representing a strong coupling case [49]. These systems are exemplified by polymethine dyes [87]. Therefore, the present review will be confined to the Frenkel exciton model. Furthermore, Section 2 will be devoted to molecular aggregates of the simplest structures, such as dimers and linear periodic chains involving N molecules, for which we shall consider various types of possible molecular orientations and related light absorption characteristics. More complicated problems, e.g., exciton – phonon interaction and photoabsorption band shape, will be discussed in Sections 3 – 5.

Because in the case under consideration the electron and the hole are located on the same molecule of the aggregate, the role of their interaction with other molecules is virtually insignificant; hence, wave functions of isolated molecular states can be employed in constructing the exciton wave function.

For simplicity, the aggregate molecules are assumed to be motionless and resided in their equilibrium positions. The wave function of the aggregate ground state can then be represented as a product of wave functions ψ_n of individual ground-state molecules, antisymmetrized over all electrons. However, exchange terms of intermolecular interaction in the lowest molecular excited states are very small; the more so such is the case in the ground state [51].[4] Therefore, exchange effects are not considered below.

In this case, the approximate wave function of the aggregate ground state can be represented as

$$\Psi_{\mathrm{G}} = \prod_{n=1}^{N} \psi_n \,. \tag{2.1}$$

[2] In the above example of a potential box, the wall displacement resulting from electron excitation occurs 'with friction'.

[3] Classification of DTSs needs a special study.

[4] This observation refers to singlet excitons. In the case of triplet excitons, it may be important to take account of exchange interaction between molecules [51].

The intermolecular interaction being neglected, the wave function of an aggregate containing a single excited molecule, e.g., molecule a, has the form

$$\phi_a = \psi_a^+ \prod_{\substack{n=1 \\ n\neq a}}^{N} \psi_n \,. \tag{2.2}$$

Wave function ϕ_a corresponds to the energy $(N-1)\varepsilon + \varepsilon^+$, where ε and ε^+ are the energies of the ground and lowest excited (singlet) states of the molecule (assuming, for simplicity, that all the molecules are alike). This state is N-fold degenerate (translational degeneracy), the aggregate energy being independent of which the molecule a is excited.

Intermolecular interaction V removes this degeneracy. The aggregate energy can be calculated in the first approximation with respect to the intermolecular interaction by constructing correct linear combinations of the functions ϕ_a that would diagonalize the matrix of the operator of intermolecular interaction.

In what follows, these linear combinations of the functions ϕ_a and the aggregate energy will be presented for a molecular dimer and a linear periodic chain of N molecules, along with specific cases of mutual orientation of aggregated molecules, believed to be inherent in J-aggregates and the so-called hypsochromic or H-aggregates.[5]

2.1 Molecular dimer

In accordance with Eqn (2.1), the ground-state dimer wave function has the form

$$\Psi_G = \psi_1 \psi_2 \,, \tag{2.1a}$$

where ψ_1 and ψ_2 are the wave functions of the isolated ground-state molecules 1 and 2.

The Hamiltonian of the dimer is defined as [54–57]

$$H = H_1 + H_2 + V \,, \tag{2.3}$$

where H_1 and H_2 are the Hamiltonians of isolated molecules, and V is the operator of intermolecular interaction.

The ground-state energy of the dimer is given by

$$E_G = \int \Psi_G H \Psi_G \, d\mathbf{r} = \varepsilon_1 + \varepsilon_2 + \iint \psi_1 \psi_2 V \psi_1 \psi_2 \, d\mathbf{r}_1 \, d\mathbf{r}_2 \tag{2.4}$$

and it is made up of ground-state energies $\varepsilon_1 = \varepsilon_2 \equiv \varepsilon$ of isolated molecules (all molecules are assumed to be alike) and the interaction energy of molecules in the ground states. Integration in formula (2.4) is performed over coordinates $\mathbf{r}$ of all electrons in molecules 1 and 2.

Wave functions and energies of excited states of the dimer are [56]

$$\Psi' = \frac{1}{\sqrt{2}}(\phi_1 + \phi_2) \,, \qquad \Psi'' = \frac{1}{\sqrt{2}}(\phi_1 - \phi_2) \tag{2.5}$$

and

$$E' - E_G = (\varepsilon^+ - \varepsilon) + D + E \,, \tag{2.6}$$

$$E'' - E_G = (\varepsilon^+ - \varepsilon) + D - E \,. \tag{2.7}$$

Here, the quantity

$$D = \iint \psi_1^+ \psi_2 V \psi_1^+ \psi_2 \, d\mathbf{r}_1 \, d\mathbf{r}_2 - \iint \psi_1 \psi_2 V \psi_1 \psi_2 \, d\mathbf{r}_1 \, d\mathbf{r}_2 \tag{2.8}$$

describes a change in the interaction energy between molecules 1 and 2 due to the excitation of one of them, which determines the displacement of the electron term of the excited state relative to the ground-state term (or D is the shift of the molecular excitation energy level owing to dimer formation, i.e., the excitonic shift), and

$$E = \iint \psi_1^+ \psi_2 V \psi_1 \psi_2^+ \, d\mathbf{r}_1 \, d\mathbf{r}_2 \tag{2.9}$$

is the interaction energy related to excitation energy transfer between molecules 1 and 2, which is responsible for splitting of the electron term of the excited state (excitonic splitting).

Intermolecular interaction V must be defined concretely if excitonic splitting E or excitonic shift D is to be calculated. Molecules being considered neutral, operator V is determined in the first approximation by the dipole–dipole interaction [88] between them. For excitonic splitting, one finds

$$E = \frac{\mathbf{M}_1 \mathbf{M}_2}{R^3} - \frac{3(\mathbf{M}_1 \mathbf{R})(\mathbf{M}_2 \mathbf{R})}{R^5} \,, \tag{2.10}$$

where

$$\mathbf{M}_{1,2} = \int \psi_{1,2}^+ \hat{\mathbf{M}}_{1,2} \psi_{1,2} \, d\mathbf{r}_{1,2} \tag{2.11}$$

is the dipole moment of transition of molecule 1 or 2 from the ground state to the lowest excited (singlet) state ($\hat{\mathbf{M}}_{1,2} \equiv \sum_i e\mathbf{r}_{1,2}^i$, where $\mathbf{r}_{1,2}^i$ is the radius vector of the ith electron in molecule 1 or 2), and R is the distance between the centers of masses of the molecules. This means that the knowledge of transition dipole moments of individual molecules, their mutual orientation, and intermolecular distance allows excitonic splitting of the dimer to be calculated. Excitonic shift D can be found in a similar way.

2.2 Special cases of relative position of transition dipole moments of molecules in a dimer

Selection rules for light absorption by a dimer are deduced from calculations of dipole moments of transition from the ground state Ψ_G to exciton states Ψ' and Ψ'':

$$\mathbf{M}' = \int \Psi' (\hat{\mathbf{M}}_1 + \hat{\mathbf{M}}_2) \Psi_G \, d\mathbf{r} \,,$$

$$\mathbf{M}'' = \int \Psi'' (\hat{\mathbf{M}}_1 + \hat{\mathbf{M}}_2) \Psi_G \, d\mathbf{r} \,.$$

Let transition dipole moments of molecules 1 and 2 be parallel ('sandwich' or 'pack-of-cards' configuration of the dimer). If state Ψ' corresponds to a lower excitation energy level, then one has

$$\mathbf{M}_2 = -\mathbf{M}_1 \tag{2.12}$$

[5] The absorption band of J-aggregates, viz. the J-band, is called bathochromic since it is shifted to the red region of the spectrum as compared to the absorption band of a monomer (see above). The absorption band of H-aggregates, i.e., the H-band, is hypsochromic or blue-shifted relative to the absorption band of a monomer.

and

$$\mathbf{M}' = 0\,, \qquad \mathbf{M}'' = \sqrt{2}\,\mathbf{M}_1\,. \tag{2.13}$$

Hence, dimer transition from the ground state to a low-lying exciton state is forbidden, while the transition to an upper state is allowed (a shift of the light absorption spectrum to a high-frequency region relative to the monomer spectrum).

As is known, the matrix element squared of a transition dipole moment can be expressed through the oscillator strength f of the corresponding transition and the cyclic light frequency Ω [89]:

$$|\mathbf{M}_1|^2 = \frac{e^2\hbar f}{2m_e\Omega}\,. \tag{2.14}$$

Then, in accordance with formula (2.13), the oscillator strength for dimer transition to the low-lying exciton state is zero, and that for transition to the upper state equals the double oscillator strength for a monomer:

$$f_d' = 0\,, \qquad f_d'' = 2f_m\,. \tag{2.15}$$

It follows from expressions (2.10) and (2.12) that the excitonic splitting is given by

$$E = -\frac{M^2}{R^3}\,. \tag{2.16}$$

From here on, $M \equiv |\mathbf{M}_1|$. Assuming the oscillator strength for the allowed electron transition to be $f_m \approx 1$ [56, 87], and the absorbed light wavelength $\lambda \approx 5000$ Å, formula (2.14) ($\Omega = 2\pi c/\lambda$) gives the transition dipole moment $M \approx 10^{-17}$ CGS units or 10 D. Quantity E computed for two intermolecular distances $R = 10$ Å and 5 Å is $-870\ \mathrm{cm}^{-1}$ and $-6960\ \mathrm{cm}^{-1}$, respectively.

According to Eqns (2.6), (2.7), excitonic splitting $\Delta E \equiv |E'' - E'|$ is twice the absolute E value. It follows from relationship (2.16) that

$$\Delta E = 2\,\frac{M^2}{R^3}\,. \tag{2.17}$$

If $R = 5$ Å, one obtains $\Delta E = 13920\ \mathrm{cm}^{-1}$. Excitonic splitting and shift effects are easy to observe because many electron bands are as wide as $3000-4000\ \mathrm{cm}^{-1}$ [56].

When transition dipole moments of constituent molecules are arranged in-line, excitonic splitting, according to formulas (2.10) and (2.12), is defined as

$$E = 2\,\frac{M^2}{R^3}\,. \tag{2.18}$$

Configuration $\rightarrow\leftarrow$ of transition dipole moments corresponds to a higher excitation energy level than configuration $\rightarrow\rightarrow$ ('head-to-tail'). Therefore, the upper exciton state Ψ'' is forbidden, while the lower one, Ψ', is allowed. Oscillator strengths of the corresponding transitions equal

$$f_d' = 2f_m\,, \qquad f_d'' = 0 \tag{2.19}$$

(a shift of the light absorption spectrum to the low-frequency region relative to the monomer spectrum; cf. formula (2.15) for the shift of the absorption spectrum to the high-frequency region). As follows from expressions (2.6), (2.7), (2.18), excitonic splitting ΔE here is twice that of the case of parallel molecular transition dipole moments:

$$\Delta E = 4\,\frac{M^2}{R^3} \tag{2.20}$$

[cf. Eqn (2.17)].

The following schemes of excitonic splitting of the monomer energy level during dimer formation [57] are usually considered: tilted transition dipole moments of constituent molecules, parallel transition dipole moments tilted to the axis connecting the molecular centers of masses, and transition dipole moments lying in different planes. All these variants are easy to analyze as described above.

2.3 Linear periodic chain of N molecules

Let vector $\mathbf{d}$ denote the chain parameter; then, $\mathbf{a} = \mathbf{d}a$ is the vector of the chain's direct 'lattice', where $a = 1, 2, \ldots, N$. The ground-state wave function of a linear aggregate containing N molecules is given by formula (2.1).

In the zero approximation, the lowest excited electron state of the aggregate may be described as a state in which one of the molecules, e.g., a, is excited, whereas the remaining ones reside in the ground state. However, the position of the excited molecule will be unstable due to translational symmetry of the aggregate and intermolecular interaction, because the excitation energy will be transferred from one molecule to another, spreading as a wave throughout the entire aggregate. In what follows, we shall focus on the stationary state of the system when the exciton wave is standing rather than traveling.

The stationary wave function of the lowest excited (singlet) state of a linear periodic chain containing N molecules is given by the expression [56][6]

$$\Psi_k = \frac{1}{\sqrt{N}}\sum_{a=1}^{N}\exp\left(\mathrm{i}\,\frac{2\pi}{N}\,ka\right)\phi_a\,, \qquad k = 0, +1, -1, +2, \ldots, \frac{N}{2} \quad (N \text{ is even})\,, \tag{2.21}$$

where the wave functions ϕ_a describing the N-fold degenerate excited state of the aggregate (translational degeneracy) are given by formula (2.2). It is easy to see that the exciton wave functions (2.21) are mutually orthogonal and normalized to unity.

Let us write down the total Hamiltonian of the system in order to find the aggregate energy:

$$H_{\mathrm{tot}} = H + V = \sum_{a=1}^{N} H_a + \frac{1}{2}\sum_{a\neq a'} V_{a,a'}\,, \tag{2.22}$$

where H_a is the Hamiltonian of molecules constituting the aggregate (they all are assumed to be alike, for simplicity), and $V_{a,a'}$ is the Coulomb interaction operator for molecules a and a', depending on their electronic and nuclear coordinates.[7]

The energy of the aggregate ground state is expressed as

$$E_G = \int \Psi_G(H+V)\Psi_G\,\mathrm{d}\mathbf{r} = N\varepsilon + \int \Psi_G V \Psi_G\,\mathrm{d}\mathbf{r}\,, \tag{2.23}$$

[6] Cyclic boundary conditions are used here.

[7] Only instantaneous Coulomb interaction between charges forming the aggregate is taken into account in operator (2.22). Therefore, excitons corresponding to operator (2.22) are called Coulomb excitons [51].

being the sum of ground-state energies ε of N isolated molecules and the interaction energy of molecules in their ground states:

$$\int \Psi_G V \Psi_G \, d\mathbf{r} ,$$

where the wave function Ψ_G is given by formula (2.1), and integration is performed over the coordinates of all the electrons in the molecules: $d\mathbf{r} \equiv d\mathbf{r}_1 \, d\mathbf{r}_2 \ldots d\mathbf{r}_N$.

The excited state energy of a linear periodic chain comprising N molecules in the nearest neighbor approximation is written out as

$$E_k = E'_k - E_G = (\varepsilon^+ - \varepsilon) + D + \Delta_k , \tag{2.24}$$

where

$$E'_k = \int \Psi_k^* (H + V) \Psi_k \, d\mathbf{r} , \tag{2.25}$$

and the quantity

$$D = \int \phi_a V \phi_a \, d\mathbf{r} - \int \Psi_G V \Psi_G \, d\mathbf{r} \tag{2.26}$$

determines a change in the energy of interaction between a molecule and its nearby environment that occurs as the molecule passes from the ground to the excited state (or else D is the shift of the excitation energy level of the molecule due to aggregation — the excitonic shift, for short), and Δ_k is the so-called zonal component:

$$\Delta_k = \left[\frac{2(N-1)}{N} \cos\left(\frac{2\pi}{N} k \right) \right] \int \phi_a V \phi_{a+1} \, d\mathbf{r} . \tag{2.27}$$

The latter is determined by matrix element $E_{a,a+1}$ of excitation energy transfer from molecule a to molecule $a+1$ (namely, by excitonic splitting E):

$$E_{a,a+1} \equiv \int \phi_a V \phi_{a+1} \, d\mathbf{r} \equiv E . \tag{2.28}$$

Thus, the example of a linear periodic chain demonstrates that aggregation of molecules results in a shift of electron excitation energy and energy level splitting forming the exciton band.

Intermolecular interaction V needs to be defined concretely if excitonic splitting E (or excitonic shift D) is to be calculated. Here, as in the case of a dimer, molecules are supposed to be neutral; therefore, operator V is defined in the first approximation by dipole–dipole interaction between molecules. Then, in conformity with formula (2.28) for excitonic splitting, one has

$$E = \frac{\mathbf{M}_a \mathbf{M}_{a+1}}{R^3_{a,a+1}} - \frac{3(\mathbf{M}_a \mathbf{R}_{a,a+1})(\mathbf{M}_{a+1} \mathbf{R}_{a,a+1})}{R^5_{a,a+1}} , \tag{2.29}$$

where $\mathbf{M}_a$ is the transition dipole moment of molecule a from the ground state to the lowest excited (singlet) state. In other words, excitonic splitting E for aggregates can be computed knowing transition dipole moments $|\mathbf{M}_a| \equiv M$ of individual molecules, their mutual orientation, and intermolecular distance $R_{a,a+1} \equiv R$. Excitonic shift D is found in a similar way.

2.4 Special cases of relative position of transition dipole moments of molecules in a chain

In the simplest case, excitonic splitting E and the appropriate zonal component $\Delta_k \equiv \Delta(k)$ are usually found for two types of chains: I — with a simple periodic structure, and II — with an alternate periodic structure (Fig. 3). In case I, the computation of E using formula (2.29) and its subsequent substitution into Eqns (2.27), (2.28) give for the zonal component [56] the following expression

$$\Delta_I(k) = -\left[\frac{2(N-1)}{N} \cos\left(\frac{2\pi}{N} k \right) \right] \frac{M^2}{R^3} (1 - 3\cos^2 \alpha) , \tag{2.30}$$

$$k = 0, +1, -1, +2, \ldots, \frac{N}{2} \quad (N \text{ is even}) ,$$

where α is the tilt angle of transition dipole moments of molecules to the axis connecting their centers of masses. By analogy, in case II one obtains [56]

$$\Delta_{II}(k) = -\left[\frac{2(N-1)}{N} \cos\left(\frac{2\pi}{N} k \right) \right] \frac{M^2}{R^3} (1 + \cos^2 \alpha) , \tag{2.31}$$

$$k = 0, +1, -1, +2, \ldots, \frac{N}{2} \quad (N \text{ is even}) .$$

Expressions (2.30) and (2.31) define splitting of the electron term of the excited molecular state with the formation of the exciton band. However, only one exciton state in case I and two in case II (two molecules in a unit cell) are optically allowed of all the N states in this band. Optically allowed and forbidden k states are found by selection rules.

2.5 Selection rules for light absorption by a molecular chain. The simplest interpretation of J- and H-bands

The intensity of aggregate optical transition from the ground state G into the kth exciton state is defined by the matrix element squared of the dipole moment

$$\mathbf{M}_k = \int \Psi_k^* \left(\sum_{a=1}^{N} \hat{\mathbf{M}}_a \right) \Psi_G \, d\mathbf{r} .$$

Simple computations give [56]

$$\mathbf{M}_k^2 = \frac{1}{N} \sum_{a=1}^{N} \sum_{b=1}^{N} \mathbf{M}_a \mathbf{M}_b \cos\left[\frac{2\pi k (a-b)}{N} \right] . \tag{2.32}$$

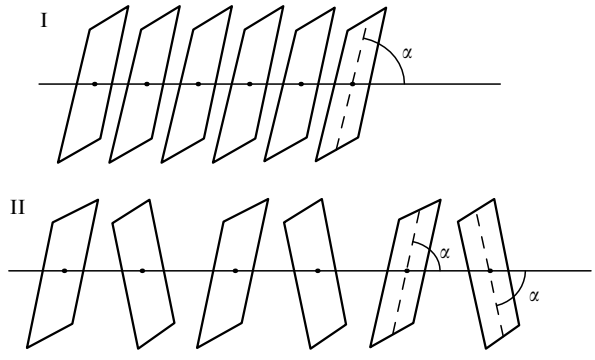

Figure 3. Two types of molecular chains: I — with a simple periodic structure, and II — with an alternate periodic structure.

Formula (2.32) yields all the selection rules for light absorption by linear periodic chains of molecules having different geometric structures.

Let us consider, as an example of using (2.32), a chain with a 'pack-of-cards' geometric structure [in case I, angle $\alpha = 90°$, Fig. 3(I)]. Bearing in mind phase relations

$$\mathbf{M}_{a+1} = -\mathbf{M}_a\,, \quad \mathbf{M}_{a+2} = -\mathbf{M}_{a+1}\,, \quad \mathbf{M}_{a+3} = -\mathbf{M}_{a+2}\,, \ \ldots \tag{2.33}$$

[analogous with Eqn (2.12) in the case of a dimer], we arrive at

$$\mathbf{M}_a\mathbf{M}_{a+1} = -\mathbf{M}^2, \qquad \mathbf{M}_a\mathbf{M}_{a+2} = \mathbf{M}^2,$$

$$\mathbf{M}_a\mathbf{M}_{a+3} = -\mathbf{M}^2\,, \text{ etc.} \tag{2.34}$$

Substitution of Eqn (2.34) into relationship (2.32) leads to

$$\mathbf{M}_k^2 = \frac{M^2}{N}\sum_{a=1}^{N}\sum_{b=1}^{N}(-1)^{a-b}\cos\left[\frac{2\pi k(a-b)}{N}\right]. \tag{2.35}$$

If $k \neq N/2$, then

$$\mathbf{M}_k^2 = 0\,, \tag{2.36}$$

if $k = N/2$, one obtains

$$\mathbf{M}_{N/2}^2 = NM^2\,, \tag{2.37}$$

so that radiative transition of the aggregate is allowed into an exciton state corresponding to the largest zonal component $\Delta(k = N/2)$ [a shift of the light absorption spectrum to the high-frequency region, see formula (2.30) at $\alpha = 90°$]; its intensity is the sum of transition intensities for N monomers making up the chain.

However, formula (2.32) is not absolutely necessary to clear up what exciton states of an aggregate with a given geometric structure corresponds to an optically allowed or forbidden transitions. Suffice it to look through all possible combinations of directions for transition dipole moments of individual molecules in a given geometric structure and choose those for which the resulting transition dipole moment differs from zero. Each combination corresponds to a certain exciton energy ($\mathbf{M}_a$-dipole interaction energy) that must be 'resided' in the exciton band depending on its value.

The selection rules being considered are illustrated by the example of a cyclic linear molecular chain with $N = 8$ in Fig. 4 for different geometric structures. Figure 4a shows schematically excitonic splitting of a monomer energy level during formation of a molecular chain in the case of a simple periodic structure, when transition dipole moments of the constituent molecules are arranged in parallel ('pack-of-cards' geometric structure, Fig. 3(I), angle $\alpha = 90°$).[8] The upper exciton state with a nonzero resulting transition dipole moment is allowed. All the remaining energetically lower exciton states have zero transition dipole moments; therefore, transitions with the participation of these states are forbidden. The scheme in question shows a shift of the light absorption band to the high-frequency spectral region relative to the monomer band.

[8] Hereinafter, excitonic shift D in the schemes [see formula (2.26)] is assumed to be zero.

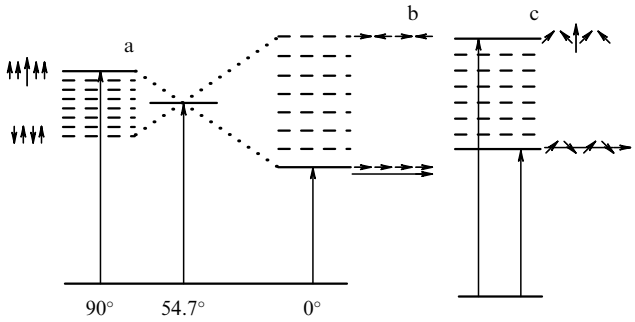

Figure 4. Exciton band and location of allowed exciton energy levels. Cases (a) and (b) correspond to the molecular chain structure in Fig. 3(I) at the angles $\alpha = 90°$ and $\alpha = 0°$. Case (c) is suited to the structure in Fig. 3(II).

Figure 4b presents a schematic of excitonic splitting of the monomer energy level during molecular chain formation in the case of a simple periodic structure with lined-up transition dipole moments of the constituent molecules [Fig. 3(I), angle $\alpha = 0$]. Here, transition to a lower exciton state is allowed, whereas transitions to all other exciton states are forbidden. This scheme implies a shift of the light absorption band to the low-frequency spectral region relative to the monomer band. Note that the width of the exciton band for the in-line geometric structure is twice that of the pack-of-cards structure, according to relationship (2.30).

Figure 4c schematically depicts exciton splitting of the monomer energy level during molecular chain formation in the case of an alternate periodic structure with tilted transition dipole moments of the constituent molecules [Fig. 3(II)]. Both the lower and the upper exciton states with nonzero transition dipole moments are allowed here. The six remaining ones with intermediate energies have zero transition dipole moments; therefore, transitions involving these states are forbidden. Oscillator strengths f' and f'' of radiative transitions to the lower (E') and upper (E'') states depend on the angle α of inclination of molecules to the axis connecting their centers of masses:

$$f' = 4f\cos^2\alpha\,, \qquad f'' = 4f\sin^2\alpha \tag{2.38}$$

(f is the transition oscillator strength for a monomer), and have mutually perpendicular polarizations. According to formula (2.38), the relationship

$$f' + f'' = 4f \tag{2.39}$$

describes the known sum rule for transition oscillator strengths in quantum mechanics [89]. The scheme under consideration illustrates, by an example of the simplest geometric structure of an aggregate, Davydov splitting [48] of the monomer's light absorption band during formation of an aggregate with two molecules in a unit cell.

To conclude the discussion of excitonic properties of the linear periodic chain of N molecules, the following fact is worthy of attention. It follows, for instance, from formula (2.30) for the exciton zonal component $\Delta(k)$ that the exciton band width in the case of a linear cyclic chain is twice that in the case of a dimer having an identical geometric structure. This circumstance is attributable to the presence of two neighbors for each molecule in the cyclic chain (in contrast to the dimer) and the nearest neighbor approximation for

interaction. When the number of interacting nearest neighbors in the chain amounts to 8, the width of the exciton band increases to 2.39 compared with that in the dimer [56].

The case exhibited in Fig. 4b and interpreted in terms of the exciton model is believed to match the experimentally examined narrow high-intensity J-band red-shifted with respect to the monomer absorption band; the case depicted in Fig. 4a corresponds to the wide blue-shifted H-band. The case in Fig. 4c may account for the high-frequency wing of the J-band for angles $\alpha \ll \pi/2$ [Fig. 3(II)], and low-frequency wing of the H-band for angles $\alpha < \pi/2$.

3. Noncanonical exciton theories of optical band shapes for molecular aggregates

The canonical exciton theory and its use for the explanation of absorption band narrowing during J-aggregation are based on the proposals by P Anderson and R Kubo [90–94] to average static and dynamic disorder in the medium by electron motion; this idea was further extended by Knapp [58] (Section 1) to the case of averaging static disorder by the motion of the Frenkel exciton. The canonical exciton theory (Sections 4 and 5) is actually a consistent formalization of Anderson's, Kubo's, and Knapp's ideas. The noncanonical exciton theories considered in the present section are based essentially on the same ideas realized less consistently.

3.1 Semiclassical model

Kuhn and co-workers have been developing the semiclassical exciton J-band model for almost 50 years, starting from the free electron model for polymethine chromophore of monomeric molecules [95] up to the review in a volume of *J-aggregates* [96]. Some calculations in this model, e.g., band-shift resulting from aggregation, were made by the quantum-chemistry methods, but on the whole (including band shape assessment) the model is a semiclassical one. On the one hand, the Khun model reflects the dramatic situation in the J-band theory, arising from the enormous difficulty of the problem and the desire to solve it at any cost; on the other hand, it stands apart from other models, not only in terms of priority. Unlike other exciton models, the Kuhn model relies on the correct idea of the relationship between unique chromophore properties in J-aggregates and the properties of the principal chromophore in their constituent monomers, i.e., an extended polymethine chain.

3.1.1 Absorption by isolated molecules. The monomer absorption band of dye molecules that form J-aggregates in a solution under certain conditions [97] is located in the visible spectral region and largely depends on the part of the π-electron charge density enclosed between nitrogen atoms. Properties of the appropriate chromophore system separated from the remaining π-electron parts are fairly well described by the free electron model in its simplest form [95] — that is, by considering $2(n+2)$ π-electrons whose charge is extended along a chain of length $L = 2(n+2)d$ (taking into account a single bond outside N atoms, and a bond length $d = 1.40$ Å, see Fig. 5) [96].

The wavelength $\lambda_{\max}$ of the absorption maximum and the oscillator strength f are in good agreement with experimental data [98]. Normally, $\lambda_{\max}$ for dyes lies in a somewhat longer-wave region than the calculated one due to the presence of unaccounted π-electron fractions which can be taken into consideration by a slight increase in the length L [96].

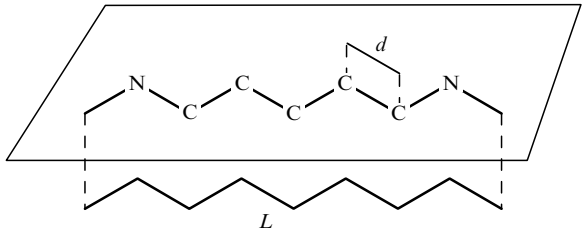

Figure 5. A polymethine dye: propagation of a π-electron cloud along a polymethine chain of length L [96].

A more detailed scrutiny takes into account the branching of the π-electron system, nitrogen atoms are treated as potential wells, and the difference between bond lengths related to the π-electron distribution is also taken into consideration [99]. The resulting $\lambda_{\max}$ values [97] reasonably agree with experimental data [96].

The understanding of spectroscopic properties of aggregates in the review by H Khun and C Khun [96] is facilitated by first considering light absorption by an isolated molecule. They use the time-dependent Schrödinger equation to derive time-dependent transition dipole moments of molecules in an electromagnetic field. The authors [96] reasoned that the problem of finding this moment is equivalent to evaluating the change x in the length of a damped classical oscillator with a frequency $v_0 = (2\pi)^{-1}\sqrt{K/m}$ (K is the force constant, and m is the mass) in the electromagnetic field. Reference [96] described equivalence conditions under classical and quantum considerations.

3.1.2 Interaction between two closely located dye molecules. The solution of two coupled Schrödinger equations in Ref. [100] yielded the time-dependent transition dipole moment $\mu(t)$ for two neighboring dye molecules in an electromagnetic field (e.g., with a sandwich type structure [96]). The problem of deriving the time evolution $\mu(t)$ is regarded in Ref. [100] as equivalent to that of time evolution $\mu(t) = x_1(t)Q_1 + x_2(t)Q_2$, where $x_1(t)$ and $x_2(t)$ denote the length changes of two coupled classical oscillators in an electric field of incident radiation (with force constants K_1 and K_2, charges Q_1 and Q_2, and damping constants ς_1 and ς_2):

$$m_1 \frac{\mathrm{d}^2}{\mathrm{d}t^2} x_1 = -K_1 x_1 - \varsigma_1 \frac{\mathrm{d}}{\mathrm{d}t} x_1 + Q_1 F_0 \cos(2\pi v t) - K_{12} x_2 , \tag{3.1}$$

$$m_2 \frac{\mathrm{d}^2}{\mathrm{d}t^2} x_2 = -K_2 x_2 - \varsigma_2 \frac{\mathrm{d}}{\mathrm{d}t} x_2 + Q_2 F_0 \cos(2\pi v t) - K_{21} x_1 . \tag{3.2}$$

The equivalence conditions under classical and quantum considerations are given in Ref. [96].

The interaction between optical electrons of two molecules leads to a shift of oscillator eigenfrequencies and a change in oscillator strengths corresponding to the radiative transitions of individual molecules.

Consideration concerning dimers is easy to generalize for the aggregates of many dye molecules and transition dipole moments of arbitrary directions [96].

Wave function antisymmetrization effects were omitted in the Kuhn model [96] for the sake of simplicity (Section 2). This model was first used to treat intramolecular interactions [100] between π-electrons and proved helpful for

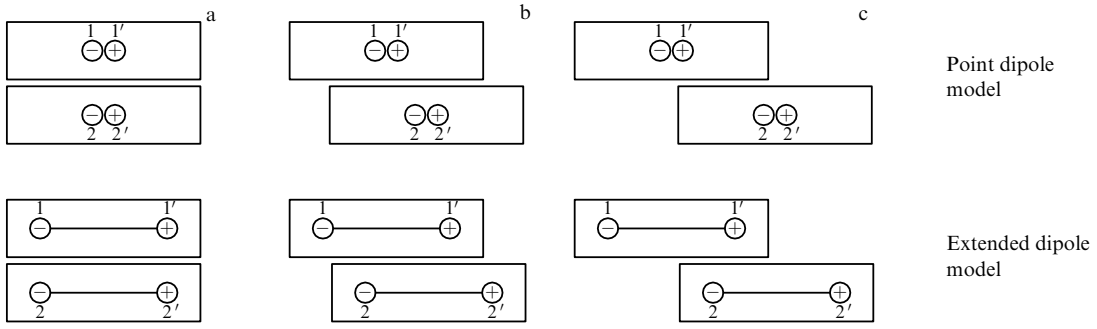

Figure 6. Charge interactions in point and extended dipole models at different relative positions of molecules [96].

explaining electronic spectra [97, 99, 101–104]. When interactions between molecules are reduced to interactions between their π-electrons, the entire molecular aggregate is regarded as a certain supermolecule in which, however, interactions of π-electrons in each constituent molecule are neglected, while intermolecular interactions are taken into account. Then, the approach under consideration is essentially similar to the exciton theory [54–57] with one important difference [96] which will be discussed in Section 3.1.3.

3.1.3 Extended dipole model. When the distance between molecules is large enough, the magnitude of exciton interaction J_{12} is given by the point dipole approximation [96]. However, this approximation is inapplicable at small distances between molecules. For example, J_{12} values in Fig. 6a, c are much greater than those obtained from accurate quantum calculations, and even have the opposite sign as those in Fig. 6b.

At small intermolecular distances, the J_{12} value can be evaluated by means of a simple and useful approximation on the assumption that transition dipole moments M_1 and M_2 are not point-like but extended along the π-electron charge density distribution: charges $-Q$ and $+Q$ at distance l, where $Q = 0.25e$ and $l = 8.9$ Å or 9.9 Å depending on the type of the polymethine dye [96, 105]. The J_{12} values obtained for the case of extended dipoles in Fig. 6 are in good agreement with quantum calculations [96, 105]. The extended dipole model [105] saves up to 99.9% of the computation time without any substantial reduction in accuracy. Figure 6b conveniently illustrates the point dipole model for the depicted geometry attaches to J_{12} a sign opposite to that given by the extended dipole moment and quantum computation. Indeed, the main contribution to J_{12} in the point dipole approximation is governed by the attraction of charges $1'$ and 2, while in the extended dipole model it depends on the repulsion of charges 1 and 2, as well as $1'$ and $2'$. This example shows how important it is to take into consideration the specific π-electron structure of dye molecules when estimating exciton interaction [96].

3.1.4 Estimation of the number of molecules in a J-aggregate and its temperature dependence. The size and shape of a coherent exciton. Let us consider J-aggregates, namely, monolayers in the form of macroscopic two-dimensional crystals [106]. The size of an excited domain N_c in these aggregates is frequently much smaller than that of the J-aggregate itself (N). According to Refs [107, 96], the size N_c depends on the competition between the attraction of in-

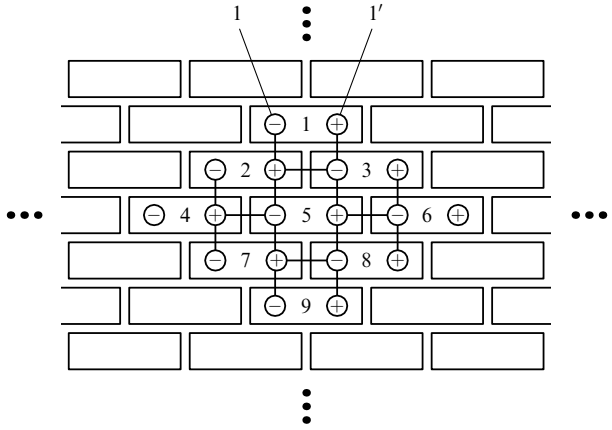

Figure 7. Aggregate with a brickwork type structure (J-aggregate). The excited domain of $N_c = 9$ molecules represented by in-phase oscillating extended dipoles illustrates the situation at room temperature [96].

phase cooperatively oscillating dipoles and thermal fluctuations tending to break the interaction of a given molecule with all the remaining molecules belonging to the excited domain:

$$N_c = \frac{0.24\ \text{eV}}{k_B T} \approx \frac{3000\ \text{K}}{T} \tag{3.3}$$

($N_c = 9$, Fig. 7).

Evidently, N_c is limited by the presence of defects, and formula (3.3) is invalid at low temperatures; however, this formula is indirectly confirmed for J-aggregates of oxacyanine in a temperature range of $20 < T < 300$ K [96]. Each extended dipole within the excited domain makes up six bonds; its breaking with cooperative motion due to thermal fluctuations can be neglected [96]. The interplay between bond formation and breaking at the boundary is responsible for the drop-like shape of the excited domain, characterized by a minimal number of molecules located at its boundary (see Fig. 7). As follows from formula (3.3), the number N_c in a J-aggregate should be about 10 at room temperature.

It was supposed above that the number N of molecules in an aggregate is much greater than the number N_c of molecules in its excited domain at 300 K ($N_c = 10$). With decreasing temperature, however, the size of the domain tends to equal that of the aggregate ($N > 150$) which depends on lattice defects and admixtures [96].[9]

[9] See the recent publication by Heijs et al. [32] concerning the temperature dependence of an exciton coherence length.

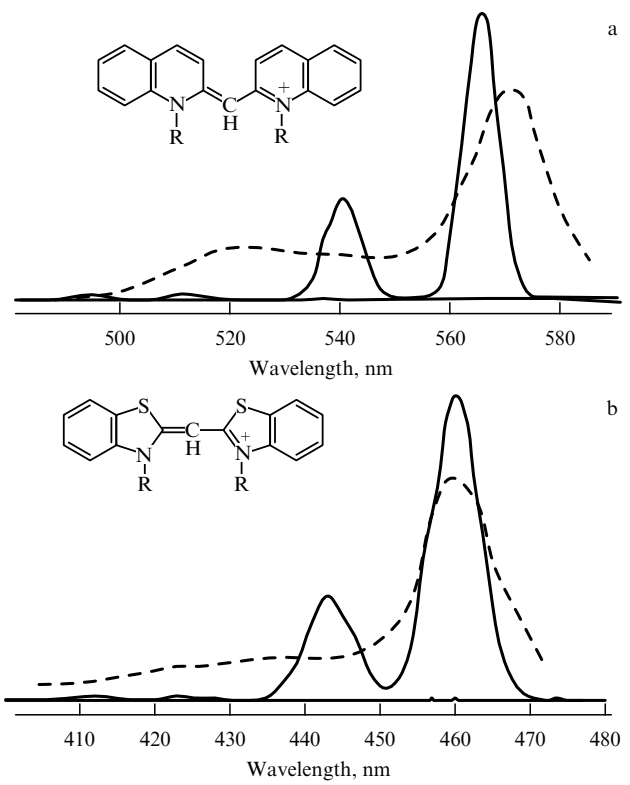

Figure 8. Theoretically simulated optical absorption spectra of pseudoisocyanine and thiacyanine J-aggregates [96] (solid lines) in comparison with experimental spectra (dashed lines). The spectra were approximated by Gaussian distributions with a half-width of 10 nm, based on the computed oscillator strengths. Experimental spectra were borrowed from Refs [106] (thiacyanine) and [109] (pseudoisocyanine in a solution of ordered polymers; the absorbed light is polarized in the polymer ordering direction).

It was believed in Ref. [96] that the small width of absorption bands in the J-aggregates at room temperatures is due to the fast motion of a sufficiently large (N_c) excited domain over the monolayer that effectively averages thermal fluctuations [107, 108]. However, the authors of review [96] emphasize that the domain size must be significantly greater than their estimate $N_c = 10$ [107].

3.1.5 Comparison of theoretical and observed J-band shapes. Figure 8 presents a typical example of comparison of calculated results from the Kuhn semiclassical model and experimental data. The authors of Ref. [96] concluded that the computed J-band position fairly well reproduces experimental findings (thiacyanine monolayer [106] and pseudoisocyanine in ordered polyvinyl alcohol [109]).

3.1.6 Summary. In order to explain the peculiar spectral characteristics of J-aggregates, H Kuhn and C Kuhn [96] first consider isolated molecules based on a simple quantum model (free electron model). Then they use the time-dependent Schrödinger equation to study a system of interacting dye molecules in the light wave field. According to paper [96], this formally leads to the same problem as the consideration of coupled classical oscillators in an alternating field of force. Terms corresponding to the interaction are defined by the molecular wave functions representing isolated dye molecules. These molecules can be approximated by the model of vibrating extended dipoles.

Spectral features of J-aggregates are described by the brickwork structure formed by dye molecules. The emerging J-band is associated with a region (domain) of in-phase oscillating excited dipoles. The size of an excited domain is a result of competition between oscillator interaction and the thermal fluctuations that destroy it.

An advantage of the theory developed by H Kuhn and his colleagues is the attempt to simulate the specific properties of extended π-electron chromophores of polymethine dyes as lengthy rather than point dipoles, in contrast to the generally accepted procedure. However, the parameters of extended dipoles are determined only by the optical band shift as a result of J-aggregation, not by the entire shape and position of the J-band. In other words, the main drawback of the semiclassical model by H Kuhn and others consists in the absence of computation of the J-band shape proper because it does not consider the interaction of oscillating dipoles (exciton) with the motion of dye nuclei and the environment.

3.2 Vibron model

3.2.1 Development of the theory in terms of the notions of standard electron-vibrational spectroscopy

Hamiltonian of an aggregate. Scherer [47] considered an aggregate of N molecules located at sufficiently large distances from each other, so as to allow the electron exchange effects to be neglected. In the framework of the Born – Oppenheimer adiabatic approximation [110], the Hamiltonian of the nth molecule in the aggregate has the form [47]

$$H_n = \sum_s \left|s^{(n)}\right\rangle \left(E_n^{(s)} + h_s^{(n)}\right) \left\langle s^{(n)}\right| , \tag{3.4}$$

where s denotes the sth singlet electronic state of the nth molecule, and $h_s^{(n)}$ is the Hamiltonian of its nuclear motion taken in the harmonic approximation and neglecting the rotation of normal coordinates (Dushinsky effect [111]):

$$h_s^{(n)} = \sum_{\mathbf{R}} \hbar\omega_{\mathbf{R},s}^{(n)} b_{\mathbf{R}}^{+(n)} b_{\mathbf{R}}^{(n)} + \zeta_{\mathbf{R},s}^{(n)} \hbar\omega_{\mathbf{R},s}^{(n)} \left(b_{\mathbf{R}}^{+(n)} + b_{\mathbf{R}}^{(n)}\right) \tag{3.5}$$

(**R** are the nuclear coordinates). The product $\left|s_1^{(1)} s_2^{(2)} \ldots s_N^{(N)}\right\rangle$ of wave functions of individual (generally speaking, different) molecules may be taken as the approximate electron wave functions of the aggregate. Taking into account electron exchange effects gives rise to an admixture of charge-separated states, corresponding to the Wannier – Mott exciton (Section 2). It can be expected based on quantum-chemical calculations that such states lie at least 1 eV above the exciton band [47]. As computations revealed, their interaction with exciton states is rather strong (ca. 500 cm^{-1}) and may be related to the strong internal electric fields [47] found in Ref. [112]. However, the consideration in Section 3.2.1 will be confined solely to the Frenkel excitons typical of molecular crystals and aggregates [47].

The ground state of an aggregate containing N molecules is approximately described by the product

$$\left|0_{\mathrm{agg}}\right\rangle = \left|0^{(1)} 0^{(2)} \ldots 0^{(N)}\right\rangle$$

[formula (2.1) written in terms of the Dirac brackets]. Each molecular excitation is a source of a group of N degenerate states represented by the products

$$\left|n, s\right\rangle = \left|0^{(1)} \ldots 0^{(n-1)} s^{(n)} 0^{(n+1)} \ldots 0^{(N)}\right\rangle$$

[cf. formula (2.2)] and coupled through intermolecular interaction, eventually leading to the formation of delocalized one-exciton states (Section 2). Simultaneous excitation of two or more molecules in an aggregate needs to be considered at higher excitation energies [36–38, 113, 114]. The matrix element of intermolecular interaction consists of a constant matrix element of electron interaction and a matrix element of interaction dependent on nuclear coordinates **R** [47]:

$$W_{ns,n's'} = W^{(0)}_{ns,n's'} + \mathfrak{R}_{ns,n's'}\left(\{b^{+(m)}_{\mathbf{R}} + b^{(m)}_{\mathbf{R}}\}\right). \qquad (3.6)$$

For the allowed dipole transitions $|0\rangle \rightarrow |s\rangle$, nondiagonal matrix elements of interaction may be regarded as roughly constant and proportional to the product $\mathbf{M}_{0s}\mathbf{M}_{0s'}$ of transition dipole moments. The electrostatic shift of energy levels $W^{(0)}_{ns,ns} \equiv D$ (Section 2) is of importance when the molecular dipole moment changes substantially during the transition $|0\rangle \rightarrow |s\rangle$. It is the sum of electrostatic interactions with all surrounding charged molecules of the aggregate.

The term $\mathfrak{R}_{ns,n's'}\left(\{b^{+(m)}_{\mathbf{R}} + b^{(m)}_{\mathbf{R}}\}\right)$ depending on nuclear coordinates is important for low-frequency deformation vibrations affecting the contact area between neighboring molecules and thereby the van der Waals interaction energy; it is equally important for vibrations active in infrared absorption. This term is practically independent of the system's electronic state, causing delocalization of vibrations and increasing their frequency, as demonstrated in an experiment on low-frequency vibrations of pseudoisocyanine [47]. As a rule, the observed frequency shifts [115] are small (10–20 cm^{-1}) and can be neglected when considering optical spectra at moderately low temperatures.

Because the spatial structure of an aggregate is not as apparent as that of a molecular crystal, translational symmetry is maintained only approximately, matrix elements $W^{(0)}_{ns,n's'}$ being 'smeared' over a certain area and also fluctuating in time. It is assumed in Section 3.2.1 below that deviation from an ideally ordered structure is not too large, and a molecular crystal of restricted size is utilized as the starting point for investigations into aggregate optical spectra.

Exciton–phonon interaction. When the optical spectra of monomeric dye exhibit a more or less resolved vibronic structure, it can be attributed to certain essentially harmonic vibrations, largely to C–C valent vibrations in the 1300–1400 cm^{-1} range [47]. Low-frequency modes are usually not observed at room temperature. However, absorption spectra at low temperatures, as well as Raman spectra, contain information about their interaction with electron transition. The unresolved sequences of these modes make an important contribution to the inhomogeneous broadening at room temperatures and to the Stokes shift between the maxima of absorption and emission spectra [47].

Reference [47] describes the vibronic spectrum of pseudoisocyanine, computed up to 1500 cm^{-1}. The results were obtained from the standard MNDO analysis of normal modes and the INDO/CI calculation of transition energies. The strongest vibronic interaction was found for three almost degenerate vibrations at ≈ 1400 cm^{-1}, in conformity with optical and Raman spectra [116]. Calculations underestimate the interaction constant $\zeta^{(n)}_{\mathbf{R},s}$ nearly two-fold [see formula (3.5)]. Some ten vibrational modes between 200 and 1000 cm^{-1} moderately interacting with electron transition are in good agreement with the Raman spectrum. The lowest-frequency modes at ≈ 35 cm^{-1} corresponding to the motion of two halves of a molecule with respect to each other also essentially interact with electron transition [47].

The interaction of intramolecular vibrations with an exciton is described by the part of formula (3.6) dependent on coordinates **R**. In the one-exciton approximation, the Hamiltonian of an aggregate has the form [47]

$$\begin{aligned} H = (N-1)E_0 + E_1 &+ \sum_{\mathbf{R},n} \hbar\omega_{\mathbf{R}} b^{+(n)}_{\mathbf{R}} b^{(n)}_{\mathbf{R}} \\ &+ \sum_{\substack{n=1 \\ \mathbf{R}}}^{N} |n\rangle\left(\hbar\omega_{\mathbf{R}}\zeta_{\mathbf{R}}(b^{+(n)}_{\mathbf{R}} + b^{(n)}_{\mathbf{R}}) + \ldots\right)\langle n| \\ &+ \sum_{\substack{n,m=1 \\ \mathbf{R}}}^{N-1} |n\rangle(V_{n,m} + \ldots)\langle m|. \end{aligned} \qquad (3.7)$$

The interaction of diagonal energies with vibrations is an inherent property of molecules, whereas modulation of exciton interaction with vibrations depends on the aggregate structure. The spectrum of Hamiltonian (3.7) eigenstates cannot be identified precisely. By analogy with a small-radius polaron [117], the problem for weak exciton–phonon interaction can be resolved by the variation method [118]. For spectra at room temperatures, the problem may be simplified by dividing vibrations into two groups: a small number of dominant high-frequency modes taken into account exactly, and an ensemble of unresolved low-frequency modes ($\hbar\omega < k_{\mathrm{B}}T$) treated as classical by the substitution of dimensionless coordinates $q_{\mathbf{R}}$ for operators $b^{+}_{\mathbf{R}}$ and $b_{\mathbf{R}}$. However, it was incorrectly supposed in Ref. [47] that temperature causes a spread in transition energies and intermolecular interaction energies. In a real situation, temperature is responsible for exciton scattering from one state into others, whereas a spread in transition energies and intermolecular interaction energies is due to static disorder in both the aggregate and the medium into which it is embedded. The role of such a spread or, in other words, of diagonal and nondiagonal disorder has been extensively studied by numerical methods [68, 119, 120) (see also Sections 4 and 5 and references cited therein).[10] The simplest example of a single intramolecular high-frequency vibrational sequence is considered below (Fig. 9). On the whole, the disorder decreases the exciton coherence length, since it tends to restrict the propagation of excitation. The resultant absorption band reflects exciton exchange narrowing and characteristic asymmetry with a broad wing on the high-energy side. The bandwidth is decreased by $\sqrt{N_{\mathrm{c}}}$ times, where the number N_{c} of coherently coupled molecules can be found from the superradiance factor as $N_{\mathrm{c}} \approx (\sigma/V)^{-0.74}$ [119] for the noncorrelated distribution of transition energies with the half-width $(8\ln 2)^{1/2}\sigma$.

Figure 9 demonstrates the example of exciton interaction with intramolecular vibration in pseudoisocyanine [47]. A model spectrum as the function of intermolecular interaction V between the nearest neighbors is shown for an aggregate of 8 molecules with periodic boundary conditions. The vibronic structure that is well apparent in the monomer spectrum rapidly disappears with increasing V.

The red shift of the lowest-energy transition is slightly smaller than $2V$ shown by the arrows in Fig. 9. (Exciton

[10] For simplicity, the more complicated case of nondiagonal disorder is not considered here.

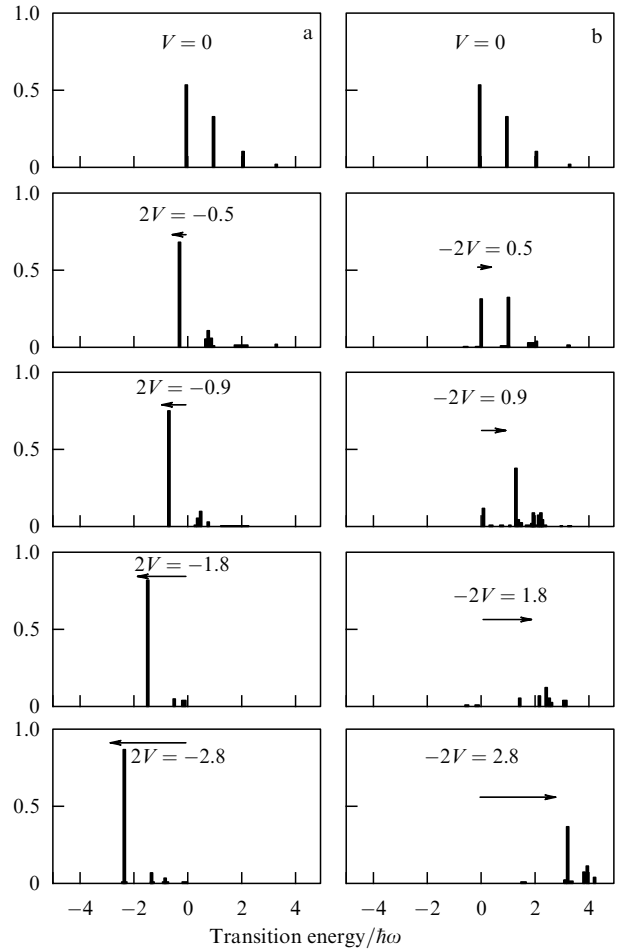

Figure 9. Interaction of an exciton with intramolecular vibrations, which illustrates transitions (a) near the lower edge of the exciton band (J-effect), and (b) near the upper edge of the exciton band (H-effect) [47]. Hamiltonian (3.7) was numerically diagonalized for a linear chain of 8 molecules with periodic boundary conditions. Electron-vibrational interaction $\zeta^2 = 0.6$ reproduces the vibrational sequence of 1368 cm^{-1} for a pseudoisocyanine monomer.

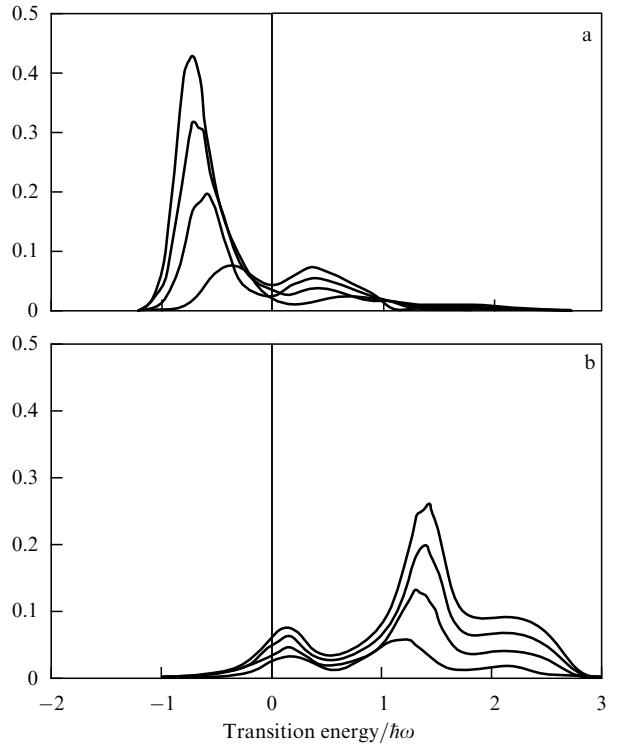

Figure 10. Absorption spectra of small linear aggregates ($N = 2, 4, 6, 8$), calculated for the Gaussian distribution of diagonal energies taking into account one high-frequency intramolecular vibration ($\zeta^2 = 0.6$) [47]. Exciton interaction between the nearest neighbors is $V = -0.46\,\hbar\omega$. (a) $k = 0$ — transitions are allowed close to the lower edge of the exciton band (J-bands); (b) $k = N/2$ — transitions are allowed close to the upper edge of the exciton band (H-bands).

interaction with intramolecular vibrations effectively decreases intermolecular interaction). In quantitative terms, the results in the case of $k = 0$ and $V < 0$ differ from the results in the case of transitions to the upper edge $k = N/2$ ($V < 0$) of the exciton band, shown in Fig. 9b. The latter results also hold true for the case of $k = 0$ and $V > 0$.

The exciton strongly mixes with intramolecular vibrations, so that the intensity for intermediate exciton interaction is distributed over zero-phonon and one-phonon lines (Fig. 9b). Such a situation is typical of dimers and H-aggregates [121 – 124]. As regards the J-band of pseudoisocyanine, it is unclear [47] whether the observed intense and broad absorption wing on the high-energy side is due to aggregates of a different (pack-of-cards) structure or represents transition to the upper edge of the exciton band of J-aggregates, which is allowed for the brickwork structure [59, 118].

Figure 10 shows the results of calculations taking into account both the high-frequency mode and strong diagonal disorder [47]. The Hamiltonian of the aggregate is diagonalized for 10^4 random sets of transition energies with the uncorrelated Gaussian distribution. In this example, the disorder decreases the exciton coherence length to ≈ 2 molecules; hence, the bandwidth depends almost not at all on the length of the molecular chain.

Solvent fluctuations. In the classical approximation, electrostatic interaction with surrounding molecules leads to the modulation of energies $\varepsilon_n^{(s)}$ of molecular electronic states, in compliance with the randomly fluctuating local electric field:

$$\varepsilon_n^{(s)}(t) = \bar{\varepsilon}_n^{(s)} + \Delta\varepsilon_n^{(s)}(t)\,.$$

Correlation times of fastest fluctuations in polar solutions are on the order of 10 – 20 fs [125]. Scherer [47] simulated molecular dynamics of water in a cube of side 20 Å surrounding a pseudoisocyanine dimer. Changes in time-dependent diagonal energies for the dimer's fixed coordinates were calculated from molecular orbital densities evaluated by quantum-chemical methods. The resulting energy fluctuations rapidly decay and can be approximated by the Gaussian function typical of the inertial motion of solvent molecules:

$$\left\langle \varepsilon(t)\varepsilon(0)\right\rangle = \Delta^2 \exp\left(-\aleph^2 t^2\right),$$

with the width $\Delta = 200$ cm^{-1} ($\Delta\omega = 4 \times 10^{13}$ s^{-1}) and decay constant $\aleph = 5 \times 10^{13}$ s^{-1}. These numerical values agree with the experimental data by van Burgel et al. [126] on the photon echo for tetrachloroimidacarbocyanine (TDBC) aggregates in water.

The fast component of fluctuations is not observed in the presence of correlations between transition energies of

different molecules in an aggregate. Its main source is the motion of solvent molecules, the volume of which is much smaller than the entire volume of the solvent. Fast fluctuations are first and foremost associated with the motion of solvent molecules closest to the aggregate. Slower fluctuations resulting from collective motion may give rise to significant correlations between transition energies of individual molecules within the aggregate [127]. Such fluctuations in a monomer lead to inhomogeneous line broadening if only $\Delta \geqslant \aleph$, as is roughly the case in a real situation. There appears one more time scale $\hbar/V$ for an aggregate, which is associated with the intermolecular interaction, where the typical value of $V/\hbar$ is also on the order of 10^{14} s^{-1}. It is therefore unclear [47] how to realize Knapp's mechanism of band narrowing [58] by the agency of 'fast moving' Frenkel exciton that must average the static disorder. The results of experiments with TDBC aggregates [126] suggest homogeneous line broadening, assuming that energy fluctuations occur for exciton states k and depend on the reduced value of $\Delta_k^2 \approx \Delta^2/N_c$ (N_c is the exciton coherence length). Nevertheless, the final solution to the problem remains to be found [47]. Reineker et al. [128–131] simulated fluctuations by a dichotomic process (binary disorder, see Section 4.5.1) and received analytical results for small aggregates. Cordan et al. [132] studied the influence of δ-correlated fluctuations. The situation is much simpler for slower fluctuations on a picosecond or larger scale [126]. Here, the description of radiative transition energies of individual molecules in an aggregate by random distribution seems to be adequate [47]. Nevertheless, determination of the degree of correlations between transition energies still encounters difficulties [47]. Nonlinear effects imply large correlation lengths at low temperatures [37], whereas hole burning studies in the spectrum give preference to the uncorrelated disorder model [133].

Quantum-chemical calculations of model structures of pseudoisocyanine aggregates [134] indicated that the two-level model is only a poor approximation for such molecules. That gave Scherer [47, 134] reason to discuss electron excitations in an aggregate beyond the framework of the simple exciton picture.

Summary. An advantage of Scherer's vibron model of the J-band [47] is the rather detailed consideration of Frenkel exciton interaction with intramolecular vibrations and nuclear motion in the medium surrounding the dye. However, this consideration is virtually inconsistent with the final result; it further incorrectly simplifies the problem for the concrete calculation of the J-band by introducing Gaussian diagonal disorder. Scherer actually reduces his vibron theory to the canonical exciton theory (Section 4). As a result, the band narrowing mechanism in J-aggregation is reduced to the Knapp mechanism [58]. In so doing, the characteristic fluctuation time of the solvent obtained by Scherer is comparable to the characteristic time of exciton motion; the author recognizes that this fact is in conflict with the band narrowing mechanism under consideration. As mentioned in the introduction to Section 3, such inaccuracies in the theory are characteristic features of all noncanonical exciton approaches. They can be overcome partly in a more sophisticated exciton model [129, 131, 132, 135–138] taking into account Anderson–Kubo [90–94] dynamic disorder (Section 12).

3.2.2 Quantum-chemical semiempirical calculations. One more attempt to solve the J-band problem in the framework of the vibron theory has been undertaken in a series of studies [139–143] based on semiempirical methods of quantum chemistry. In quantum-chemical calculations, exciton interaction is present only in the implicit form, as opposed to the theory considered in Section 3.2.1, where it is present in the explicit form. Here, the simplest task on the way to the solution of the J-band problem was numerical simulation of the band shape in organic dyes (not necessarily polymethine ones) and their dimers [139–142].

References [141, 142] present semiempirical quantum-chemical calculations of electronic absorption spectra in streptopentamethinecyanine and pseudoisocyanine dimers. Two methods were used to compute changes in the energy of the 0–0 transition during dimer formation. The first was based on the supermolecule approximation in which a dimer was regarded as a large single molecule. The corresponding calculations were made by the CNDO/S [144] method taking into account interactions of all singly excited electron configurations of the $\pi\pi^*$ type. In the second case, the CNDO/S method was used in the one-configuration approximation to obtain wave functions of the ground and singly excited electronic states of a $\pi\pi^*$-type monomer. Thereafter, the electronic absorption spectrum of the dimer was calculated by the configuration interaction method on the basis of the obtained many-electron wave functions of monomers.

The shape of the absorption band was simulated by the method suggested in Refs [139, 140, 145, 145] in which the empiric field of force for the ground electronic state of a molecule was combined with the quantum-chemical computation of the transition energy from the ground state to the electronically excited state. Such an approach allows the volume of computational work to be significantly reduced.

The main assumptions underlying the semiempirical quantum-chemical calculations under consideration are related to the Born–Oppenheimer adiabatic approximation and the Franck–Condon principle. The adiabatic approximation in quantum-chemical calculations works well for sufficiently small molecules.[11] For large polymethine dye molecules usually making up dimers, J- and H-aggregates, the Born–Oppenheimer approximation is markedly violated, which dictates invoking of alternative methods to the theory [69–73]. Sometimes, it can be expected that the Born–Oppenheimer approximation valid for theoretical description of relatively small molecules will be strongly violated for their aggregates. It appears that the authors of Refs [139–143] encountered exactly such a situation, since their results are still in agreement with experiment in the case of monomers, but disagree with those in the case of dimers [141, 142] and J-aggregates of 4 or 9 molecules [143].

3.2.3 Phenomenological explanation of the J-band shape based on the Hamiltonian resolvent method. Eisfeld and Briggs [147] drew attention to the fact that delocalized electron excitation of an aggregate comprising N monomers or the Frenkel exciton exemplifies entangled quantum states (see, for instance, reviews [80, 81] and references cited therein) which occur at the mesoscopic level and that the J-band is one of their experimental manifestations.[12] The authors of Ref. [147] considered an exciton model containing various exciton–

[11] To be precise, the problem at issue concerns the size of a spatial region covered by electron charge density redistribution during excitation.

[12] Our view on the relationship between the J-band and entangled quantum states was expounded in Section 1.

phonon interactions in the implicit form as a result of a direct relationship between the absorption bands of the aggregate and the monomer. The exact relation depends on the aggregate geometry. This approach, based on the Hamiltonian resolvent method [148 – 150], allows a rather simple determination of the aggregate spectrum shape from the known monomer spectrum.

The expression for the absorption band shape $(-G)$ of a linear J-aggregate is given by the monomer line shape $(-g_i)$ and difference C [148] between the average absorption energies of the monomer and J-aggregate bands [147]:

$$G = \frac{1}{C} \frac{Cg_i}{(1 - Cg_r)^2 + C^2 g_i^2}, \tag{3.8}$$

where

$$g_r(E) = \frac{1}{\pi} \mathrm{P} \int_{-\infty}^{\infty} \frac{g_i(E')}{E' - E} \, \mathrm{d}E' \tag{3.9}$$

is the principal-value integral. It follows from expressions (3.8), (3.9) that the Eisfeld – Briggs model has no free parameters. In many cases, however, the wings of the monomer spectrum are poorly known. Therefore, for practical purposes, it is better to approximate g_i by known functions and consider C as a fitting parameter [147].

It was shown in Ref. [147] that the calculated spectrum of a TDBC J-aggregate for $C = -2416$ cm^{-1} is in excellent agreement with experimental data [151]. The simple structure of relation (3.8) makes it possible to easily explain the band shape of the J-aggregate. The $g_r(E)$ dependence calculated by formula (3.9) is such that expression (3.8) for $g_r(\lambda) = 1/C$ has two poles: at $\lambda = 575$ nm, and 540 nm [147]. The pole at 575 nm is responsible for the J-band peak in the absorption spectrum [147]. It can be seen from formula (3.8) that Cg_i plays the role of the bandwidth. Monomer absorption, hence $-g_i$, being very small in this region, the bandwidth is also small and the J-band is narrow. This result exhibits a generic character; specifically, strong narrowing of the J-band can be expected when the absolute value of parameter C is large enough to shift the pole to the region where the monomer does not absorb. Physically, the case when $|C|$ is larger than the monomer absorption bandwidth corresponds to the strong exciton interaction between monomers in an aggregate [147]. The pole at 540 nm, lying in the monomer absorption region, possesses, on the contrary, large width Cg_i. It is responsible for the wide sloping absorption wing in the short-wave part of the J-band [147].

Exciton coherence naturally poses the problem of its control [147]. The problem of application and control of quantum coherence is presently very popular in connection with the development of quantum computers. Rydberg atomic dimers arising by dipole – dipole interaction have been suggested as a model for two-position registers [152, 153]. Their exciton analogs are dimers of polymethine dyes in which the excited state is just a pair of levels (Section 2.1), in full analogy with a pair of Rydberg atoms [147].

A drawback of the Eisfeld – Briggs model [147] is the inclusion of two experimental quantities, viz. the monomer band shape and the difference between the average energies of the J-aggregate and monomer absorption bands. Another disadvantage is the fact that the monomer band shape playing the role of the starting element for computation of the J-band undergoes uncontrolled modification as a result of aggregation (Section 4.2). Finally, this model (as well as the exciton approach at large) does not consider explicitly the specific electronic structure of polymethine dyes (Sections 7 and 8).[13]

4. Canonical exciton theory of optical band shapes for molecular aggregates

4.1 General information about dye aggregates and a comparative characteristic of calculation methods for their optical bands

As pointed out in the Introduction, studies of dye molecule aggregation in solutions were pioneered by the classical works of Jelly [42, 43] and Scheibe [44, 45], who observed the appearance of a very narrow and intense band in the long-wave region of the pseudoisocyanine absorption spectrum with increasing concentration of the solution. The authors associated this band with the formation of J-aggregates.

Absorption band narrowing during formation of J-aggregates was also observed in experiments with other cyanine dyes, besides pseudoisocyanine. At the same time, aggregation of thiazine dyes decreased their absorption capacity, whereas aggregation of xanthene and acridine dyes, and some other compounds led to the splitting of the absorption band into two or more subbands (see review [154] and references cited therein). These differences in changing the optical properties under aggregation are usually attributed to the different sizes and geometrical structures of molecular aggregates formed by dyes of various classes.

The size and the structure of molecular aggregates are determined not only by the type of dye but also by the nature of the solvent [154]; the last effect depends on the extent to which solvation spheres of molecules facilitate or hamper their aggregation. Aggregation is most efficacious in aqueous solutions [155 – 159]. The addition of organic solvents considerably inhibits the formation of aggregates [156, 160 – 162]. In due course, a drop in temperature promotes aggregation [163 – 170].

Experimental determination of the molecular aggregate size encounters great difficulties and frequently gives conflicting results. By way of example, the size of pseudoisocyanine aggregates in water varies from dozens [171] to hundreds and even a thousand [172] of molecules, and that of crystal violet from 2 to 18 molecules (see Refs [173 – 177]), depending on the experimental technique.

It is generally accepted that aggregates are formed by van der Waals forces [178 – 185]. Calculations done by Coulson and Davies [180] showed that van der Waals forces for large molecules may be as large as dozens of kcal mol^{-1}. On the other hand, Refs [186 – 193] reported strong dependence of aggregation efficiency on the dye molecular structure and the solvent type, which is characteristic of hydrogen bonding. This means that the nature of intermolecular forces in an aggregate must be discussed separately for each concrete situation.

Theoretical analysis of the optical properties of molecular aggregates is based on a variety of exciton models. The most popular of them is the canonical exciton model (CEM) [58, 60 – 66, 68, 119, 128, 130, 194 – 207], in terms of which dye molecules are regarded as simple two-level quantum systems

[13] It is implicitly taken into account in the experimentally obtained monomer band shape.

with randomly distributed transition energies. Transition energy disorder referred to as diagonal disorder takes into account molecular vibrations (considered in the classical approximation in the framework of this approach), the inhomogeneous local environment (inhomogeneous broadening), and other factors responsible for the molecular absorption spectrum. The popularity of CEM is attributable to its relative simplicity, which makes possible the calculation of very large systems (up to 10^6 molecules) [128]. At the same time, such more complicated models as the vibron model [47, 59, 118, 141–143, 147, 208–211] (Section 3.2) or exciton model with dynamic disorder[14] [129, 131, 132, 135–138] are characterized by a very fast rise in the number of equations with increasing aggregate size. This precludes calculations for aggregates composed of more than 5–10 molecules. Thus, CEM is the optimal option when dye optical properties change during aggregation due to delocalization of electron excitation over a large number of molecules. In particular, CEM permits reproducing characteristic features of the absorption spectra of J-aggregates, such as shifts, narrowing, and asymmetry of optical bands.

In the beginning, CEM was used to study the optical properties of molecular aggregates by the methods of the perturbation theory [58, 194–200]. Later on, numerical calculations were given priority [60–66, 68, 119, 128, 130, 201–207]. However, computational methods reported in the literature had very low efficiency and frequently brought in a high noise level in the resultant spectra. We proposed several methods based on the introduction of a fluctuating origin of the energy scale that substantially increase computation efficiency and yield rather exact spectra by a reasonable amount of calculations [60, 61, 63, 65].

Section 4 presents the description of CEM and offers a concise derivation of the expression for the band shape needed for further application. Also considered are the main analytical and numerical methods used in the literature to characterize optical bands of molecular aggregates in the framework of CEM; the results obtained with the help of these methods are reviewed in this section. Section 5 considers a highly efficient computation tool (proposed within the scope of CEM) for the most common case of aggregates with the Gaussian diagonal disorder and discusses results of calculations by this method [60–64, 66]. The general method for aggregates with arbitrary disorder is also expounded [65, 66]. References [66, 212] report computed optical bands for aggregates of different types of molecules that differ either in mean transition energy alone or in transition dipole moments, too. For simplicity, the authors of Refs [66, 212] consider only the effects of violation of the selection rules for quantum transitions to the exciton band, leading to the redistribution of the oscillator strength between the states in the band, but disregard nondiagonal disorder in the Hamiltonian, including that related to the dependence of intermolecular interaction energy on the type of molecules.

4.2 Model description: Hamiltonians of a molecule and a molecular aggregate, and interaction with radiation

The current molecular theory implies that the mass of an atomic nucleus is many orders of magnitude bigger than the electron mass, which accounts for the lower velocity of nuclear motion compared with the electronic one. This permits using the adiabatic Born–Oppenheimer approximation [110, 77] in terms of which the problem of electron-nuclear motion in a molecule is resolved in two stages. First, the Schrödinger equation for the electron wave function is solved for motionless nuclei located at given distances from one another. Then, movements of the nuclei are considered using the dependence (found at the previous stage) of the ground-state eigenenergy on the position of the nuclei as the potential energy surface.

The Hamiltonian of a molecule with nuclei at rest has the form

$$H_{\mathrm{mol}} = \frac{1}{2m_{\mathrm{e}}} \sum_i \mathbf{p}^{(i)2} + u(\mathbf{r}, \mathbf{R}) \,, \tag{4.1}$$

where $\mathbf{p}^{(i)}$ is the momentum operator of the ith electron, $\mathbf{r}$ and $\mathbf{R}$ are the sets of coordinates of all electrons and nuclei in the molecule, respectively, and $u(\mathbf{r}, \mathbf{R})$ is the electrostatic energy of interaction between them.

In the framework of CEM, movements of atomic nuclei are considered in the classical approximation (Section 3.2.1) where the probability of their being found at the position $\mathbf{R}$ is determined by the Boltzmann distribution (see, for instance, Ref. [213]):

$$P(\mathbf{R}) \propto \exp\left(-\frac{E^{(0)}_{\mathrm{mol}}(\mathbf{R})}{k_{\mathrm{B}}T}\right), \tag{4.2}$$

where $E^{(0)}_{\mathrm{mol}}(\mathbf{R})$ is the ground-state energy of the molecule.

Let us consider light absorption by an ensemble of noninteracting molecules. Due to nuclear vibrations, individual molecules are characterized at each instant of time by different values of vector $\mathbf{R}$. As a result, individual molecules of the ensemble have different absorption frequencies. In the long-wave approximation (see, for instance, Ref. [89]), light absorption intensity I at frequency Ω is determined by averaging the modulus squared of the transition dipole moment $\mathbf{M}_{0f}$ of molecules over the ensemble:

$$I(\Omega) \propto \int \mathrm{d}\mathbf{R}\, P(\mathbf{R}) \left|\mathbf{M}_{0f}(\mathbf{R})\right|^2 \delta\left[E^{(f)}_{\mathrm{mol}}(\mathbf{R}) - E^{(0)}_{\mathrm{mol}}(\mathbf{R}) - \hbar\Omega\right], \tag{4.3}$$

where f denotes electron-excited state of the molecule, $\mathrm{d}\mathbf{R}$ is the product of differentials of all nuclear coordinates of the system, and $P(\mathbf{R})$ is the multidimensional probability distribution (4.2). For the molecules in a solution, an important role is played not only by nuclear vibrations but also by inhomogeneous broadening, i.e., deviations in the transition energy under the effect of the local surrounding medium. In this case, averaging over the ensemble requires integration not only over atomic nucleus coordinates but also over coordinates of the nearby solvent molecules.

Let us now consider a molecular aggregate of N molecules. Its Hamiltonian [see formula (2.22)] consists of Hamiltonians of constituent molecules and electrostatic interactions between them and depends on the coordinates of all electrons ($\mathbf{r}$) and nuclei ($\mathbf{R}$). Intermolecular interactions cause delocalization of electron excitation, which results in producing collective excitations or Frenkel excitons [23] (Section 2).

It is usually supposed, in analogy with molecular crystals, that overlap integrals of electron wave functions of neighboring molecules in aggregates are very small. Therefore, the aggregate wave functions can be written without antisymme-

[14] For more about dynamic disorder, see Section 12.

trization over electrons belonging to different molecules (Section 2).

Let us consider a case when the separation between electronic levels in a molecule is much greater than the energy of intermolecular interaction and deviations in the transition energy. In such a case, the Hamiltonian of the aggregate may be written down taking account of only the ground ($f = 0$) and one excited ($f = u$) molecular state [50]. Moreover, only a minor fraction of molecules in the system is excited at the small electromagnetic radiation densities being considered. It is therefore possible to disregard aggregate states with two or more excited molecules. In other words, we may confine ourselves to considering the basis consisting of the aggregate ground state and states in which one of the molecules is excited. On this basis, aggregate Hamiltonian (2.22) takes the form [50, 51, 214 – 218]

$$H = \sum_n |n\rangle \varepsilon_n \langle n| + \sum_{\substack{n,m \\ n \neq m}} |n\rangle V_{nm} \langle m| \,, \tag{4.4}$$

where ε_n is the transition energy of the nth molecule in the aggregate, and V_{nm} is the energy of resonance interaction between the nth and mth molecules; the ground-state energy of the aggregate is taken as the origin.

Similar to the case of noninteracting molecules considered earlier, eigenenergies and eigenfunctions of aggregate molecules depend on atomic nucleus coordinates $\mathbf{R}$ and the location of the nearest solvent molecules. Molecular vibrations and an inhomogeneous local environment give rise to different transition energies ε_n and transition dipole moments $\mathbf{M}_n$ of various molecules in the aggregate.

Disordering of energies ε_n is otherwise called diagonal disorder; disordering of energies V_{nm} of intermolecular resonance interaction due to the disorder of transition dipole moments and intermolecular distances is referred to as nondiagonal disorder. The majority of theoretical studies on the shape of optical bands in molecular aggregates (see Refs [58, 68, 128, 194 – 207]) are restricted to the diagonal disorder, whereas $\mathbf{M}_n$ and V_{nm} quantities are regarded as fixed ones. We also stick to this approximation in our works [60 – 65], except where dealing with aggregates with disordered transition dipole moments [212] (Section 4.1).

Now, let us consider the interaction of a molecular aggregate with electromagnetic radiation. In the framework of our model, the Hamiltonian of the aggregate has $N + 1$ eigenstates: the ground state $|0 \ldots 0\rangle$, and N excited states described by the wave functions ψ_k. These excited states [eigenstates of Hamiltonian (4.4)] make up the exciton band E_k [eigenenergies of Hamiltonian (4.4)] having a width roughly corresponding to the mean total energy of resonance interaction of a molecule with its neighbors in the aggregate.

Let us assume that the outer dimensions of the aggregate is much smaller than the light wavelength. In this case, the long-wave approximation is applicable not only to individual molecules but also to the aggregate as a whole.

It was noted above that most publications (see Refs [58, 68, 119, 128, 130, 194 – 207]) deal with aggregates in which all molecules have identical transition dipole moments: $\mathbf{M}_n = \mathbf{M}$ for all n. In this case, the dipole moment of transition from the ground state to the kth excited state takes the form

$$\mathbf{M}_{0k} = \mathbf{M}\sqrt{N}\langle S|\psi_k\rangle \,, \tag{4.5}$$

where

$$|S\rangle = \frac{1}{\sqrt{N}} \sum_{n=1}^{N} |n\rangle \tag{4.6}$$

is the quantum state with the zero wave vector (all molecules in the aggregate are excited with equal amplitudes and phases).

Let us consider light absorption by an ensemble of molecular aggregates. Similar to individual molecules, different aggregates in the ensemble are characterized by specific sets of energies ε_n and, therefore, possess different absorption frequencies. The expression for light absorption intensity at frequency Ω can be derived by averaging $|\mathbf{M}_{0k}|^2$ [see formula (4.5)] over the ensemble after summation over all k states in the exciton band. Omitting Ω-independent multipliers and taking into account that the transition energy is much greater than the optical band width lead to

$$I(\Omega) \propto \int \ldots \int \mathrm{d}\varepsilon_1 \ldots \mathrm{d}\varepsilon_N \, P(\varepsilon_1, \ldots, \varepsilon_N) \times \sum_{k=1}^{N} \left|\langle S|\psi_k(\varepsilon_1, \ldots, \varepsilon_N)\rangle\right|^2 \delta\left[E_k(\varepsilon_1, \ldots, \varepsilon_N) - \hbar\Omega\right] , \tag{4.7}$$

where $P(\varepsilon_1, \ldots, \varepsilon_N)$ is the multidimensional probability distribution for the transition energies of aggregated molecules. When the transition energies of all molecules in the aggregate are distributed similarly and independently of one another, the distribution of interest assumes the form

$$P(\varepsilon_1, \ldots, \varepsilon_N) = \prod_{n=1}^{N} p(\varepsilon_n) \,, \tag{4.8}$$

where $p(\varepsilon_n)$ is the transition energy distribution for the nth molecule.

The distribution $p(\varepsilon_n)$ has a simple physical meaning. If intermolecular interaction V_{nm} in Hamiltonian (4.4) is put to zero for all n and m, the absorption spectrum given by expression (4.7) coincides with distribution $p(\varepsilon_n)$. Then, it may be assumed in the first approximation that $p(\varepsilon_n)$ represents the absorption spectrum of noninteracting molecules. This is, however, a rough approximation because it disregards modification of potential energy surfaces of the molecules forming the aggregate. For this reason, the optical absorption spectra of aggregates of concrete substances should be computed with regard for the specific properties of their constituent molecules, thus taking the distribution $P(\varepsilon_1, \ldots, \varepsilon_N)$ from relevant quantum-chemical calculations. However, such calculations are cumbersome and for practical purposes $P(\varepsilon_1, \ldots, \varepsilon_N)$ is usually substituted by a simple model distribution known from the probability theory, e.g., the Gaussian distribution [58, 68, 119, 128, 130, 194 – 199, 201 – 207], or binary distribution [128, 199, 200].

As is known, the disorder associated with local environment fluctuations has the Gaussian form (see, for instance, Ref. [77]). At the same time, it was shown in paper [201] that small molecular vibrations also lead to Gaussian disorder. Therefore, the many-dimensional Gaussian distribution is most frequently used as $P(\varepsilon_1, \ldots, \varepsilon_N)$ when calculating the optical properties of molecular aggregates. The model of aggregates with the Gaussian disorder permits, despite its simplicity, reproducing characteristic features of experimental spectra of J-aggregates, including shifts, narrowing, and

asymmetry of the optical band [42–45, 68, 171]. Hence the wide application of this model. In many cases, however, e.g., when the potential energy surface of the ground state of aggregate-forming molecules has two or more minima (i.e., when the molecules can exist in different isomeric forms), the Gaussian disorder approximation is inapplicable. In such cases, calculations need to be made using more complicated distributions that reflect the specific properties of the molecules of interest (Section 5.5).

4.3 On the shape of the absorption band in the perturbation-theory approximation

There are a large number of theoretical works in which the optical properties of molecular aggregates were investigated with the use of CEM by both approximate analytical [58, 194–200] and exact numerical [68, 119, 128, 130, 201–207) methods. This section and Section 4.4 are devoted to the works using approximate methods.

Crystal lattice disorder is known to result in localization of a system's eigenstates (Anderson localization [219, 220]). In a three-dimensional case there is a certain level of threshold disorder, below which the states remain delocalized. In a one-dimensional case, localization occurs even in the presence of infinitesimal disorder [220–223], while the delocalization length (coherence length) approaches infinity as the disorder tends to zero. (In two-dimensional geometry, all the states are also localized in the absence of a magnetic field and spin-orbital interaction [224, 225].) This implies the possibility of distinguishing two fundamentally different cases when considering excitons in disordered linear molecular aggregates. In one of them, the exciton coherence length N_c is much greater than the aggregate length N. In the other, $N_c \ll N$.

Let us first discuss the former case analyzed by Knapp [58] with the use of the perturbation theory by an example of one-dimensional molecular chains with interaction only between nearest neighbors:

$$V_{nm} = V(\delta_{n,m+1} + \delta_{n,m-1}) .$$

The choice of the one-dimensional chain as a model structure is dictated by the fact that J-aggregates most frequently look like long thin filaments [43, 109, 171]. The case in question takes place when aggregates are not too large and disorder is rather weak, i.e., when [58]

$$\frac{1}{\pi}\left(\frac{\sigma}{V}\right)^2\left(\frac{N}{2\pi}\right)^3 \ll 1 , \tag{4.9}$$

where N is the aggregate size (the number of molecules in the chain), and σ is the root-mean-square deviation of transition energies from a mean value of $\langle\varepsilon_n\rangle \equiv \hbar\Omega_0$. Inequality (4.9) suggests the possibility of using the perturbation theory for calculating corrections to exciton energies and wave functions. Its physical sense is that the magnitude of disorder, $\sigma/N^{1/2}$, reduced by exciton movements [see formula (4.14) below] must be much smaller than the minimal separation $3\pi^2 V/N^2$ between exciton energy levels in linear aggregates.

Let the deviation of the transition energy ε_n for the nth molecule from $\hbar\Omega_0$ be denoted as Δ_n. Further, let the exciton Hamiltonian (4.4) of the aggregate be written down in the form

$$H = H_0 + H' , \tag{4.10}$$

where

$$H_0 = \sum_n \left[\hbar\Omega_0|n\rangle\langle n| + V\big(|n\rangle\langle n+1| + |n+1\rangle\langle n|\big)\right] \tag{4.11}$$

is the Hamiltonian of the ordered aggregate, and

$$H' = \sum_n \Delta_n|n\rangle\langle n| \tag{4.12}$$

may be regarded as a minor correction to unperturbed Hamiltonian H_0. Let us assume $V < 0$, confine ourselves to the consideration of cyclic molecular chains, and use below standard formulas of the perturbation theory. For strong inequality (4.9), it is possible to take into account only the first order of the perturbation theory. Let us consider the case of uncorrelated Gaussian disorder in formula (4.7):

$$P(\varepsilon_1, \ldots, \varepsilon_N) = \frac{1}{(\sqrt{2\pi}\sigma)^N}\exp\left[-\sum_{n=1}^{N}\frac{(\varepsilon_n - \hbar\Omega_0)^2}{2\sigma^2}\right] . \tag{4.13}$$

Consideration gives the expression for the absorption band shape of a one-dimensional aggregate with weak Gaussian disorder [66]. It being rather cumbersome, we do not write it down here. The shape of this band possesses the following main characteristics. First, the absorption maximum of the aggregate is shifted by $2V$ with respect to the absorption band maximum of a monomer. Second, the long-wave wing of the band has an approximate Gaussian form, and the short-wave wing an approximate Lorentzian form. Finally, the half-width w_N of the aggregate band is defined by the simple relation [58]

$$w_N = \frac{w_1}{\sqrt{N}} , \tag{4.14}$$

where w_1 is the half-width of the monomer band. Thus, CEM permits reproducing all characteristic features of experimentally examined optical bands of J-aggregates.

In the general case of occurring correlation between the transition energies of different molecules in an aggregate (Section 5.2), relation (4.14) is replaced by the expression [58]

$$w_N = \frac{w_1}{\sqrt{N}}\left[\left(\frac{1-\beta^N}{1+\beta^N}\right)\left(\frac{1+\beta}{1-\beta}\right)\right]^{1/2} , \tag{4.15}$$

where β is the correlation parameter. In the absence of correlation ($\beta = 0$), relation (4.15) transforms into formula (4.14); in the case of complete correlation ($\beta \to 1$), the half-width of the aggregate band coincides with that of the monomer.

4.4 Shape of the absorption band in the average *t*-matrix and coherent potential approximations

Let us consider now the opposite case, when the aggregate length is much greater than the exciton delocalization length. In this case, neither the dynamics nor the optical properties of excitons depend on the aggregate length; therefore, it may be regarded as tending to infinity. Then, Hamiltonian eigenvalues make up a quasicontinuous spectrum.

We are interested here in the case of weak scattering: $|\sigma/V| \ll 1$. Unfortunately, the 'exact' solution to the problem with the help of the perturbation theory is impossible here. It is therefore necessary to introduce additional simplifications and apply various approximate methods, such as the average t-matrix method [194–196] or coherent potential method [196–200].

Let us rewrite expression (4.7) for the aggregate absorption spectrum through the Hamiltonian resolvent [58, 150]:

$$I(\Omega) \propto \left\langle \operatorname{Im} \left\langle S \left| (\hbar\Omega + \mathrm{i}\gamma - H)^{-1} \right| S \right\rangle \right\rangle , \tag{4.16}$$

where $\gamma \to 0$, and the external brackets $\langle \ldots \rangle$ denote averaging over the ensemble. The exciton's Green function is given by

$$G_{nm}(E) = \left\langle n \left| (E + \mathrm{i}\gamma - H)^{-1} \right| m \right\rangle . \tag{4.17}$$

Substitution of the Hamiltonian in the form of expressions (4.10) – (4.12) and its expansion in power series yield

$$G_{nm} = G^0_{nm} + \sum_l G^0_{nl} \Delta_l G^0_{lm} + \sum_{l,l'} G^0_{nl} \Delta_l G^0_{ll'} \Delta_{l'} G^0_{l'm} + \ldots , \tag{4.18}$$

where

$$G^0_{nm}(E) = \left\langle n \left| (E + \mathrm{i}\gamma - H_0)^{-1} \right| m \right\rangle \tag{4.19}$$

is the Green function of the ordered aggregate. In the case of interaction only between the nearest neighbors, it takes the form [66]

$$G^0_{nn}(E) = -\left[(E - \hbar\Omega_0)^2 - 4V^2 \right]^{-1/2} . \tag{4.20}$$

Let us rewrite expansion (4.18) in terms of the t-matrix. The introduction of [226]

$$t_n(E) = \frac{\Delta_n}{1 - \Delta_n G^0_{nn}(E)} \tag{4.21}$$

transforms expression (4.18) into

$$G_{nm} = G^0_{nm} + \sum_l G^0_{nl} t_l G^0_{lm} + \sum_{l \neq l'} G^0_{nl} t_l G^0_{ll'} t_{l'} G^0_{l'm} + \ldots . \tag{4.22}$$

The introduction of the t-matrix obviates summation over repeating indices in the third term of the series. Unfortunately, such a summation partly remains in the highest terms of expansion (4.22). Therefore, averaging the Green function over the ensemble is performed in the average t-matrix approximation [226 – 230]:

$$\langle t_n^m \rangle = \langle t_n \rangle^m . \tag{4.23}$$

This approximation takes into consideration the scattering of each exciton only from a single molecule and neglects its subsequent scattering from other molecules [195, 226, 231].

Suppose that all Δ_n are distributed identically and independently of one another. Then, averaging expansion (4.22) over the ensemble, using approximation (4.23), and summing the series lead to [195, 226]

$$\left\langle G_{nm}(E) \right\rangle = \left\langle n \left| \left[E - H_0 - \Sigma(E) \right]^{-1} \right| m \right\rangle , \tag{4.24}$$

where

$$\Sigma(E) = \frac{\left\langle t_n(E) \right\rangle}{1 + \left\langle t_n(E) \right\rangle G^0_{nn}(E)} . \tag{4.25}$$

Let us rewrite expression (4.16) for the absorption spectrum $I(\Omega)$ in terms of $G_{nm}(E)$ [see formula (4.17)] and substitute the averaged Green functions in the form (4.24). Then we arrive at

$$I(\Omega) \propto \operatorname{Im} \left\langle S \left| \left[\hbar\Omega - H_0 - \Sigma(E) \right]^{-1} \right| S \right\rangle . \tag{4.26}$$

Because $|S\rangle$ is the eigenstate of the Hamiltonian H_0 with the energy E^0_1, the expression

$$I(\Omega) = \frac{\operatorname{Im} \Sigma(E)}{\left[\hbar\Omega - E^0_1 - \operatorname{Re} \Sigma(E) \right]^2 + \left[\operatorname{Im} \Sigma(E) \right]^2} \tag{4.27}$$

is correct up to the constant. Thus, the asymmetry of the absorption band is due to the different character of the Σ dependence on E inside and outside the exciton band.

For energies E inside the exciton band, where the Green function G^0_{nn} [see formula (4.20)] is a complex quantity, expression (4.25) gives [taking into account Eqn (4.21) for the aggregates with weak Gaussian disorder ($|\sigma/V| \ll 1$)] [195]

$$\Sigma(E) = \sigma^2 G^0_{nn}(E) . \tag{4.28}$$

Outside the exciton band, where the Green function is real, one finds

$$\begin{aligned} \operatorname{Re} \Sigma(E) &= \sigma^2 G^0_{nn}(E) , \\ \operatorname{Im} \Sigma(E) &= -\left(\frac{\pi}{2} \right)^{1/2} \sigma^{-1} \left[G^0_{nn}(E) \right]^{-2} \exp \frac{\left[G^0_{nn}(E) \right]^{-2}}{2\sigma^2} . \end{aligned} \tag{4.29}$$

Expressions (4.28) and (4.29) hold true when

$$\left| (E - \hbar\Omega_0)^2 - 4V^2 \right| \gg \sigma^2 ,$$

i.e., when they describe the absorption band everywhere except a narrow region close to the exciton band edge. Substitution of Eqn (4.29) into Eqn (4.27), taking into account formula (4.20) and the fact that the band width in a weak disorder case is much smaller than the exciton band width, yields the following expression for the low-frequency wing of the spectrum [195]:

$$I(\Omega) = \frac{2(2\pi)^{1/2}}{\sigma \left[\hbar(\Omega - \Omega_0)/V - 2 \right]} \exp \left\{ - \frac{\left[\hbar(\Omega - \Omega_0)/V \right]^2 - 4}{2(\sigma/V)^2} \right\} . \tag{4.30}$$

For the high-frequency wing, one obtains

$$I(\Omega) = \frac{2|V|^{-1} \left[\hbar(\Omega - \Omega_0)/V - 2 \right]^{1/2} (\sigma/V)^2}{4 \left[\hbar(\Omega - \Omega_0)/V - 2 \right]^3 + (\sigma/V)^4} . \tag{4.31}$$

It follows from Eqns (4.30) and (4.31) that CEM in the average t-matrix approximation makes it possible to reproduce characteristic asymmetry of optical bands for the J-aggregates. However, the band widths obtained in this approximation are significantly different from the results of exact numerical calculations.

More accurate results can be obtained by the coherent potential method [230, 232 – 235, 197, 198] (see also Ref. [66]). Let us find such $\Sigma(E)$ [see formula (4.25)] at which $G^0_{nm}\left[E - \Sigma(E) \right]$ best approximates the averaged Green function $\left\langle G_{nm}(E) \right\rangle$ of the aggregate. To accomplish this, $G^0_{nm}\left[E - \Sigma(E) \right]$ must make the average t-matrix $\langle t_n \rangle$ vanish, as follows from expression (4.22). Substitution of $G^0_{nn}\left[E - \Sigma(E) \right]$ into the definition of t-matrix (4.21) instead of $G^0_{nn}(E)$ and replacement of Δ_n by $\Delta_n - \Sigma(E)$ lead to the

equation for $\Sigma(E)$ in the coherent potential approximation [232, 235]. As a result, for aggregates with weak Gaussian disorder ($|\sigma/V| \ll 1$) one finds [197, 198]

$$\Sigma(E) = \sigma^2 G_{mn}^0\big[E - \Sigma(E)\big]. \tag{4.32}$$

Substituting expression (4.20) for the Green function of a one-dimensional ordered aggregate and taking into account that $\Sigma(E) \approx \Sigma(\hbar\Omega_0 + 2V)$ at weak disorder, the result for $\Sigma(\hbar\Omega_0 + 2V)$ is realized [198]. Substituting it into formula (4.27), we get the following expression for the absorption spectrum of one-dimensional aggregates:

$$I(\Omega) = 3^{1/2}2^{-5/3}\left|\frac{\sigma}{V}\right|^{4/3} \times \left\{\left[\frac{\hbar(\Omega-\Omega_0)}{V} - \left(2 - 2^{-5/3}\left|\frac{\sigma}{V}\right|^{4/3}\right)\right]^2 + \left[3^{1/2}2^{-5/3}\left|\frac{\sigma}{V}\right|^{4/3}\right]^2\right\}^{-1}. \tag{4.33}$$

Formula (4.33) describes a symmetric band having a Lorentz shape. However, it is known from direct numerical calculations that the low-frequency wing must be a Gaussian one (see Section 4.5). This discrepancy is due to the neglect of the Σ dependence on E in the approximation used that determines the Gaussian character of the low-frequency wing of the absorption band. At the same time, formula (4.33) adequately reproduces the dependence of the band half-width on the degree of disorder for one-dimensional aggregates: $w_N/|V| \propto (\sigma/|V|)^{4/3}$ [see Section 4.5.1, formula (4.34)], with its absolute value differing from the results of numerical calculations by less than 10–20% [198]. However, such agreement holds only for one-dimensional aggregates; for three-dimensional systems, both the character of the dependence and the absolute values of half-widths are significantly different [196]. It can be concluded that the coherent potential method, as well as other approximate analytical methods, is suitable even at weak disorder only for qualitative analysis of optical band shapes possessed by large molecular aggregates; quantitative analysis requires exact numerical calculations.

4.5 Numerical simulation of optical band shapes for aggregates

4.5.1 Calculation methods and main results. In a series of studies [201–203], optical properties were calculated for one-, two-, and three-dimensional aggregates with Gaussian diagonal disorder and interaction only between nearest neighbors. Absorption spectra were computed using expression (4.7), in which δ-functions were replaced by certain normalized functions $\Delta(x)$ with a small but finite width γ. Such replacement was necessary because otherwise numerical integration would produce a 'fence' of δ-functions instead of the continuous spectrum being sought. The respective integral was computed by the Monte Carlo method. Generation of normally distributed random energies $\varepsilon_1, \ldots, \varepsilon_N$ was followed by numerical diagonalization of Hamiltonian (4.4) to find the corresponding eigenenergies E_k and eigenfunctions ψ_k.

Calculations in Refs [201–203] were made for one-dimensional chains of 30 molecules, square lattices of 13×12 molecules, and simple cubic lattices of $10 \times 9 \times 8$ molecules. Resonance interactions between all nearest neighbors in two- and three-dimensional lattices were assumed to be identical. Absorption spectra [201], density of exciton states, and oscillator strength per state [202] were thus obtained for different values of the disorder parameter $\sigma/|V|$. These data were used to build up dependences of the absorption band half-width on the degree of disorder. The following relation was found in the studied interval of parameters ($0.25 \leqslant \sigma/|V| \leqslant 1$) for one-dimensional aggregates:

$$\frac{w_N}{|V|} \propto \left(\frac{\sigma}{|V|}\right)^{4/3}. \tag{4.34}$$

Comparison of formulas (4.34) and (4.14) indicates that the exciton coherence length must depend on the degree of disorder as $|\sigma/V|^{-2/3}$, in agreement with the results reported in Refs [236, 237]. For two- and three-dimensional aggregates, it was obtained that

$$\frac{w_N}{|V|} \propto \left(\frac{\sigma}{|V|}\right)^{2} \tag{4.35}$$

and

$$\frac{w_N}{|V|} \propto \left(\frac{\sigma}{|V|}\right)^{3}, \tag{4.36}$$

respectively. Note that in the first two cases, the character of the dependence coincides with that predicted by the perturbation theory in the coherent potential approximation [196–200] that gives

$$\frac{w_N}{|V|} \propto \left(\frac{\sigma}{|V|}\right)^{4/(4-l)}, \tag{4.37}$$

where l is the system's dimensionality. The authors of Ref. [201] ascribe the discrepancy for three-dimensional systems to the fact that the density of exciton states near the band edge tends to zero, which makes it more sensitive to disorder.

The optical properties of one-dimensional aggregates consisting of 100 and 250 molecules were calculated in Refs [68, 119] taking into account resonance interactions between all molecules of the aggregate. It was shown that consideration of long-range interactions does not lead to a substantial change in the absorption band shape. At the same time, the exciton coherence length increases more than two-fold compared with that in the nearest neighbor approximation. This effect was explained in Ref. [120]. Moreover, taking into account all intermolecular interactions leads to the loss of symmetry in the energy dependence of the exciton density of states.

A somewhat different method than that in Refs [68, 119, 201–203] was employed in works [128, 130]. Let us employ the representation of the absorption spectrum of a molecular aggregate in the form of the Hamiltonian (4.16) resolvent, where calculations will be made at a small but finite value of the parameter γ instead of $\gamma \to 0$. This is equivalent to the replacement of δ-functions in the integrand of formula (4.7) by Lorentz functions with a half-width γ. Let us rewrite formula (4.16) as follows:

$$I(\Omega) \propto \int\!\ldots\!\int \mathrm{d}\varepsilon_1 \ldots \mathrm{d}\varepsilon_N\, P(\varepsilon_1, \ldots, \varepsilon_N)\, \mathrm{Im}\,\big\langle S\,\big|X(\Omega; \varepsilon_1, \ldots, \varepsilon_N)\big\rangle, \tag{4.38}$$

where the vector $|X\rangle$ is the solution of a system of linear equations

$$(\hbar\Omega + i\gamma - H)\,|X\rangle = |S\rangle\,. \tag{4.39}$$

If only interactions between the nearest neighbors are taken into account, system (4.39) is reduced to the recurrent relation [128, 130]

$$VX_{n-1} + (\hbar\Omega - \varepsilon_n + i\gamma)X_n + VX_{n+1} = 1\,, \tag{4.40}$$

where X_n are the components of the vector $|X\rangle$. Then, formula (4.38) rewritten in terms of X_n acquires the form

$$I(\Omega) \propto \int \ldots \int d\varepsilon_1 \ldots d\varepsilon_N\, P(\varepsilon_1, \ldots, \varepsilon_N) \times \sum_n \operatorname{Im} X_n(\Omega; \varepsilon_1, \ldots, \varepsilon_N)\,. \tag{4.41}$$

Generating random energies $\varepsilon_1, \ldots, \varepsilon_N$ in accordance with the distribution $P(\varepsilon_1, \ldots, \varepsilon_N)$ and finding the solution to the recurrent dependence (4.40) at different values of frequency Ω, we obtain the desired absorption spectrum of the molecular aggregate. In doing so, the use of Eqns (4.39)–(4.41) permits avoiding the laborious procedure of numerical diagonalization of the Hamiltonian and thereby facilitates calculations for extremely large aggregates.

Recurrent dependence (4.40) was applied in Refs [128, 130] to calculate absorption bands of one-dimensional aggregates involving 10^6 [128] and 10^3 [130] molecules with Gaussian and binary disorders. The binary disorder is described by the distribution

$$P(\varepsilon) = \frac{1}{2}\,\delta\left(\varepsilon - \hbar\Omega_0 - \frac{a}{2}\right) + \frac{1}{2}\,\delta\left(\varepsilon - \hbar\Omega_0 + \frac{a}{2}\right) \tag{4.42}$$

and corresponds to the case of an aggregate containing two types of molecules with different transition energies [199, 200]. The band shape is determined here by substitution disorder, while band narrowing under the influence of molecular vibrations and inhomogeneous local environment is negligibly small. The calculated absorption spectra of aggregates with binary disorder for $a > 2|V|$ were shown to have several peaks. This testifies to the fact that the cluster effects play the main role in the present case [66]. Calculations made in the presence of Gaussian disorder for $N = 10^6$ [128] confirm the relation (4.34) for the band half-width derived earlier [201] for aggregates of 30 molecules.

4.5.2 Comparison of theoretical and experimental results. Comparison of the results of calculations made in the framework of CEM was reported in Refs [68, 204–207]. Figure 11 displays the recorded absorption spectrum of J-aggregates of pseudoisocyanine bromide from Ref. [68] and the calculated exciton spectrum of a one-dimensional chain of 250 molecules with Gaussian diagonal disorder, reported by the same authors. Despite the high noise level in the computed spectrum, it fairly well reproduces experimental spectra of J-aggregates. A similarly good agreement between experimental and theoretical spectra was obtained in Refs [204, 205], where the measured absorption bands of J-aggregated carbocyanine dyes were approximated by exciton spectra of molecular chains. The authors of Refs [204, 205] also considered aggregate size disorder, besides diagonal disorder.

Similar comparisons were undertaken for a two-dimensional case in Refs [206, 207] where CEM was used to calculate absorption and emission spectra of two-dimensional aggregates in cyanine dye monolayers. Square lattices of 28×28 and 38×38 molecules with Gaussian diagonal disorder served as the model structures. Similar to the one-dimensional case, exciton spectra calculated in Refs [206, 207] correctly reproduced characteristic features of experimental optical bands.

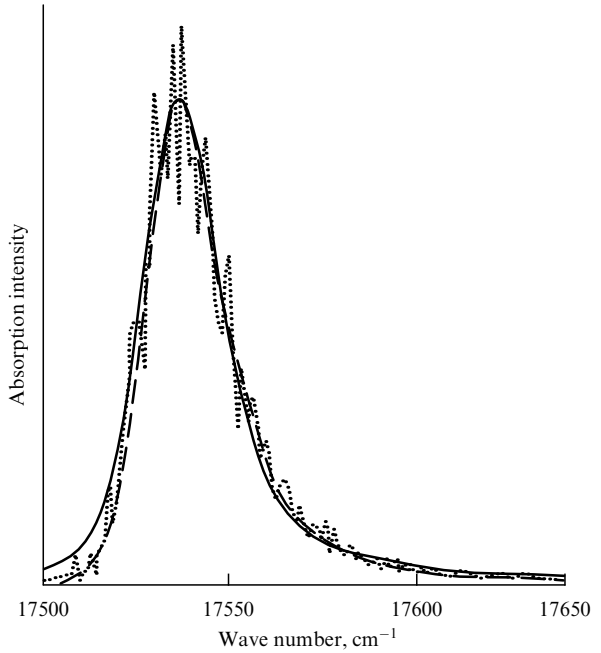

Figure 11. Absorption band of one-dimensional aggregates comprising $N = 250$ molecules with Gaussian diagonal disorder ($\sigma = 64\ \text{cm}^{-1}$) taking into account resonance interaction between all molecules in the aggregate ($V = -600\ \text{cm}^{-1}$). Points are numerical calculations from work [68]. Dashed line is the results of our numerical calculations [60, 61]. Solid line is the experimental absorption band of J-aggregates of pseudoisocyanine bromide [68].

4.5.3 Computation accuracy. It can be seen from Fig. 11 that the computed absorption spectrum [68] is characterized by a very high level of noise attributable to the extremely low efficiency of the calculation methods usually used in the literature. On the one hand, parameter γ determining the width of functions $\Delta(x)$ must be sufficiently small to enable these functions to adequately approximate δ-functions, for which they are substituted in formula (4.7). Moreover, this condition gives a large number of spectral points subject to calculation. On the other hand, integration by the Monte Carlo method requires that a sufficiently large number of Hamiltonian eigenvalues with random energies ε_n lie in the γ-vicinity of each Ω point. Diagonalization of a vast number of random Hamiltonians is needed to simultaneously meet these two conditions, which is sometimes difficult to realize even with the use of powerful modern computers. By way of example, this number was not large enough in Refs [68, 119]. The relatively smooth spectra obtained in Refs [128, 130, 201] compared with Refs [68, 119] was due to two factors. First, the authors of these works used the nearest neighbor approximation that markedly reduced the labor-intensiveness of numerical diagonalization [or computation of Hamiltonian resolvent using expression (4.38)] and thereby permitted the use of a greater number of random Hamiltonians. Second, parameter γ in studies [128, 130] was chosen to be an order of magnitude larger than in Refs [68, 119], which resulted in a

somewhat impaired accuracy of calculations. Hence the necessity of a more efficacious method to compute rather exact exciton spectra with a reasonable volume of calculations. Such a method was proposed in the works by Makhov, Egorov, Bagatur'yants, and Alfimov [60, 61, 63, 65] (hereinafter the MEBA method [15]). It may be used, for example, to determine the half-width of optical bands with an accuracy sufficient for the formerly impossible estimation of its dependence on the degree of disorder, as well as the size and the structure of aggregates (Section 5.4).

5. The exciton theory: high-performance analytical methods in band-shape numerical simulations

5.1 Gaussian diagonal disorder

As indicated in Section 4.2, the Gaussian distribution is most frequently used as a model probability distribution $P(\varepsilon_1, \ldots, \varepsilon_N)$ for the transition energies of molecules in calculating the optical bands of molecular aggregates in the framework of the exciton theory. For this reason, the discussion below (except Section 5.5) concerns aggregates with Gaussian disorder.

To begin with, there is a case in which transition energies of individual molecules are distributed independently of one another:

$$\langle \varepsilon_n \varepsilon_m \rangle = \sigma^2 \delta_{nm} . \tag{5.1}$$

Then, $P(\varepsilon_1, \ldots, \varepsilon_N)$ is given by formula (4.13).

The substance of the MEBA method [60, 61, 63, 65] in the simplest case is illustrated by the example of dimers [61]. Here, eigenenergies of Hamiltonian (4.4) and the corresponding transition dipole moments can be expressed explicitly. The change of variables in the expressions (4.7), (4.13) for the absorption band shape is analogous to the separation of the center-of-mass motion from the relative motion of molecules inside a dynamical system [60, 61]. Transition dipole moments are independent of the variable analogous to the center-of-mass motion (variable x), and transition energies entering the argument of δ-functions are linear in it. This makes it possible to analytically integrate the expression for the dimer band shape over variable x. In this way, the integration eliminates δ-functions from the integrand.

In the general case of aggregates containing N molecules, eigenenergies and the related transition dipole moments cannot be expressed explicitly. Hence the analogous change of variables directly in the aggregate Hamiltonian (4.4). It is convenient to apply the following linear orthogonal transformation [60, 61]:

$$\varepsilon'_k = \sum_{n=1}^{N} c_{nk} \varepsilon_n , \tag{5.2}$$

where

$$c_{nk} = \frac{1}{\sqrt{N}} \left[\sin\left(\frac{2\pi}{N} (n-1)(k-1) \right) + \cos\left(\frac{2\pi}{N} (n-1)(k-1) \right) \right] . \tag{5.3}$$

[15] As mentioned in Section 1, this method is known in the Western literature as the smoothing technique [67] or smoothening technique [30].

Here, $\varepsilon'_1/\sqrt{N}$ is the arithmetical mean of all energies ε_n. Thus, transformation (5.2), (5.3) distinguishes (with an accuracy of up to a constant) the average transition energy of all molecules in the aggregate as one of the new independent variables.

The transformation (5.2), (5.3) being orthogonal, the old variables are easy to express through new ones:

$$\varepsilon_n = \sum_{k=1}^{N} c_{kn} \varepsilon'_k . \tag{5.4}$$

By substituting relationship (5.4) into Eqn (4.4), we resolve the aggregate Hamiltonian into two components:

$$H = \frac{\varepsilon'_1}{\sqrt{N}} + H' , \tag{5.5}$$

where

$$H' = \sum_{n=1}^{N} |n\rangle \left(\sum_{k=2}^{N} c_{kn} \varepsilon'_k \right) \langle n| + \sum_{\substack{n,m \\ n \neq m}} |n\rangle V_{nm} \langle m| \tag{5.6}$$

is a reduced Hamiltonian dependent on quantities $\varepsilon'_2, \ldots, \varepsilon'_N$ alone. Thus, we separated fluctuations of the mean transition energy $\varepsilon'_1/\sqrt{N}$ from relative fluctuations in the transition energies in aggregated molecules [60, 61]. This procedure, as in the dimer case, is analogous to the usual separation of the center-of-mass motion from the relative motion inside a dynamical system. In short, we passed to a coordinate system with the fluctuating origin of the energy scale $\varepsilon'_1/\sqrt{N}$. Advantages of this system will be demonstrated below.

It is easy to see that

$$E_k = \frac{\varepsilon'_1}{\sqrt{N}} + E'_k \tag{5.7}$$

and

$$\psi_k = \psi'_k , \tag{5.8}$$

where E'_k and ψ'_k are the eigenenergies and eigenfunctions of the reduced Hamiltonian H'. At the same time, it follows from the orthogonality of transformation (5.2), (5.3) that

$$\sum_{n=1}^{N} \varepsilon_n^2 = \sum_{k=1}^{N} \varepsilon_k'^2 \tag{5.9}$$

and

$$\left| \det \| c_{nk} \| \right| = 1 . \tag{5.10}$$

As a result, after changing variables (5.2), (5.3) the integral (4.7), (4.13) transforms to

$$I(\Omega) \propto \int \ldots \int \mathrm{d}\varepsilon'_1 \ldots \mathrm{d}\varepsilon'_N \exp\left(-\frac{\varepsilon_2'^2 + \ldots + \varepsilon_N'^2}{2\sigma^2} \right) \times \sum_{k=1}^{N} \left| \langle S | \psi'_k(\varepsilon'_2, \ldots, \varepsilon'_N) \rangle \right|^2 \exp\left[-\frac{(\varepsilon'_1 - \hbar\Omega_0\sqrt{N})^2}{2\sigma^2} \right] \times \delta\left[\frac{\varepsilon'_1}{\sqrt{N}} + E'_k(\varepsilon'_2, \ldots, \varepsilon'_N) - \hbar\Omega \right] . \tag{5.11}$$

Because reduced Hamiltonian (5.6) does not depend on variable ε'_1, its eigenenergies E'_k and eigenfunctions ψ'_k are also ε'_1-independent. Hence the possibility of analytically integrating expression (5.11) over ε'_1. Such integration eliminates δ-functions from the integrand, as in the case of dimers; after it, the expression for the shape of the aggregate optical band takes the final form

$$I(\Omega) \propto \int \dots \int \mathrm{d}\varepsilon'_2 \dots \mathrm{d}\varepsilon'_N \exp\left(-\frac{\varepsilon'^2_2 + \dots + \varepsilon'^2_N}{2\sigma^2}\right) \times \sum_{k=1}^{N} \left|\left\langle S \left| \psi'_k(\varepsilon'_2, \dots, \varepsilon'_N) \right\rangle\right|^2 \times \exp\left\{-\frac{\left[E'_k(\varepsilon'_2, \dots, \varepsilon'_N) - \hbar(\Omega - \Omega_0)\right]^2}{2(\sigma/\sqrt{N})^2}\right\}. \quad (5.12)$$

Multidimensional integral (5.12) is computed by the Monte Carlo method. The values of E'_k and ψ'_k are found by numerical diagonalization of the reduced Hamiltonian (5.6), which does not require more computation time than diagonalization of the initial Hamiltonian (4.4). On the other hand, due to the absence of δ-functions in the integrand during calculations with the use of Eqn (5.12), daigonalization of each random Hamiltonian makes a contribution at all band frequencies at the same time, but not only in the small vicinities of its eigenvalues, as in the direct use of expressions (4.7), (4.13). A substantial enhancement of calculation efficiency is achieved in this way compared with the routine method.

The high calculation efficiency of the MEBA method is clearly demonstrated in Fig. 11 [60, 61] where the dashed line shows the spectrum computed with the use of expression (5.12) and the points reproduce results of similar calculations done in Ref. [68], where the authors applied the expressions (4.7), (4.13), having replaced δ-functions by high narrow rectangles. Evidently, the MEBA method provides an absolutely smooth spectrum, while the spectrum from Ref. [68] is characterized by a high noise level even though both were obtained by diagonalization of a similar number (500) of random Hamiltonians. In a word, the MEBA method substantially enhances the accuracy of calculations without increasing computer time.

5.2 Correlated Gaussian disorder

Let us consider now aggregates with Gaussian disorder in the presence of correlation between transition energies of individual molecules. For brevity, our consideration is limited to cyclic one-dimensional aggregates, although to equal advantage it can be generalized to linear molecular chains, and two- and three-dimensional systems [66].

The intermolecular correlation for one-dimensional cyclic aggregates is introduced in the following way [58, 61]:

$$\langle \varepsilon_n \varepsilon_m \rangle = \sigma^2 \frac{\beta^{N/2-|n-m|} + \beta^{-N/2+|n-m|}}{\beta^{N/2} + \beta^{-N/2}}. \quad (5.13)$$

The case of $\beta = 0$ corresponds to the absence of correlation [as $\beta \to 0$, expression (5.13) turns into (5.1)], and $\beta = 1$ to the complete correlation ($\langle \varepsilon_n \varepsilon_m \rangle = \sigma^2$) when all molecules in the aggregate possess identical transition energies. The following probability distribution for transition energies ensues from relation (5.13) in the case of correlated Gaussian disorder [58, 61]:

$$P(\varepsilon_1, \dots, \varepsilon_N) \propto \exp\left\{-\frac{1}{2\sigma^2}\left(\frac{1+\beta^N}{1-\beta^N}\right)\left(\frac{1-\beta}{1+\beta}\right) \times \sum_{n=1}^{N}\left[(\varepsilon_n - \hbar\Omega_0)^2 + \frac{\beta}{2(1-\beta)^2}\left((\varepsilon_n - \varepsilon_{n-1})^2 + (\varepsilon_n - \varepsilon_{n+1})^2\right)\right]\right\}, \quad (5.14)$$

where $\varepsilon_0 \equiv \varepsilon_N$, and $\varepsilon_{N+1} \equiv \varepsilon_1$.

As in the case of uncorrelated disorder, we shall make use of linear transformation (5.2), (5.3). This not only singles out the arithmetical mean of all transition energies ε_n in cyclic aggregates, but also diagonalizes the quadratic form in expression (5.14). As a result, the new variables ε'_k prove to be distributed independently of one another. The sole difference from the case of uncorrelated disorder consists in the fact that the probability distributions for different variables ε'_k have various widths σ'_k:

$$P(\varepsilon'_1, \dots, \varepsilon'_N) = \frac{1}{(\sqrt{2\pi}\sigma)^N} \exp\left[-\frac{(\varepsilon'_1 - \hbar\Omega_0\sqrt{N})^2}{2\sigma'^2_1} - \frac{\varepsilon'^2_2}{2\sigma'^2_2} - \dots - \frac{\varepsilon'^2_N}{2\sigma'^2_N}\right], \quad (5.15)$$

where

$$\sigma'_k = \sigma\left[\left(\frac{1+\beta^N}{1-\beta^N}\right)\left(\frac{1+\beta^2}{1-\beta^2}\right) \times \left(1 - \frac{2\beta}{1+\beta^2}\cos\frac{2\pi(k-1)}{N}\right)\right]^{-1/2}. \quad (5.16)$$

Analogously with what was done in Section 5.1, the substitution of variables (5.2), (5.3) and integration over ε'_1 give the following expression for the optical band shape of an aggregate with correlated Gaussian disorder [61]:

$$I(\Omega) \propto \int \dots \int \mathrm{d}\varepsilon'_2 \dots \mathrm{d}\varepsilon'_N \exp\left(-\frac{\varepsilon'^2_2}{2\sigma'^2_2} - \dots - \frac{\varepsilon'^2_N}{2\sigma'^2_N}\right) \times \sum_{k=1}^{N} \left|\left\langle S \left| \psi'_k(\varepsilon'_2, \dots, \varepsilon'_N) \right\rangle\right|^2 \times \exp\left\{-\frac{\left[E'_k(\varepsilon'_2, \dots, \varepsilon'_N) - \hbar(\Omega - \Omega_0)\right]^2}{2(\sigma'_1/\sqrt{N})^2}\right\} \quad (5.17)$$

[cf. expression (5.12)].

In the case of linear molecular chains or two- and three-dimensional aggregates, in contrast to cyclic aggregates, the transformation (5.2), (5.3) does not diagonalize the quadratic form in the corresponding expression for the probability distribution $P(\varepsilon_1, \dots, \varepsilon_N)$, and the new variables ε'_k remain correlated. This complicates the problem but does not pose fundamental difficulties for computation [61, 66].

5.3 On the computation method representing band shape through the Hamiltonian resolvent

Another frequently employed method, besides the calculation of optical bands of molecular aggregates based on numerical diagonalization of the Hamiltonian, relies on expressing the

absorption band shape through the Hamiltonian resolvent of the aggregate:

$$I(\Omega) \propto \int \dots \int \mathrm{d}\varepsilon_1 \dots \mathrm{d}\varepsilon_N P(\varepsilon_1, \dots, \varepsilon_N) \times \mathrm{Im} \left\langle S \left| (\hbar\Omega + \mathrm{i}\gamma - H)^{-1} \right| S \right\rangle, \quad (5.18)$$

where $\gamma \to 0$ [see formulas (4.16) and (4.38)]; in numerical calculations, parameter γ is given a certain small but finite value (Section 4.5.1). The integral (5.18) is computed by the Monte Carlo method, and quantities $\langle S|(\hbar\Omega + \mathrm{i}\gamma - H)^{-1}|S\rangle$ are found by solving the relevant systems of linear equations separately for each Ω value. As pointed out in Section 4.5.1, an advantage of this approach is the possibility of avoiding the laborious procedure of numerical Hamiltonian diagonalization. This advantage most prominently manifests itself in calculations of optical bands for extremely large aggregates because the computer time needed to numerically diagonalize the matrix rapidly increases with its dimension. Similar to applying the method based on numerical diagonalization of the Hamiltonian, the efficiency of calculations using expression (5.18) can be substantially increased by separating fluctuations of the average transition energy from relative fluctuations of the transition energies of aggregated molecules [63].

5.4 Calculated results

Presented in this section are the results of computation by the MEBA method in the case of Gaussian diagonal disorder (Sections 5.1 – 5.3); they are expounded in greater detail in Refs [61, 62, 64, 65]. Papers [61, 62, 64] report computed optical bands for one-dimensional aggregates of different sizes, and two-dimensional aggregates of 6×6 molecules with a brickwork structure at various values of structure parameters.

Reference [61] presents the dependences of the relative half-width $\tilde{w}_N \equiv w_N/|V|$ of the optical band on the degree of disorder $\tilde{\sigma} \equiv \sigma/|V|$ for one-dimensional aggregates with $N = 5$, 10, 20, 40, and 80. In parallel, the respective dependences for the exciton coherence (delocalization) length N_c were obtained from the ratio of the radiative lifetime of the excited monomer state to the exciton lifetime in the aggregate:

$$N_c = \left\langle \max_k \frac{|\mathbf{M}_{0k}|^2}{|\mathbf{M}|^2} \right\rangle = N \left\langle \max_k |\langle S|\psi_k\rangle|^2 \right\rangle \quad (5.19)$$

[see formula (4.5)]. For $\tilde{\sigma} > 10$, excitation is practically localized on a single molecule, and the aggregate absorption spectrum coincides with the spectrum of isolated molecules; in other words, the half-width $w_N = w_1 \propto \sigma$. A decrease in $\tilde{\sigma}$ results in delocalization of electron excitation. As long as the delocalization length N_c is smaller than the aggregate length N, the half-width of the optical band equals $\tilde{w}_N \propto \tilde{\sigma}^{4/3}$. In this region, aggregates with different numbers of molecules have a similar band half-width. As $\tilde{\sigma}$ further decreases, electron excitation becomes delocalized over the entire aggregate, and the dependence $\tilde{w}_N = \tilde{w}_N(\tilde{\sigma})$ moves to relationship (4.14) ($\tilde{w}_N = \tilde{w}_1/\sqrt{N} \propto \tilde{\sigma}$).

Calculations for two-dimensional aggregates of 6×6 molecules under free boundary conditions reveal the presence of satellite lines in the spectrum, besides the principal line [62, 64]. Under periodic boundary conditions, the absorption band consists of practically one principal line, meaning that the satellite lines result from the aggregate border effect essential for such small systems.

The dependence of the absorption band shift on the structure of a two-dimensional aggregate was calculated in Refs [62, 64]. In the framework of CEM, this dependence allows for the determination of parameter regions corresponding to J- and H-aggregates (Section 2.5).

The authors of Refs [61, 66] studied the dependence of relative band half-width w_N/w_1 and delocalization length N_c on the correlation parameter β at different degrees of disorder $\tilde{\sigma}$. For very small $\tilde{\sigma}$, the computed dependence $w_N = w_N(\beta)$ completely coincides with the result obtained in the perturbation theory [see formula (4.15)]. For large $\tilde{\sigma}$, when the strong inequality (4.9) is violated, the computed half-widths exceed the predictions of the perturbation theory.

Opinions differ as to the degree of disorder correlation in real molecular aggregates. It is stated in Refs [37, 238] based on research into nonlinear effects that the correlation length N_{cor} in J-aggregates of pseudoisocyanine is on the order of 100 molecules. Such a length corresponds to $\beta \cong \exp(-1/N_{cor}) \approx 0.99$. However, the aggregate absorption band at such the large β must be much wider and have a symmetric Gaussian shape, as in monomer spectra. Meanwhile, optical bands of J-aggregates exhibit a very small width and asymmetry as their characteristic features that are correctly reproduced in the calculated spectra at $\beta = 0$ (see Fig. 11). Malyshev et al. [239] thoroughly studied the linear optical properties of one-dimensional disordered systems as a function of the correlation length. They found that the absorption band width monotonically grows as $N_{cor}^{2/3}$ at small N_{cor} and becomes saturated when the correlation length N_{cor} is equal to the exciton delocalization length N_c. It was shown in Ref. [239] that the N_{cor} value experimentally obtained in Ref. [240] and amounting to a few hundred molecules for TDBC J-aggregates is at variance with $N_c \approx 40$ estimated in the same work. Thus, the degree of correlation between the transition energies of aggregated molecules remains to be clarified (see also Section 3.2.1).

5.5 On the computation method for aggregates with arbitrary diagonal disorder. Calculated results

The case of aggregates with Gaussian diagonal disorder is most often considered in the literature because deviations in transition energies due to both inhomogeneity of the local environment and small molecular vibrations obey exactly the Gaussian distribution (Section 4.2). Nevertheless, there are many cases in which the Gaussian disorder is inapplicable, in particular, when the probability distribution $P(\varepsilon_1, \dots, \varepsilon_N)$ for the transition energies of molecules in an aggregate has several maxima. Unlike the Gaussian distribution, the new integrand in the arbitrary distribution $P(\varepsilon_1, \dots, \varepsilon_N)$ obtained with the help of transformation (5.2), (5.3) and subsequent integration over ε_1' is a rather complicated function of $\varepsilon_2', \dots, \varepsilon_N'$ variables and the parameter Ω, whose numerical integration by the Monte Carlo method is very difficult to realize. To obviate this difficulty, Ref. [65] proposed a general computation method that has all the advantages of the approach described in Refs [60, 61, 63] (Sections 5.1 – 5.3) and can be effectively utilized not only in the case of Gaussian disorder but also at any continuous distribution of transition energies in aggregate molecules. It was shown with this method that any random energy distributed according to the same law as the molecular transition energy (diagonal disorder) may be chosen as a fluctuating origin of the energy

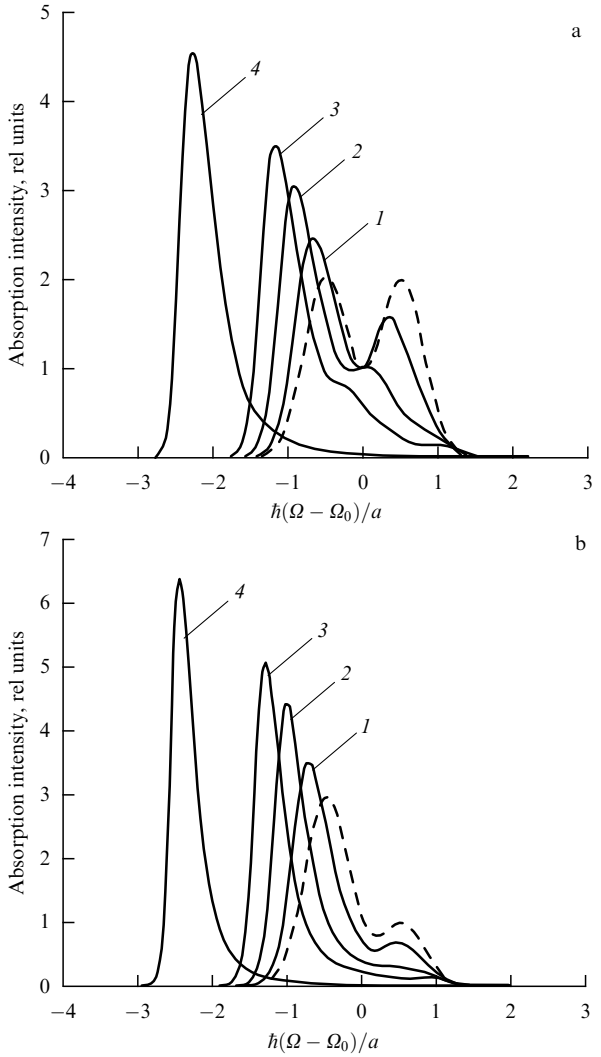

Figure 12. Absorption bands of one-dimensional aggregates of $N = 100$ molecules with bi-Gaussian diagonal disorder [see Eqn (5.20)] at the following parameter values: $\sigma/a = 0.3$; $V/a = -0.1$ (*1*), -0.25 (*2*), -0.4 (*3*), -1 (*4*); $b = 1/2$ (a), $3/4$ (b) [65]. Dashed lines display monomer bands ($V = 0$).

scale. In the specific case of Gaussian disorder, the general method [65, 66] is equivalent to the method used in Refs [60, 61] and expounded in Section 5.1. Moreover, it may be applied, as in paper [63] (Section 5.3), to the case in which the absorption band shape is presented through the Hamiltonian resolvent [65, 66].

Let us examine possibilities provided by the general MEBA method [65], when $P(\varepsilon_1, \varepsilon_2, \ldots, \varepsilon_N)$ is represented by the bi-Gaussian distribution

$$P(\varepsilon_1, \ldots, \varepsilon_N) = \frac{1}{\sigma^N (2\pi)^{N/2}} \times \prod_{n=1}^{N} \left[b \exp\left(-\frac{(\varepsilon_n - \hbar\Omega_0 + a/2)^2}{2\sigma^2} \right) + (1-b) \exp\left(-\frac{(\varepsilon_n - \hbar\Omega_0 - a/2)^2}{2\sigma^2} \right) \right], \quad a > 0, \quad 0 < b < 1. \tag{5.20}$$

Calculations were made for one-dimensional aggregates involving $N = 100$ molecules at $\sigma/a = 0.3$, $b = 1/2, 1/4, 3/4$ and $V/a = -0.1, -0.25, -0.4, -1, -10, -100$. Some of the results are shown in Fig. 12. In the case of $b = 1/2$ (Fig. 12a) corresponding to the symmetric spectrum of a monomer, inclusion of intermolecular interaction even at $V/a = -0.1$ leads to a noticeable asymmetry of the optical band whose left peak becomes higher than the right one. Asymmetry increases as intermolecular interaction becomes stronger. The right peak turns into a kink at $V/a = -0.4$ and disappears at $V/a = -1$, while the aggregate absorption spectrum looks like a single narrow line with Gaussian low-frequency and Lorentzian high-frequency wings, as in the case of Gaussian disorder. Similar band transformation takes place in the case of $b = 3/4$, corresponding to the monomer spectrum with high low-frequency and low high-frequency peaks (Fig. 12b), not infrequently observed in experiment.

6. Merits and demerits of the canonical exciton theory of the J-band

Advantages of the canonical exciton theory of the J-band include relative simplicity and the possibility of adequately reproducing experimental data (long-wave shift, small width, high intensity, and asymmetry of the J-band). Disadvantages are due either to those of CEM proper or to general physical disadvantages.

The former include the inability of CEM to reproduce the shape of optical bands for H-aggregates, whereas J- and H-bands are interpreted equivalently in the elementary model (Section 2.5). CEM gives equally intense narrow bands for H- and J-aggregates at the same exciton interaction value, in direct contrast to experiment [75, 78, 79, 121 – 124] yielding moderately intense broad bands for H-aggregates.[16]

On the other hand, nobody has tried to interpret the H-band in terms of a purely statistical exciton model. It could be described if CEM were supplemented by the consideration of exciton – phonon interaction leading to a considerable broadening of the H-band due to fast downward relaxation of the exciton. In the framework of this approach, Vitukhnovsky and co-workers [25] have recently adjusted the shape and the width of the H-band for a 'herring-bone' aggregate of dichloro-substituted thiacarbocyanine (THIATS).

Let us turn back to the drawbacks of the purely exciton model with quasistatic disorder. It is assumed in CEM that the disorder does not change as the Frenkel exciton moves along a molecular chain. However, some calculations and experimental data indicate that characteristic times of

[16] In the framework of CEM, the H-band is mirror-symmetric with the J-band relative to the midst of the exciton band. This observation follows from the selection rules for the elementary model and the fact that disorder removes exclusion for transitions to higher states of the exciton band for J-aggregates, and to lower states for H-aggregates. In the framework of the vibron model [47] (Section 3.2.1), the large width of the H-band in the case of weak exciton interaction is attributable to the strong band-shape asymmetry of molecules making up an H-aggregate — that is, to the wide short-wave wing of certain monomeric polymethine dyes, arising from high-frequency intramolecular vibrations. According to Scherer [47], exciton interactions in H-aggregates are responsible for the markedly enhanced intensity of the short-wave wing relative to the main band portion (see Figs 9, 10 where strong shape asymmetry of the monomer band is simulated by a single vibrational mode with a frequency of 1368 cm^{-1}). However, J-band effects are obscure in the case of weak exciton interaction (see Fig. 10). This implies that H-aggregates should display a weaker exciton interaction than J-aggregates. At the same time, their concrete structure suggests a much stronger exciton interaction than in J-aggregates (see Sections 16.1 and 16.2).

changes of disorder and exciton motion can be of the same order (see Section 3.2.1 and references cited therein). This puts in doubt the exciton exchange narrowing mechanism due to the 'quickly moving' Frenkel exciton [58] that averages static disorder. In this case, it is necessary to apply exciton models taking into account dynamic disorder (Anderson – Kubo disorder; see, for instance, Refs [138, 241]).[17] However, these models are too complicated and contain many fitting parameters. Under conditions in which the exciton exchange narrowing mechanism is *a priori* realizable, an important problem of the degree of disorder correlation between transition energies of aggregated molecules remains open. There is reason to think that it may be very high (Sections 3.2.1 and 5.4 and references cited therein). In such a case, the exciton exchange narrowing mechanism becomes inefficient, and the J-band is not narrow but is as wide as the optical band of a monomer (Section 4.3).

One disadvantage of the canonical exciton theory of the J-band, having a general physical sense, lies in the fact that it 'turns over' computation of the band shape for monomeric polymethine dyes (estimation of diagonal disorder) to quantum chemistry and molecular spectroscopy. However, it will be shown in the second part of this review (Sections 10, 11, 16.5, 16.6) dealing with charge transfer that the solution to this problem in the framework of modern quantum chemistry encounters serious difficulties. On the other hand, the canonical exciton theory of the J-band disregards the specific electronic structure of monomeric polymethine dyes. Consideration of this structure poses the problem of its ability to ensure strong enough resonance intermolecular (exciton) interaction used in CEM to account for the J-band effect. Anyway, it is clear that a theory of the optical band shape for J-aggregates is needed that could also explain the band shape of the constituent polymethine dye monomers. This issue will be discussed at greater length in Sections 7 and 8.

7. Elementary excitation dynamics of an extended electron system as an alternative to the exciton approach

Resonance intermolecular interactions in the statistical exciton theory must be sufficiently strong to ensure the effect of the narrow intense J-band. All characteristic features of the optical spectrum of monomer molecules in a J-aggregate tend to degrade with increasing interaction strength [65, 66] (see, for instance, curves *4* in Fig. 12). However, as shown in the discussion of the J-band problem (Section 1), it is natural to think of a new alternative approach having the opposite sense, in which a certain characteristic feature of the monomer spectrum further develops as a result of J-aggregation [69 – 73]. This feature is the most intense absorption band roughly in the midst of the polymethine series of one and the same dye [69 – 71], in which the polymethine chain length varies over a broad range (see Ref. [75] and Fig. 1). The new approach duly takes into consideration the specific structure of a polymethine dye monomer, viz. the extended distribution of π-electron density alternating along the quasilinear polymethine chain. Also, it attributes the most intense band in the polymethine series to weak electron-nuclear resonance arising at a 'mean' length of the polymethine chain in connection with peculiarities of quantum transition dynamics [69 – 73]. It will be shown in Section 13 that this resonance band intensifies as a result of the formation of J-aggregates, so as to transform into the J-band [71, 73]. Therefore, we think that the absorption band shape of J-aggregates should be interpreted with regard to the explanation of the band shape of their constituent monomers; the solution to the J-band problem lies beyond the statistical exciton theory [69 – 71].

At first sight, the employment of computational techniques of quantum chemistry instead of statistical methods may improve the exciton approach. However, the existing quantum-chemical methods disregard dynamic effects of the transient electron – phonon state, important for extended electron systems, as appears from the discrepancy between calculated and experimental results. This situation was exemplified in Refs [141 – 143] (Section 3.2.2).

Thus, the new approach implies the necessity of a unified theory encompassing the characteristic property of π-electron systems, i.e., its significant linear extension, for the description of optical band shapes of both J-aggregates and dye monomers [69 – 71, 73]. Hence, such a theory has nothing in common with the exciton theory [48 – 51]. In other words, consideration of exciton dynamics should be preceded by a study of the elementary excitation dynamics of an extended electron system that simulates a π-electron system and interacts with the surrounding medium in the case of a dye-monomer polymethine chain and in the case of a J-aggregate. This condition being fulfilled, further studies might be in order to elucidate the exciton dynamics that may be of importance, for example, in the formation of the H-band [69 – 71, 73] (Section 16.2).

8. The ideal polymethine state. Simulation of an optical transition by electron phototransfer

The main element of a chromophore in a polymethine dye is markedly extended π-electron charge density alternating along the polymethine chain (Fig. 13) and alternatively redistributed upon optical excitation [11]. Dähne [242] formulated the concept of the ideal polymethine state (IPS) as early as 1978 (see also Ref. [11]).

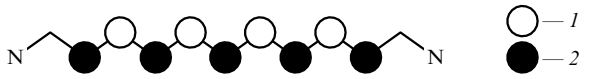

Figure 13. Ideal polymethine state [11, 242]. Charges are on carbon atoms of the polymethine chain in the ground state. Charge: *1* — positive, *2* — negative.

For the IPS, the distribution of π-electron density along the polymethine chain is maximally alternated, and π-bond orders are equalized in both ground and excited states. Optical excitation of the IPS is associated with maximum changes in π-electron density and minimal changes in π-bond orders [11]. Accordingly, we construct such a model of electronic structure for the IPS in which the distribution of the absolute charge value on carbon atoms is uniform along the polymethine chain both in the ground and excited states, with equal linear charge density corresponding to the equal reorganization energy of nuclei in the nearby environment in either state [69 – 71]. Then, the π-electron transition in the IPS may be described by the new theory of elementary electron

[17] Dynamic disorder is considered in Section 12.

charge transfer [70, 73], which is based in its present form on the assumption of equal reorganization energies in the initial and final states. This theory is briefly outlined in Section 10 and is discussed at length in Section 16.5. It was shown in experiment that dyes with an odd number of methine groups in the polymethine chain symmetrically flanked by nitrogen atoms are very close to the IPS [242]. It is easy to see that thiapolymethinecyanine (see Fig. 1) is one such dye.

Because π-electron charge density strongly alternates along the polymethine chain (see Fig. 13) and is alternatively distributed upon optical excitation, the wave functions of ground and excited states are strongly overlapped. This accounts for small tunnel effects in the extended π-electron system being excited. Note that this inference ensues from the sole fact that the properties of the main chromophore in polymethine dyes can be roughly estimated from H Kuhn's free electron model (see Section 3.1.1 and references cited therein). Thus, one has to neglect tunnel effects in the description of photoexcitation of an extended π-electron system in the theory of photoinduced electron transfer. Hence the necessity to ascribe a new physical sense to the extent L of electron transfer; namely, tunnel effects being neglected, quantity L is regarded as the extent of the π-electron system [69 – 71, 73].

In a word, complete charge transfer along the entire length of the polymethine chain is the sum of many acts of transfer of a relatively small number of charges over the small distance between neighboring carbon atoms. Therefore, tunnel effects are small. Thus, the problem of transfer of an alternating charge along the polymethine chain is reduced to that of electron transfer by formal substitution of the large number $\eta \leqslant 1$ for the Gamow tunnel factor [69 – 71, 73].

To conclude, the nature of optical transition in polymethine dyes is reduced to that of elementary electron transfer [69 – 71, 73].

9. The standard theory of elementary electron-charge-transfer processes: classical nuclear motion reorganizing environment. Transient state dynamics problem

In the standard Landau – Zener theory [243, 244], electron charge transfer is regarded either as nonadiabatic transition in the crossover region of adiabatic electron terms (i.e., nuclear potential energy surfaces) or as the motion of an 'electron + medium' system over the potential energy surface, during which electron movements are adiabatically adjusted to the nucleus displacements in the medium (Fig. 14) [245 – 248]. The probability of the nonadiabatic transition per unit time is given at high temperatures by the formula

$$W_{\mathrm{if}} = \frac{|V_{\mathrm{if}}|^2}{\hbar\sqrt{\lambda_{\mathrm{r}} k_{\mathrm{B}} T}} \exp\left[-\frac{(\Delta - \lambda_{\mathrm{r}})^2}{4\lambda_{\mathrm{r}} k_{\mathrm{B}} T}\right], \tag{9.1}$$

where V_{if} is the electronic matrix element of the interaction operator leading to the transition, λ_{r} is the environmental nuclear reorganization energy, and Δ is the thermal effect of the transition. For adiabatic transitions, one has

$$W_{\mathrm{if}} = \omega \exp\left[-\frac{(\Delta - \lambda_{\mathrm{r}})^2}{4\lambda_{\mathrm{r}} k_{\mathrm{B}} T}\right], \tag{9.2}$$

where ω is the vibrational frequency of the nuclei in the initial and final states (assumed here to be identical, for the sake of simplicity). Formulas (9.1) and (9.2) differ among each other only in preexponent, with

$$\frac{|V_{\mathrm{if}}|^2}{\hbar\sqrt{\lambda_{\mathrm{r}} k_{\mathrm{B}} T}} \ll \omega, \tag{9.3}$$

i.e., the probability of nonadiabatic transitions is significantly smaller than that of adiabatic ones. Formulas (9.1) and (9.2) are frequently referred to as Marcus formulas. However, they were obtained earlier in the theory of multiphonon processes (see review [76]): for optical transitions by Pekar [249, 250] (see also Ref. [251]), and for nonradiative transitions by Krivoglaz [252]. Formulas (9.1) and (9.2) were derived on the assumption that a classical particle ('reaction coordinate' [253], e.g., solvent polarization [248]) travels in the crossover region of electron terms with a constant velocity [243, 244].

Zusman [254] suggested a variant of the Landau – Zener theory taking into account medium viscosity; in this case, the motion of the reaction coordinate has the form of a random walk. As a result, the reaction coordinate spends much more time in the crossover region of electron terms than in the Landau – Zener model. The transition rate is limited by medium relaxation rather than by the electron transition proper. Thus, nonadiabatic transition in the Landau – Zener model may become adiabatic in the Zusman model. Worthy of note is the voluminous literature on the theory of elementary electron-charge-transfer processes (e.g., Refs [69 – 73, 117, 245 – 248, 253 – 294]), the review of which is beyond the scope of the present communication.

The Landau – Zener picture of transitions is still poorly substantiated even if it looks plausible.[18] It follows from the Born – Oppenheimer theory [110] that potential energy surfaces are dynamic invariants only for initial and final states but not for the transient one (see, for instance, Ref. [77]). Hence the importance and topicality of searching for dynamic invariants for the transient state.

These invariants were found in Ref. [71] (see also Ref. [72]). Moreover, the author of Refs [70, 73] elaborated a strict quantum-mechanical theory of elementary charge transfer that properly takes into account transient state dynamics. Also, the aforementioned standard Landau – Zener theory proved to be its certain limiting case [69 – 73] (Sections 10.3 and 11.2).

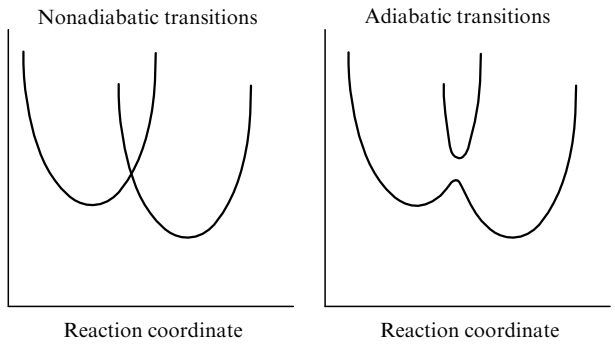

Figure 14. Landau – Zener picture of elementary electron charge transfer processes [243 – 248].

[18] The Landau – Zener problem [243, 244] has remained the focus of attention for more than 70 years. Some details related to this problem are expounded in recent publications by Dufey [295] (see also Ref. [73]) and Di Giacomo and Nikitin [296].

As stated above, the standard theory suggests a notion of a classical particle (reaction coordinate) related to the assumption of classical nuclear motion reorganizing environment [248]. Our theory [70, 73] considers the general case of nuclear reorganization motion — that is, quantum reorganization of nuclei at which their motion is inseparable from the electron one. Therefore, the limiting passage from our theory [70, 73] to the standard one [248] may be regarded as the passage from the quantum description of nuclear reorganization to its quasiclassical description.

Thus, the problem of description of transient state dynamics is the problem of theoretical consideration of the effects of the relationship between electron and nuclear movements. In other words, it is the problem of the search for an alternative to the Born–Oppenheimer adiabatic approximation having the opposite effect (it separates the electron motion from the nuclear one). Such an alternative is the solution to the problem based on the Green function method.

10. The microscopic theory of photoinduced electron transfer

10.1 Consideration of the quantum character of nuclear reorganization

Compared with the Hamiltonian in the theory of multiphonon transitions (see Ref. [76]), the Hamiltonian in the theory of elementary electron transfer [70, 73] is complicated only by an additional electron potential well $V_2(\mathbf{r}-\mathbf{L})$ spaced from the initial well $V_1(\mathbf{r})$ by distance $L \equiv |\mathbf{L}|$:

$$H = -\frac{\hbar^2}{2m}\,\Delta_{\mathrm{r}} + V_1(\mathbf{r}) + V_2(\mathbf{r}-\mathbf{L}) + \sum_{\kappa} V_{\kappa}(\mathbf{r})q_{\kappa} + \frac{1}{2}\sum_{\kappa}\hbar\omega_{\kappa}\left(q_{\kappa}^2 - \frac{\partial^2}{\partial q_{\kappa}^2}\right), \tag{10.1}$$

where $\mathbf{r}$ is the electron's radius vector, q_{κ} are the real normal phonon coordinates, ω_{κ} are the eigenfrequencies of normal vibrations, and κ is the phonon index; the term $\sum_{\kappa} V_{\kappa}(\mathbf{r})q_{\kappa}$ ensues from electron–phonon interaction.

Our purpose being to find 'good' dynamic invariants for the transient state [71, 72], which would be alternative to the Born–Oppenheimer adiabatic invariants (potential energy surfaces), we are seeking the solution of the Schrödinger equation

$$H\Psi = E_H\Psi \tag{10.2}$$

for an 'electron + surrounding medium' system by the Green function method. In the beginning, identical transformations of the Schrödinger equation (10.2) in this method may be regarded as alternatives to the identical transformations for distinguishing the nonadiabaticity operator in the Born–Oppenheimer method. The former are needed to maximally conserve the relationship between electronic and nuclear motions, while the latter are used to separate slow nuclear motion from fast electron motion.

The solution of Eqn (10.2) is written down as [70, 73]

$$\Psi_1 = G_H\tilde{V}\Psi_1^{\mathrm{BO}}, \tag{10.3}$$

where

$$G_H = G + G\tilde{V}G + G\tilde{V}G\tilde{V}G + \ldots \tag{10.4}$$

is the Green function of Hamiltonian (10.1), and G is the Green function of the Hamiltonian $H-\tilde{V}$:

$$G(\mathbf{r},\mathbf{r}';q,q';E_H+\tilde{V}) = \sum_s \frac{\Psi_s(\mathbf{r},q)\Psi_s^*(\mathbf{r}',q')}{E_H+\tilde{V}-E_s-\mathrm{i}\gamma} \tag{10.5}$$

(spectral representation), with

$$\tilde{V} \equiv \sum_{\kappa} V_{\kappa}(\mathbf{r})(q_{\kappa}-\tilde{q}_{\kappa}), \tag{10.6}$$

where $\tilde{q}_{\kappa}$ are the shifts of normal phonon coordinates corresponding to the shifts of nuclear equilibrium positions in the medium, which are caused by the presence of an electron on donor 1 or acceptor 2. Superscript BO in formula (10.3) and hereafter indicates that the given quantity is taken in the adiabatic Born–Oppenheimer approximation.

The infinitesimal imaginary addition $\mathrm{i}\gamma$ is usually introduced when the Green function is written down in the spectral representation [see formula (10.5)] to avoid zero in the denominator [here, at $\tilde{V}(q=\tilde{q})=0$, see formula (10.6)]. Contrary to this, we regard quantity γ as having a finite value, which gives it the physical sense of a measure of chaos in environmental nuclear reorganization caused by electron movement from the donor to the acceptor. We call quantity γ the dissipation energy.[19] In other words, the dissipation energy γ characterizing the measure of chaos in the transient-state nuclear motion is introduced in the theory of elementary electron transfer, in addition to the nuclear reorganization energy $E_{\mathrm{r}} \equiv \sum_{\kappa}\hbar\omega_{\kappa}\tilde{q}_{\kappa}^2$. The introduction of the dissipation energy γ helps to avoid singularity in probabilities of extended transitions (electron transfer) related to the incommensurability of masses of the electron and its environmental nuclei in the surrounding medium. Physically, it means introduction in the transient state of a mechanism that first transforms part of the nuclear vibrational motion into translational motion and then the resulting translational motion back into the vibrational one. Because chaos in the electron-nuclear motion develops only in the transient state and is absent in the initial and final states, it is called *dozy chaos*; then, the corresponding dissipation energy γ is the *dozy chaos energy*.

The proposed introduction of the finite γ value performs one more important function, in addition to damping singular electron-nuclear motion; it allows introducing the small parameter into the theory [70, 73]:

$$\tilde{V}G \sim \frac{\tilde{V}}{\gamma} \sim \frac{\hbar\omega_{\kappa}}{\gamma} \ll 1. \tag{10.7}$$

Hence it follows that

$$G \gg G\tilde{V}G \gg G\tilde{V}G\tilde{V}G \gg \ldots,$$

and according to Eqn (10.4) we arrive at

$$G_H \approx G. \tag{10.8}$$

We thus obtain the solution, in accordance with formula (10.3), that describes the electron transfer state

$$\Psi_1 \approx G\tilde{V}\Psi_1^{\mathrm{BO}}, \tag{10.9}$$

where $G = G(E_H = E_H^{\mathrm{BO}}; \mathrm{i}\gamma, \gamma \gg \hbar\omega_{\kappa})$.

[19] Quantity γ usually defines the rule for detouring singular points in contour integration. But in our charge transfer theory [70, 73], a certain mathematical method [272, 297] is used for the exact summation over intermediate states related to γ. This procedure 'relieves γ from previous obligations' and allows it to achieve a new status.

It is clear from Eqn (10.7) that smallness in the transition amplitude

$$A_{12} = \left\langle \Psi_2(\mathbf{r}-\mathbf{L},q)\middle| V \middle|\Psi_1(\mathbf{r},q)\right\rangle \tag{10.10}$$

can be avoided if the system's wave function for an electron localized on acceptor 2 should be taken not in the form (10.9) but in the adiabatic approximation:[20] $\Psi_2 = \Psi_2^{\mathrm{BO}}$.

On the strength of Eqn (10.7), the series for the transition probability, corresponding to series (10.4) for the Green function G_H, has a small parameter $(\bar{n}_1\hbar\omega_\kappa/\gamma)^2 \ll 1$, where $\bar{n}_1$ is the Planck distribution function.[21] Hence, the small parameter of the problem for $k_\mathrm{B}T > \hbar\omega_\kappa/2$ is given by

$$\left(\frac{k_\mathrm{B}T}{\gamma}\right)^2 \ll 1\,. \tag{10.11}$$

Acting further in compliance with the rules of quantum mechanics (in the framework of the 'Fermi golden rule') and using the method described in Refs [272, 297] that generalizes the generating polynomial method of Krivoglaz and Pekar [251, 252] in the theory of multiphonon transitions [76], we arrive at the general expression for the probability of electron phototransfer (for optical absorption K) [70, 73]. Calculations in Refs [70, 73] are simplified by applying the Fermi zero-range approximation [298, 299] for electron potential wells.

10.2 Analytical result for optical absorption

Based on the general expression for optical absorption K and applying exact methods of the theory of functions of complex variables in the framework of the Einstein nuclear vibration model, we obtained an analytical result fully expressed in elementary functions [69, 70, 73]:

$$K = K_0 \exp W\,, \tag{10.12}$$

$$W = \frac{1}{2}\ln\left(\frac{\omega\tau\sinh\beta_T}{4\pi\cosh t}\right) - \frac{2}{\omega\tau}\left(\coth\beta_T - \frac{\cosh t}{\sinh\beta_T}\right) + (\beta_T - t)\,\frac{1}{\omega\tau\Theta} - \frac{\sinh\beta_T}{4\omega\tau\Theta^2\cosh t}\,, \tag{10.13}$$

$$1 \ll \frac{1}{\omega\tau\Theta} \leqslant \frac{2\cosh t}{\omega\tau\sinh\beta_T}\,, \tag{10.14}$$

where $\beta_T \equiv \hbar\omega/2k_\mathrm{B}T$, and

$$t = \frac{\omega\tau_\mathrm{e}}{\theta}\left[\frac{AC+BD}{A^2+B^2} + \frac{2\Theta(\Theta-1)}{(\Theta-1)^2+(\Theta/\theta_0)^2} + \frac{\theta_0^2}{\theta_0^2+1}\right], \tag{10.15}$$

$$|\theta_0| \gg \frac{E_\mathrm{r}}{2J_1}\,, \tag{10.16}$$

$$\theta \equiv \frac{\tau_\mathrm{e}}{\tau} = \frac{LE_\mathrm{r}}{\hbar\sqrt{2J_1/m}}\,, \qquad \Theta \equiv \frac{\tau'}{\tau} = \frac{E_\mathrm{r}}{\Delta}\,, \qquad \theta_0 \equiv \frac{\tau_0}{\tau} = \frac{E_\mathrm{r}}{\gamma}\,, \tag{10.17}$$

$$\tau_\mathrm{e} = \frac{L}{\sqrt{2J_1/m}}\,, \qquad \tau = \frac{\hbar}{E_\mathrm{r}}\,, \qquad \tau' = \frac{\hbar}{\Delta}\,, \qquad \tau_0 = \frac{\hbar}{\gamma}\,, \tag{10.18}$$

where, in turn, the following notation is used:

$$A = \cos\left(\frac{\theta}{\theta_0}\right) + \Lambda + \left(\frac{1}{\theta_0}\right)^2\mathcal{N}\,, \qquad B = \sin\left(\frac{\theta}{\theta_0}\right) + \frac{1}{\theta_0}\,\mathcal{M}\,, \tag{10.19}$$

$$C = \theta\left[\cos\left(\frac{\theta}{\theta_0}\right) - \frac{1-\xi^2}{2\theta_0}\sin\left(\frac{\theta}{\theta_0}\right)\right] + \mathcal{M}\,, \tag{10.20}$$

$$D = \theta\left[\sin\left(\frac{\theta}{\theta_0}\right) + \frac{1-\xi^2}{2\theta_0}\cos\left(\frac{\theta}{\theta_0}\right)\right] - \frac{2}{\theta_0}\,\mathcal{N}, \tag{10.21}$$

$$\xi \equiv \left(1 - \frac{E_\mathrm{r}}{J_1}\right)^{1/2} \qquad (J_1 > E_\mathrm{r} \text{ by definition})\,, \tag{10.22}$$

and where, finally:

$$\Lambda = -(\Theta-1)^2\mathcal{E} + \left[\frac{(\Theta-1)\theta}{\rho} + \Theta(\Theta-2)\right]\mathcal{E}^{(1-\rho)/(1-\xi)}\,, \tag{10.23}$$

$$\mathcal{M} = 2\Theta(\Theta-1)\mathcal{E} - \left[\frac{(2\Theta-1)\theta}{\rho} + 2\Theta(\Theta-1)\right]\mathcal{E}^{(1-\rho)/(1-\xi)}\,, \tag{10.24}$$

$$\mathcal{N} = \Theta\left[\Theta\mathcal{E} - \left(\frac{\theta}{\rho} + \Theta\right)\mathcal{E}^{(1-\rho)/(1-\xi)}\right], \tag{10.25}$$

$$\mathcal{E} \equiv \exp\left(\frac{2\theta}{1+\xi}\right), \qquad \rho \equiv \sqrt{\xi^2 + \frac{1-\xi^2}{\Theta}}\,. \tag{10.26}$$

Factor K_0 has the form

$$K_0 = K_0^\mathrm{e}K_0^\mathrm{p}\,, \tag{10.27}$$

where

$$K_0^\mathrm{e} = \frac{2\tau^3 J_1}{m}\,\frac{(A^2+B^2)\,\rho^3\Theta^4\xi}{\theta^2\left[(\Theta-1)^2 + (\Theta/\theta_0)^2\right]^2\left[1+(1/\theta_0)^2\right]} \times \exp\left(-\frac{4\theta}{1-\xi^2}\right) \tag{10.28}$$

and

$$K_0^\mathrm{p} = \frac{1}{\omega\tau}\left[1 + \frac{\sinh(\beta_T - 2t)}{\sinh\beta_T}\right]^2 + \frac{\cosh(\beta_T - 2t)}{\sinh\beta_T}\,. \tag{10.29}$$

In formulas (10.71) and (10.18), J_1 is the electron binding energy in the initial state 1, Δ is the thermal effect related to heat absorption (or heat release) in elementary electron transfer processes, and γ is the dissipation energy or dozy chaos energy (Section 10.1). The energy $\hbar\Omega$ of the absorbed photon and thermal effect Δ are related by the law of conservation of energy:

$$\hbar\Omega = J_1 - J_2 + \Delta\,, \tag{10.30}$$

where J_2 is the electron binding energy in the final state.

Quantity $K = K(\Theta,\theta_0)$ and the corresponding optical extinction

$$\varepsilon = \frac{4\pi^2 q^2 N_\mathrm{A}\Omega}{3\hbar c n_\mathrm{ref}}\,K \tag{10.31}$$

(q is the amount of electron charge transferred in an extended multiphonon transition, c and n_ref are the speed of light in vacuum and the refractive index, respectively, and N_A is the

[20] Perturbation V in formula (10.10) is taken in the usual long-wave approximation (see, for instance, Ref. [89]).

[21] Factor $\bar{n}_1$ appears due to taking into consideration the equilibrium population distribution for n_1 initial phonon states.

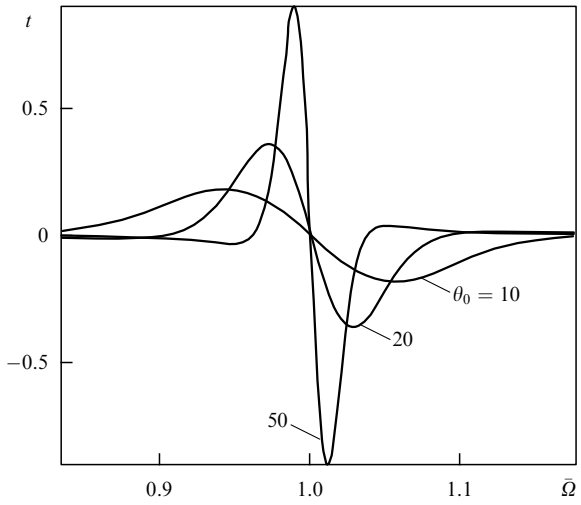

Figure 15. The electrodynamics of extended multiphonon transitions in the vicinity of the singular point ($\bar{\Omega} = 1, \theta_0 = \infty$) is illustrated by the behavior of function $t = t(\bar{\Omega}, \theta_0)$ [70]. Here, it is formally assumed for simplicity that $J_2 - J_1 = 0$; then, $\Theta^{-1} = \hbar\Omega/E_r \equiv \bar{\Omega}$. The following parameters of the 'electron + environment' system are used: $J_1 = 5$ eV, $E_r = 1$ eV, $m = m_e$, $\omega = 5 \times 10^{13}$ s^{-1}, and $L = L^* \approx 0.44$ nm (transferon resonance, Section 11.2).

Avogadro constant) have singularity at point ($\Theta = 1$, $\theta_0 = \infty$) or ($\Delta = E_r$, $\gamma = 0$). The character of this singularity is determined by singularities of functions $t = t(\Theta, \theta_0)$ and $K_0^e = K_0^e(\Theta, \theta_0)$. The singularity in function $K_0^e = K_0^e(\Theta, \theta_0)$ is removable:

$$\frac{K_0^e(\Theta = 1, \theta_0 \to \infty)}{2\tau^3 J_1/m} = \frac{\xi}{\theta^2}\left[\exp\left(\frac{2\theta}{1+\xi}\right) - \frac{\theta^2}{2} - \theta - 1\right]^2 \times \exp\left(-\frac{4\theta}{1-\xi^2}\right). \quad (10.32)$$

In function $t = t(\Theta, \theta_0)$ [see Eqn (10.15)], the singularity at point ($\Theta = 1, \theta_0 = \infty$) is unremovable. The behavior of function $t = t(\Theta, \theta_0)$ in the vicinity of point ($\bar{\Omega} \equiv \Theta^{-1} = 1$, $\theta_0 = \infty$) is illustrated in Fig. 15. It should be noted that the result (10.12)–(10.29) is invariant with respect to a change in the sign of γ. This invariance is in line with the physical fact that both virtual processes of conversion of electron motion (energy) into nuclear reorganization motion (energy) and the inverse processes occur in the intermediate state of the 'electron + environment' system [73]. For certainty, in Fig. 15 and hereinafter, we put $\gamma > 0$.

When the dissipation energy γ exceeds the nuclear reorganization energy E_r, the complex expression for the dynamic quantity t may be represented in a simple form [70, 73, 272]:

$$t = \omega\tau_e, \quad (10.33)$$

where τ_e is given by one of the formulas (10.18). This simple case was applied to the theoretical treatment of electron transfer in Langmuir–Blodgett films [73, 286, 300] and Brönsted relations [73, 277, 301–303] for proton transfer reactions.

10.3 Passage to the standard result

The limiting passage from expressions (10.12)–(10.29) for optical absorption K to the standard result in the theory of multiphonon transitions [76] could be realized by directing the dissipation energy (dozy chaos energy) γ either to zero or to infinity. However, in the former case, K is infinite, in the latter it vanishes. The physical sense of $K(\gamma \to 0) \to \infty$ in the absence of adiabatic approximation is related to the incommensurability of masses of the electron and its environmental nuclei in the surrounding medium (Section 10.1). The physical sense of $K(\gamma \to \infty) \to 0$ (Section 11.2, Fig. 17) is dictated by the impossibility of electronic quantum transition coupled to nuclear reorganization at absolutely chaotic (random) movements of nuclei in the transient state (i.e., at infinite 'friction' in the electron-nuclear system). For all that, it is possible to get rid of γ in expressions (10.12)–(10.29) and obtain the standard result by directing γ to infinity in the expression for t [$t \to 0$; see Fig. 15, where $\theta_0 = E_r/\gamma$ in compliance with Eqn (10.17)] and to zero in K_0^e [see Eqn (10.32)]. Hence, we obtain a formula of the (9.1) or (9.2) type for optical absorption K (for $k_B T > \hbar\omega/2$) [70]:

$$K = \frac{a^2\hbar}{\sqrt{4\pi\lambda_r k_B T}} \exp\left(-\frac{2L}{a}\right) \exp\left[-\frac{(\Delta - \lambda_r)^2}{4\lambda_r k_B T}\right], \quad (10.34)$$

where $a \equiv \hbar/\sqrt{2mJ_1}$, $\lambda_r \equiv 2E_r$.

This brings us to the end exposition of the formal theory of elementary charge transfer and opens the way to the treatment of its results at the qualitative physical level.

11. The physics of elementary charge transfer

11.1 The simplest example: a potential box with a movable wall

The example of a potential box with a movable wall is presented in the well-known book by Dogonadze and Kuznetsov [248] to explain the adiabatic approximation and the conditions under which nonadiabatic transitions of a quantum particle occur.

Let the right wall of the box undergo harmonic vibrations with frequency ω:

$$L = L_0 + L_1 \sin\omega t, \qquad L_1 < L_0$$

(Fig. 16). At small ω, a particle adjusts itself adiabatically to the slowly changing box size L without affecting the

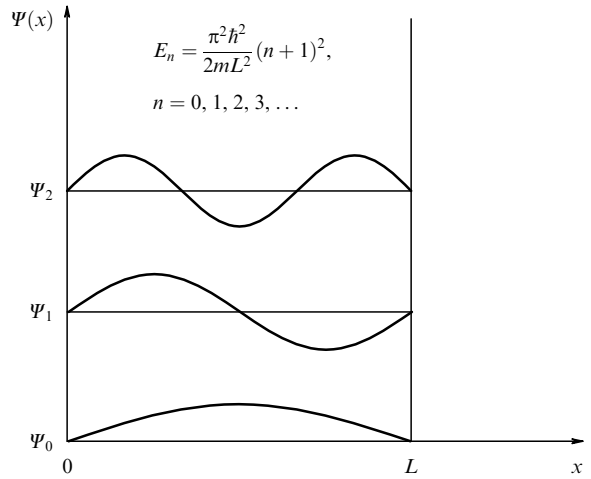

Figure 16. Potential box with a movable wall: the simplest illustration of the physics of extended electron-vibrational transitions [73].

quantum number n. The adiabaticity criterion is a smallness of $\hbar\omega$ with respect to the energy level spacing $\Delta E = E_1 - E_0$ in the box:

$$\hbar\omega \ll \Delta E\,.$$

At a sufficiently high frequency of wall vibrations and

$$\hbar\omega \cong \Delta E\,,$$

the particle undergoes nonadiabatic transition. This is a gedanken experiment by Dogonadze and Kuznetsov. We shall draw two more conclusions from the case of the potential box with a movable wall.

First, there is one important aspect of nonadiabatic transition that will be needed in the discussion below. Namely, the nonadiabatic transition corresponds to resonance $\hbar\omega = \Delta E$. In other words, resonance can be interpreted as an alternative to the adiabatic approximation.

Second, the potential box with a movable wall exposes characteristic features of elementary electron transfer. Let us consider the thought experiment with the potential box in a different respect. Suppose that the wall is fastened to the abscissa axis by a freely movable joint and can move under certain friction or without friction against the axis. Such a wall simulates environmental nuclear reorganization in the electron transfer problem [73], where dissipation energy γ plays the role of friction.

Let us first consider the case of nonzero friction. Let an electron pass from the ground state to the first excited state under the effect of light. The charge in the excited state concentrates close to the box walls (see Fig. 16). This produces pressure that causes the wall to move and thereby enlarges the box width. The energy level E_1 lowers, which increases the probability of electron transition. This situation simulates electron transition in the case of dissipation: $\gamma \neq 0$.

Our example with a potential box also includes singularity [73] discussed in Section 10. Indeed, if the wall moves without friction, its shift upon electron transition to an excited state is infinitely fast, the growth of the box size is unrestricted, and the energy level E_1 lowers infinitely fast till it merges with E_0; this situation corresponds to the infinitely large electron transition probability. This is the model of electron transition in the case of $\gamma = 0$. Note that the case of rather small $\gamma \neq 0$ in our thought experiment refers to the J-band: intense optical transition is accompanied by its shift to the long-wave region.

This rough model having been discussed, we return to the problem of transient state dynamics. Two circumstances need to be recalled. First, transient state dynamics is a problem of the search for an alternative to the adiabatic approximation (Section 9). Second, it was concluded from the example of a potential box that resonance may be regarded as an alternative to the adiabatic approximation. This means that the solution to the problem of transient state dynamics should be sought in the search for a certain resonance or, generally speaking, certain resonances. On the other hand, consideration of any simple problem in quantum mechanics at the qualitative level is underlain by the Heisenberg uncertainty relation. These two observations will be applied in Section 11.2 to the electron transfer problem. In other words, we shall find these resonances and establish their connection with the uncertainty relation [71 – 73].

11.2 Dynamic pumping of electron transfer by dissipative reorganization of the environment. Dynamic resonance-invariants for a transient state: the transferon and dissipon

The five principal parameters of the problem, viz. electron mass m, electron – donor binding energy $J_1 \equiv J$, distance between the donor and the acceptor L, environmental reorganization energy E_r, and dissipation (dozy chaos) energy γ, may be combined into three quantities:

$$\tau_e = \frac{L}{\sqrt{2J/m}}\,, \qquad \tau = \frac{\hbar}{E_r}\,, \quad \text{and} \quad \tau_0 = \frac{\hbar}{\gamma} \tag{11.1}$$

having a time dimension [cf. (10.18)] and representing two physically meaningful resonances [71 – 73]:

$$(2\tau_e)^{-1} = \tau^{-1} \quad \text{and} \quad (2\tau_e)^{-1} = \tau_0^{-1}\,. \tag{11.2}$$

The former resonance is between the extended electron motion and the ordered constituent of the environmental nuclear reorganization motion. The latter is between the electron motion and, conversely, the chaotic constituent of nuclear reorganization. These resonances can be regarded as the simplest dynamic invariants for the transient state (TS). Dynamic resonance-invariants are alternative to the Born – Oppenheimer adiabatic invariants (potential energy surfaces). In other words, these two resonances are the simplest manifestation of the relationship between electron and nuclear movements in the TS.

It follows from the above discussion and Refs [71 – 73] that resonances (11.2) are connected with the Heisenberg uncertainty relation

$$\Delta p \Delta x = \frac{\hbar}{2}\,. \tag{11.3}$$

We shall first consider the resonance $(2\tau_e)^{-1} = \tau^{-1}$. It can be written as the uncertainty relation (11.3) assuming that

$$\Delta p = \frac{E_r}{\sqrt{2J/m}} \quad \text{and} \quad \Delta x = L\,. \tag{11.4}$$

The equality $\Delta p \Delta x = \hbar/2$ is known to belong to the Gaussian wave packet of width Δx, describing a free-moving quantum particle. Therefore, this quantum particle may be regarded in terms of elementary electron transfer as a free electron – phonon quasiparticle with the momentum

$$p_0 \approx \Delta p = \frac{E_r}{\sqrt{2J/m}}\,. \tag{11.5}$$

In paper [71], this quasiparticle is referred to as a transferon (see also Refs [72, 73]). Thus, in the case of resonance between the extended electron motion and the ordered nuclear reorganization motion in the medium, the electron transfer may be interpreted as the motion of a transferon being created as the electron becomes detached from the donor and annihilating upon its attachment to the acceptor.

The same line of reasoning also applies to the second resonance in formula (11.2), i.e., $(2\tau_e)^{-1} = \tau_0^{-1}$, which originates from the former one when the nuclear reorganization energy E_r is replaced by the dissipation (dozy chaos) energy γ. The corresponding quasiparticle is called a dissipon [71 – 73].

It is easy to estimate the masses of both transferon (tr) and dissipon (dis), their mean free time between the donor and the acceptor, and wave packet broadening $\Delta x'/\Delta x$:

$$m_{\rm tr} \approx \frac{E_{\rm r}}{2J}\, m \ll m \quad \text{and} \quad m_{\rm dis} \approx \frac{\gamma}{2J}\, m \ll m\,, \tag{11.6}$$

$$\tau_{\rm tr} = \frac{L}{\sqrt{2J/m}} = \frac{\hbar}{2E_{\rm r}} \quad \text{and} \quad \tau_{\rm dis} = \frac{L}{\sqrt{2J/m}} = \frac{\hbar}{2\gamma}\,, \tag{11.7}$$

$$\frac{\Delta x'}{\Delta x} \approx 2\,. \tag{11.8}$$

The mean free time between the donor and the acceptor (11.7) is supplemented by the time of transferon or dissipon formation at the donor. This parameter is related to the dynamics of quasiparticle birth and life in the donor-bound state before transition to the free one. It may also be called the dynamic pumping time of a quasiparticle. In other words, dynamic pumping time of a quasiparticle is the time needed for the transient state to form in these two simplest cases of transient state dynamics. These times for the transferon ($E_{\rm r} \gg \gamma$) and dissipon ($\gamma \gg E_{\rm r}$) are as follows [71–73]:

$$\tau_{\rm tr}^{\rm p} = \frac{\hbar}{2\gamma} \quad \text{and} \quad \tau_{\rm dis}^{\rm p} = \frac{\hbar}{2E_{\rm r}}\,. \tag{11.9}$$

Clearly, the dynamic pumping time is much greater than the mean free time:

$$\tau_{\rm tr}^{\rm p} \gg \tau_{\rm tr} \quad \text{and} \quad \tau_{\rm dis}^{\rm p} \gg \tau_{\rm dis}\,. \tag{11.10}$$

Thus, the simplest case of elementary electron transfer may be interpreted as transferon or dissipon transfer [71–73]. The picture of electron transfer viewed as dissipon transfer is complementary to that of transferon transportation. This complementarity is due to the fact that environmental nuclear reorganization dynamics possesses two constituent components, namely, ordered and chaotic nuclear motions. Such duality of transient state dynamics in the elementary electron transfer theory is analogous with the corpuscular-wave dualism in quantum mechanics; it is one more form of expression of the Bohr principle of complementarity [304]. In other words, both corpuscular and wave motions are intrinsic properties of a quantum particle. Similarly, ordered and disordered movements are inherent properties of environmental nuclear reorganization dynamics.

The transferon corresponds to the quantum nuclear reorganization motion in the medium when the de Broglie wavelength for dissipation energy γ is much greater than for nuclear reorganization energy $E_{\rm r}$ [73, 304]:

$$\hat{\lambda}_\gamma \gg \hat{\lambda}_{E_{\rm r}} > L\,, \tag{11.11}$$

where

$$\hat{\lambda}_\gamma = \frac{\hbar}{p_\gamma}\,, \qquad p_\gamma \equiv \frac{\gamma}{\sqrt{2J/m}}\,,$$

and

$$\hat{\lambda}_{E_{\rm r}} = \frac{\hbar}{p_{E_{\rm r}}}\,, \qquad p_{E_{\rm r}} \equiv \frac{E_{\rm r}}{\sqrt{2J/m}}\,.$$

The dissipon answers to the quasiclassical nuclear reorganization motion when the de Broglie wavelength for dissipation energy γ is much smaller than for nuclear reorganization energy $E_{\rm r}$ [73, 304]:

$$\hat{\lambda}_\gamma \ll L < \hat{\lambda}_{E_{\rm r}}\,. \tag{11.12}$$

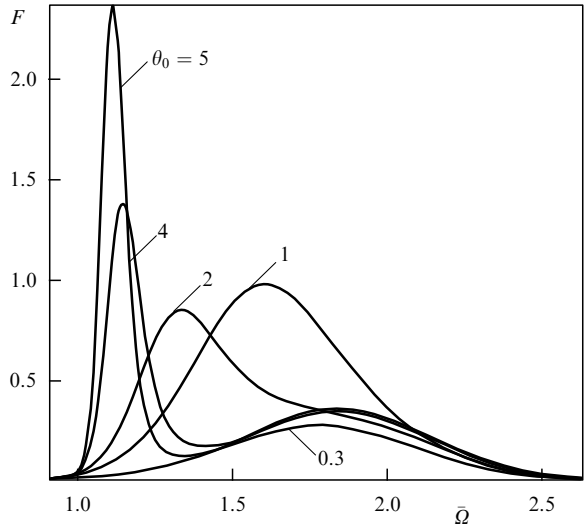

Figure 17. Variation of the absorption band shape $F = F(\bar{\Omega})$ ($F \equiv K \times 10^6/(2\tau^3 J_1/m)$) with changing dissipation energy γ (with the change in $\theta_0 \equiv E_{\rm r}/\gamma$) in transferon resonance $\sqrt{J_1/2m}/L = E_{\rm r}/\hbar$ [see Eqns (11.1), (11.2)] [70–72]. It is formally assumed that $J_2 - J_1 = 0$; the frequency $\bar{\Omega} \equiv \hbar\Omega/E_{\rm r}$. System parameters are as follows: $J_1 = 5$ eV, $E_{\rm r} = 1$ eV, $m = m_{\rm e}$, $\omega = 5 \times 10^{13}$ s^{-1}, and $T = 300$ K.

It should be emphasized that the transferon is actually a new quasiparticle [71–73] that has no analog in the former theories of elementary electron transfer. Conversely, the complementary dissipon is analogous to a classical particle [71–73] or 'reaction coordinate' [253] (e.g., solvent polarization [248]) appearing in the theories [247, 248, 254] of the Landau–Zener type [243, 244].

Figure 17 shows different shapes of optical absorption bands corresponding to the transferon and dissipon [71–73]. Curves with a peak ($\theta_0 = 5, 4$) represent the transferon, and those in the form of the Gauss function ($\theta_0 = 1, 0.3$) correspond to the dissipon.[22] The transferon peak degrades as parameter θ_0 decreases (and γ increases) and is absorbed by the Gauss-like wing of the band. The result is the same as ensues from the standard Landau–Zener picture of adiabatic ($\theta_0 = 1$) and nonadiabatic ($\theta_0 = 0.3$) transitions (Sections 9 and 10.3).

The transferon is depicted by a narrow optical band, and the dissipon by a broad one [71–73]. Strictly speaking, the dissipon is a certain broad resonance rather than (narrow) resonance proper [73].

To conclude this section, it was demonstrated, following Refs [71–73], that the dynamics of non-Landau–Zener elementary electron transfer processes may be described by the Heisenberg uncertainty relation. This brings us to a new concept of dynamic organization of elementary processes

[22] Strictly speaking, the intermediate case of $\theta_0 = 1$ may refer either to the dissipon or the transferon. The case of $\theta_0 = 0.3$ refers to the finite, but not free, dissipon motion since it meets the uncertainty relation in the form of inequality $\Delta p_\gamma \Delta x = \hbar/0.6 > \hbar/2$, where $\Delta p_\gamma = \gamma/\sqrt{2J/m}$. See Refs [71–73] for a more detailed transferon–dissipon picture of elementary charge transfer.

[305], the physical basis of which is that the transient state is spontaneously pumped by dissipative reorganization of the environment.

12. Anderson – Kubo motional narrowing and transferon resonance: the similarity and the difference

In the framework of the Anderson – Kubo statistical theory [90 – 94], the optical absorption band shape is given by the following infinite fraction [94, 306]:

$$F_{\rm st}(\Omega) = \frac{1}{\pi}\,{\rm Re}\left(i\Omega + \frac{\Delta_{\rm st}}{i\Omega + \Gamma_{\rm cor} + 2\Delta_{\rm st}/(i\Omega + 2\Gamma_{\rm cor} + \ldots)}\right)^{-1}, \tag{12.1}$$

where $\Delta_{\rm st}$ is the root-mean-square deviation of electron transition frequencies attributed in paper [94] to statistical fluctuations due to environmental motion; in other words, $\Delta_{\rm st}$ is the amplitude of statistical fluctuations, and $\Gamma_{\rm cor}$ is the inverse correlation time between statistical fluctuation amplitudes or the modulation rate of random amplitudes. Figure 18 displays optical band shapes computed by formula (12.1). In the limit of slow modulation

$$\frac{\Gamma_{\rm cor}}{\Delta_{\rm st}} \equiv \alpha_{\rm AK} \ll 1 \tag{12.2}$$

(static disorder), the band has a Gaussian shape that reflects the distribution of random amplitudes themselves. In the limit of fast modulation

$$\alpha_{\rm AK} \gg 1 \tag{12.3}$$

(dynamic disorder), the Gaussian band shape turns into the Lorentzian one with a width of $\Delta_{\rm st}^2/\Gamma_{\rm cor}$. Optical band narrowing frequently referred to as Anderson – Kubo motional narrowing [138, 241] occurs between these two limiting cases with increasing modulation rate. This effect is explained by the fact that each realization of a random process for smaller correlation times between statistical environmental fluctuation amplitudes is more efficiently averaged over the dipole phase evolution associated with electron transition in a molecule [138, 241].

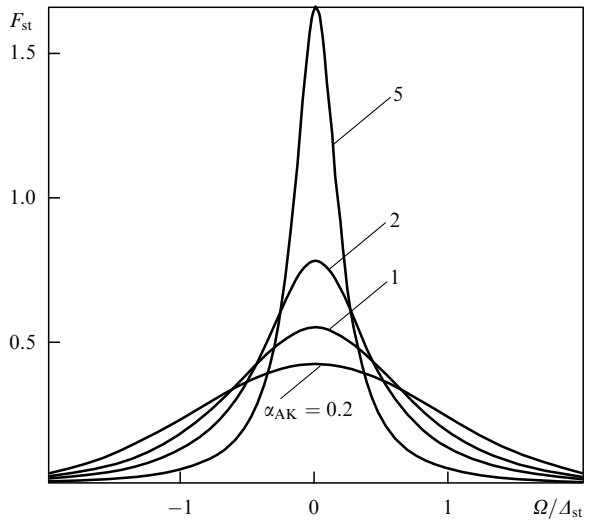

Figure 18. Motional narrowing in terms of the Anderson – Kubo statistical theory [90 – 94] [see formulas (12.1) – (12.3)].

The Anderson – Kubo theory is a phenomenological theory [138] disregarding the optical electron response to the environmental motion [94], whereas our theory [70, 73] is a microscopic theory in which the optical electron motion is by definition self-consistent with the environmental motion. This explains the lack of exact correspondence between the parameters of the two theories. Nevertheless, data on optical band narrowing in the Anderson – Kubo theory (see Fig. 18) and in our theory (see Fig. 17) may be compared by formally setting $E_{\rm r} \equiv J_1^2/\hbar\Delta_{\rm st}$ and $\gamma \equiv J_1^2/\hbar\Gamma_{\rm cor}$, and taking $J_1 \cong E_{\rm r} \cong \hbar\Delta_{\rm st}$ [73]. In this case, our parameter $\theta_0 \equiv E_{\rm r}/\gamma$ corresponds to $\alpha_{\rm AK} \equiv \Gamma_{\rm cor}/\Delta_{\rm st}$ from the Anderson – Kubo theory (i.e., $\theta_0 \equiv \alpha_{\rm AK}$); then, one and the same quantity is plotted on the abscissa in Figs 17 and 18. Comparison of these figures indicates that in the static disorder limit ($\theta_0 \equiv \alpha_{\rm AK} \ll 1$) our curve for dissipon resonance and the Anderson – Kubo curve have a similar shape close to the Gaussian curve [73]. Conversely, in the dynamic disorder limit ($\theta_0 \equiv \alpha_{\rm AK} \gg 1$), our transferon resonance in the form of a narrow low-frequency peak with an adjoining broad high-frequency band is substantially different from the Lorentzian curve in the Anderson – Kubo theory [73]. It may be concluded that our optical band narrowing as the parameter $\theta_0 \equiv \alpha_{\rm AK}$ increases reflects the formation of an intense narrow (transferon) peak against the background of a wide band, which is shifted to the low-frequency region, whereas the Anderson – Kubo theory gives only symmetrical narrowing of the increasingly intense band. Also, in our case, the optical band barely extends beyond the absorption frequency range $\Omega > 0$ (see Fig. 17), whereas in the Anderson – Kubo theory half of the band lies in the frequency range $\Omega < 0$ (see Fig. 18).[23]

13. Examples of applying the new charge-transfer theory to the explanation of fundamental experimental data

13.1 Inconsistency of applying the standard electron-transfer theory to charge transfer in a polymethine dye chromophore

The problem of alternating charge transfer (see Fig. 13) along the main chromophore of a polymethine dye (polymethine chain) is reduced to that of elementary electron transfer by the formal substitution of the large number $\eta \leqslant 1$ for the Gamow tunnel factor [69 – 71, 73] (Section 8).

Let us consider the most intense optical absorption band in the known Brooker series (Fig. 1) corresponding to the polymethine chain length $L = 1.4$ nm. The band is first treated based on the result of the standard electron transfer theory (10.34), (10.30). The band half-width

$$w_{1/2} = 2\sqrt{2\ln 2}\,\sqrt{2\lambda_{\rm r} k_{\rm B} T} \approx 0.09 \text{ eV}$$

($T = 300$ K) is used to estimate the Marcus energy $\lambda_{\rm r} \equiv 2E_{\rm r}$ of environmental nuclear reorganization. The result is $\lambda_{\rm r} \approx 0.03$ eV. The standard theory gives the Gaussian function for the band shape. Therefore, it does not explain the explicitly asymmetric band shape observed in experiment.

[23] For simplicity, we formally assume in Figs 18 and 17 the energy gap $J_2 - J_1 \equiv 0$ between excited and ground states.

It was supposed that the explanation could be deduced from the new theory (see Section 10) on the assumption that the most intense band in the Brooker series corresponds to transferon resonance [see relations (11.2), the first resonance]. Equations (11.2) give $\lambda_r \approx 0.63$ eV [see Eqn (11.1), where $L = 1.4$ nm and $J \cong 5$ eV]. Thus, this reorganization energy is 21 times (!) that in the standard theory [71, 73].

The gross underestimation of nuclear reorganization energy in the standard approach is due to the fact that it is based on the Franck–Condon principle that treats electron transitions as instantaneous. For this reason, the application of the standard theory to such an extended system as a polymethine dye leads to some local, but not total, environmental nuclear reorganization energy [71, 73].

13.2 Nature of the shape of a polymethine dye optical band: the charge transfer effect with regard for the quantum character of environmental nuclear reorganization. Explaining the experimental data of Brooker and co-workers

Figure 19 presents the results of fitting [71, 73] our theoretical extinction (10.12)–(10.31) [with the substitution of $\eta \leqslant 1$ for the Gamow factor $\exp\left(-4\theta/(1-\xi^2)\right) \equiv \exp\left(-2L/a\right)$ in formula (10.28)] to Brooker's experimental data (see Fig. 1). The fitting was realized in terms of the maximum position, maximum intensity, and band half-width. The theoretical band shape proved very similar to the experimental one.

The appropriate choice of numerical values of system parameters in the theoretical expression was possible because the assumption made in Section 13.1 proved justified; indeed, the most intense band in the Brooker series corresponds to transferon resonance. It allows the nuclear reorganization energy of the environment (methanol) to be estimated from the polymethine chain length [71, 73].

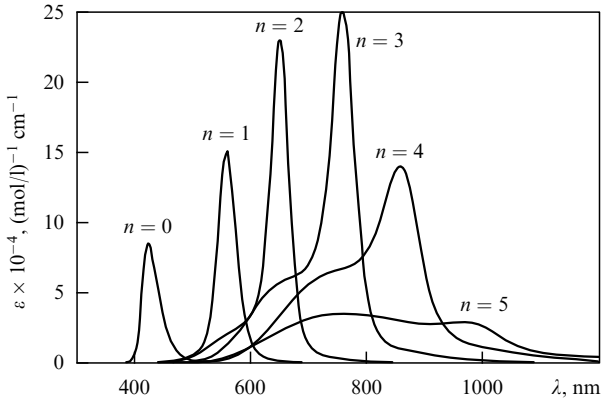

Figure 19. Theoretical dependence of optical absorption ($\lambda = 2\pi c/\Omega n_{ref}$) of an ideal polymethine dye (thiapolymethinecyanine) [71] on the polymethine chain length $2(n+2)d$, where d are certain roughly equal bond lengths in the chain. Absorption bands are computed by formulas (10.12)–(10.31) with $\eta \leqslant 1$ instead of the Gamow exponent $\exp(-4\theta/(1-\xi^2))$ when fitting them to experimental data of Brooker and co-workers (see Fig. 1) in terms of wavelength λ_{max}, extinction ε_{max}, and half-width $w_{1/2}$ with a high degree of accuracy. The following parameters of the 'dye + environment' system were used: $q = e$, where e is the electron charge, $m = m_e$, $\omega = 5 \times 10^{13}$ s^{-1}, $d = 0.14$ nm, $n_{ref} = 1.33$; for $n = 0, 1, 2, 3, 4, 5$ one has $J_1 = (5.63, 5.40, 4.25, 3.90, 3.74, 3.40)$ eV, $J_1 - J_2 = (1.71, 1.31, 1.11, 0.90, 0.74, 0.40)$ eV, $E_r = (0.245, 0.248, 0.256, 0.275, 0.297, 0.496)$ eV, and $\gamma = (0.402, 0.205, 0.139, 0.120, 0.129, 0.131)$ eV, respectively; for $n = 0, 1, 2, 3$ factor $\eta = 1$, and for $n = 4, 5$ factor $\eta = 0.55, 0.1$, respectively; $T = 298$ K.

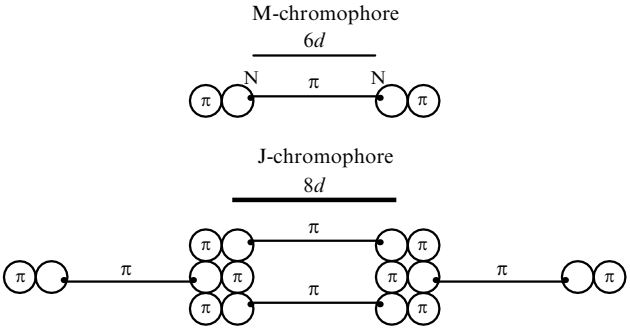

Figure 20. A polymethine dye molecule and its brickwork-structured J-aggregate [75, 79, 96]. Dye chromophore lengthening is a result of J-aggregation through $\pi-\pi$ electron interaction between the heterocyclic rings, where d is a certain unitary bond length in each chromophore [69, 70].

The successful explanation of Brooker's experimental data based on our theoretical expressions (10.12)–(10.31) for the band shape is attributable to the fact that the new charge-transfer theory [70, 73] in which this expression was derived takes account of the quantum character of environmental nuclear reorganization.

13.3 Nature of the J-band: transferon resonance effect. Explanation of Herz's experimental data

Similar to the most intense band in the Brooker series, the narrow intense J-band is also explained by transferon resonance [69–71, 73]. The J-band, the main subject of interest in this review, appears during aggregation of polymethine dyes. It is thought that aggregating monomers cannot reach the transferon state because their polymethine chain length L is not sufficiently large. In the Brooker series (see Figs 1, 19), the band corresponding to a monomer lies left of the most intense band. The length of a monomeric π-electron chromophore in a J-aggregate increases due to its coupling with the π-electron system of benzene rings of the neighboring molecules. It brings the chromophore to transferon resonance, as shown schematically in Fig. 20. Coupling of the π-electron systems of benzene rings to the π-electron system of monomer polymethine chain alters the spatial structure of the π-system from one- to two-dimensional, and thereby markedly enhances its interaction with the environment. As a result, the transferon state arising from J-aggregation proves much more 'powerful' than the state resulting from simple polymethine chain lengthening in the Brooker series [69–71, 73].

Figure 2 shows Herz's known experimental data on the concentration dependence of optical absorption by benzimidacarbocyanine in water. It can be seen that the monomer band loses intensity with increasing dye concentration and eventually disappears; instead, a narrow intense J-band appears in the long-wave region of the spectrum. Herz band intensity is a measure of monomer and aggregate concentrations. Herz believes that only one type of aggregates is formed; otherwise, experimental absorption spectra could not be analyzed. Figure 2b depicts concentrations of the dye in monomeric and aggregated forms. They can be used to calculate the number of molecules in a J-aggregate based on the law of mass action. Herz estimated it as four.

Figure 21 presents the results of analysis of Herz's experimental data in the framework of the new charge-

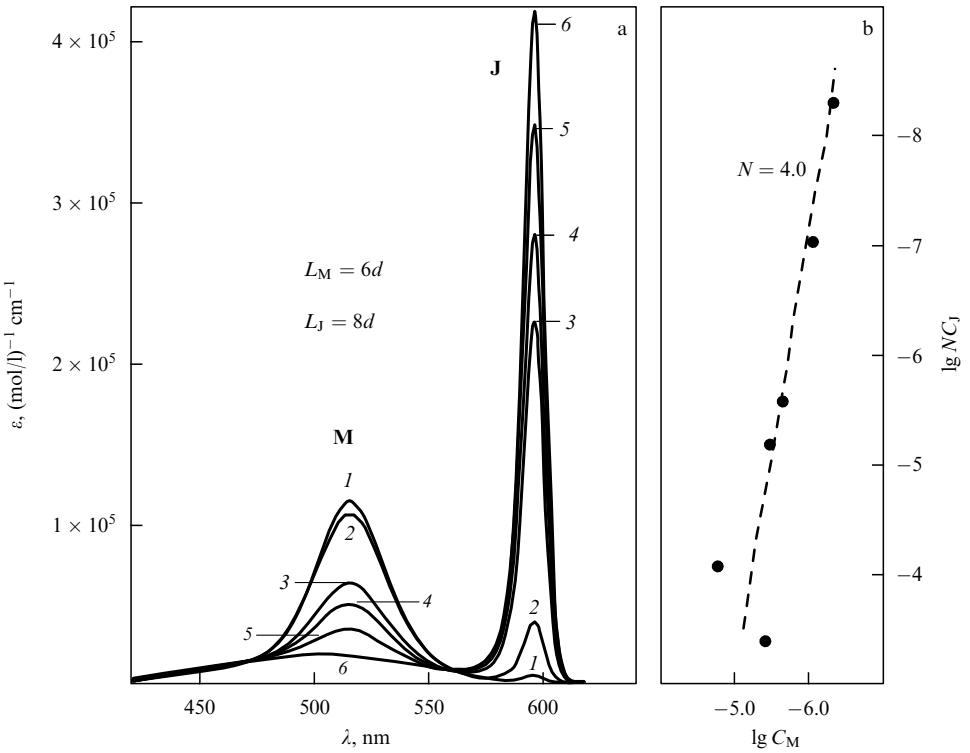

Figure 21. Theoretical dye-concentration dependence of optical absorption by benzimidacarbocyanine at 25 °C [69, 70]. (a) Absorption bands of monomer (M) and J-aggregate (J) calculated by formulas (10.12)–(10.31) with $\eta = 1$ instead of the Gamow exponent $\exp(-4\theta/(1-\xi^2))$ in a high-accuracy fitting of Herz's experimental data (see Fig. 2) in terms of wavelength λ_{max}, extinction ε_{max}, and half-width $w_{1/2}$, when 1% (*1*) and 99% (*6*) of the dye is converted into the J-state, respectively. The intermediate relative concentrations of the dye are: 9% (*2*), 53% (*3*), 66% (*4*), and 82% (*5*). (b) Molar concentrations of the dye in the monomeric (C_M) and aggregated (C_J) forms are derived from absolute concentrations reported by Herz (see the caption to Fig. 2) and relative concentrations obtained by our fitting. They give the number of molecules N in a J-aggregate. The following parameters of 'J-aggregate + environment' and 'monomer + environment' systems were used in the fitting: $m_J = 0.86m_e$ and $m_M = 0.97m_e$, $\omega = 5 \times 10^{13}$ s^{-1}, $d = 0.14$ nm, $n_{ref} = 1.33$; $J_{1J} = J_{1M} = 5$ eV, $J_{1J} - J_{2J} = 1.11$ eV, and $J_{1M} - J_{2M} = 1.37$ eV, $E_{r,J} = 0.420$ eV and $E_{r,M} = 0.315$ eV, $\gamma_J = 0.067$ eV and $\gamma_M = 0.231$ eV; the total charges transferred along chromophores $L_J = 8d$ and $L_M = 6d$ of J-aggregate and monomer are $q_J \cong \sqrt{2\varepsilon_d L_J E_{r,J}} \approx 1.28e$ and $q_M \cong \sqrt{2\varepsilon_d L_M E_{r,M}} \approx 0.96e$, where permittivity $\varepsilon_d = 2.5$ [96] (contribution from σ-electrons and the solvent).

transfer theory [69, 70, 73]. Absorption bands of the monomer and the J-aggregate were calculated by the formulas for optical extinction (10.12)–(10.31) [with the replacement of the Gamow factor $\exp(-4\theta/(1-\xi^2)) \equiv \exp(-2L/a)$ in formula (10.28) by the number $\eta = 1$]. Similar to Herz, we found out that the J-aggregate is composed of 4 molecules. However, our analysis of experimental data obtained at high concentrations of the dye reveals their lower accuracy than reported by Herz. The discrepancy is due to instability of J-aggregates with respect to the formation of colloid particles [69–71, 73].

14. Prediction of new effects

14.1 High-intensity narrow absorption bands for small-extent electron–phonon transitions

In the preceding text, we presented a theoretical interpretation of the two transferon peaks [69–71, 73] observed by Brooker and co-workers and by Herz. Evidently, Herz's transferon peak is much narrower and more intense than Brooker's one (cf. Figs 21 and 19). Let us try to elucidate the origin of this discrepancy [71, 73]. To this end, we shall compare the numerical parameters of either system responsible for dissipative nuclear reorganization dynamics in the nearby environment. In other words, we should compare dissipation (γ_J) and reorganization ($E_{r,J}$) energies in the experiments by Herz and Brooker and co-workers ($n = 3$).

It turns out that the 'Herz gamma' is twice as small as the 'Brooker gamma': $\gamma_J/\gamma = 0.067$ eV$/0.120$ eV ≈ 0.56. This finding is due to the fact that electron-nuclear interaction in the Herz transferon state is 1.5 times stronger than in the Brooker transferon state. It is easy to see from the comparison of reorganization energies: $E_{r,J}/E_r = 0.420$ eV$/0.275$ eV ≈ 1.53. The stronger interaction decreases the chaoticity of environmental nuclear reorganization during charge transfer along a chromophore. Thus, the dissipation energy γ falls as the reorganization energy E_r increases. This means that our theory [70, 73] admits the possibility of more intense and narrower electron–phonon bands compared to the J-band [71, 73].

Now, what are these bands? The answer must be sought with a great deal of scepticism — that is, even more intense and narrower bands should be predicted for the most unfavorable dependence $\gamma = \gamma(E_r)$. The worst prediction is derived from the hyperbolic dependence [71, 73].

A convenient starting object for our prediction is provided by three optical bands in the Brooker series, corresponding to a shorter length of the polymethine chain than that producing the transferon band ($n = 3$). In Fig. 19, these three bands can be seen to the left of the transferon band. Evidently, each of them can be brought to the transferon state by adequate enhancement of interaction between its π-electron chromo-

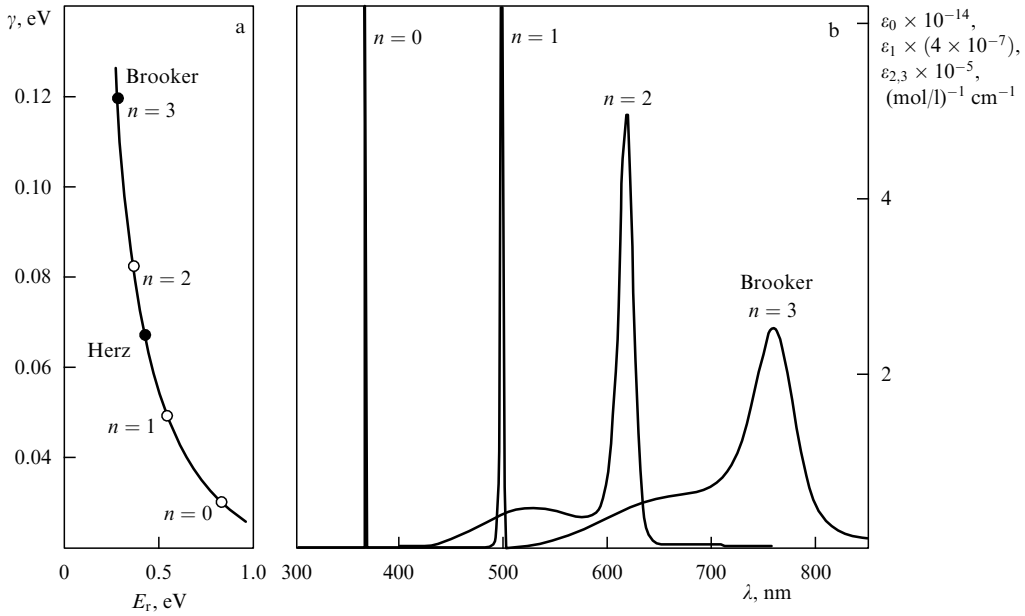

Figure 22. Strong electron–phonon interaction in transferon resonance $\sqrt{J/2m}/L = E_r/\hbar$ [see formulas (11.1), (11.12)] leads to the appearance of narrow intense bands [71]. (a) The dependence $\gamma = \gamma(E_r)$ of dissipation energy on nuclear reorganization energy is approximated by a hyperbolic function using our theoretical interpretation [see Fig. 19 ($E_r = 0.275$ eV, $\gamma = 0.120$ eV) and Fig. 21 ($E_{r,J} = 0.420$ eV, $\gamma_J = 0.067$ eV)] of the experimental resonance states of Brooker and co-workers (see Fig. 1, $n = 3$) and Herz (see Fig. 2, J-band). (b) Transferon resonance for the data of Brooker and co-workers is enhanced by increasing electron–phonon interaction in the same way as nonresonance states $n = 2, 1, 0$ (see Fig. 19) are converted one after another into resonance states $n = 2, 1, 0$ as the interaction increases.

phore and the environment, i.e., by increasing the environmental reorganization energy E_r. To this effect, the dissipation energy γ should be assumed to decrease with an increase in E_r, in agreement with the hyperbolic dependence shown in Fig. 22a. Transferon absorption bands obtained in this case are presented in Fig. 22b. Evidently, even the worst prediction gives high-intensity narrow absorption bands for small-extent electron–phonon transitions [71, 73]; the shortest transition has the greatest effect[24] (Fig. 22b, $n = 2, 1, 0$).

Thus, our theory [70, 73] admits the possibility of much stronger transferon effects than the effect yielding the J-band [71, 73]. It should be recalled that the transferon effect is that of spontaneous pumping of charge transfer state by the ordered environmental motion. In other words, the medium fosters electron charge transfer. This effect is an example of the dynamic self-organization of electron-vibrational transitions.[25] It may be assumed that self-organization of this kind is in the nature of biological functions. It justifies the search for more pronounced transferon effects than the effect responsible for the J-band, e.g., in biological objects [71, 73].

14.2 Abnormal temperature dependence of the J-band

Calculations of optical absorption bands by formulas (10.12)–(10.30) demonstrated that J-band intensity grows with temperature, the rise in peak intensity being much greater than that in wing intensity (Fig. 23) [70, 73]. There is a sort of peak pumping by phonons. This phenomenon is due to the fact that more vibrational quanta are transformed to the ordered environmental nuclear motion at higher temperatures than at lower ones. In other words, the environment more efficiently promotes electron charge transfer (Section 14.1).

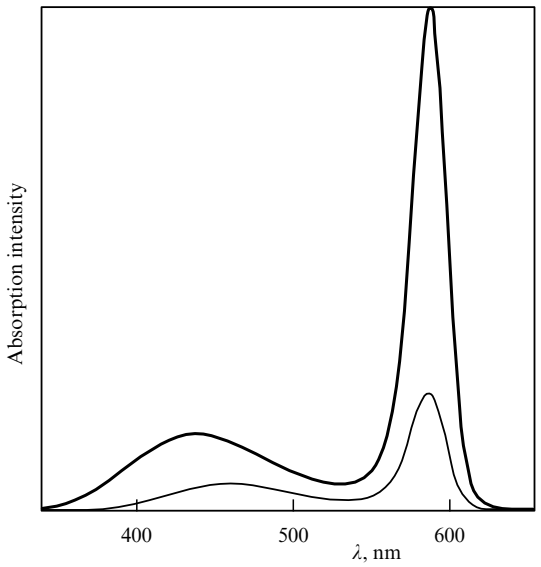

Figure 23. A rise in optical absorption intensity of J-aggregates with temperature in the case of their hindered decomposition into constituent molecules [70]: $T = 200$ K — thin line, and $T = 300$ K — thick line. The following parameters were used in formulas (10.12)–(10.30): $J_1 = 5$ eV, $J_2 = 4$ eV, $E_r = 1$ eV, $\gamma = 0.2$ eV, $m = m_e$, $\omega = 5 \times 10^{13}$ s^{-1}, and $L = L^* \approx 0.44$ nm (transferon resonance).

However, such temperature dependence of J-band intensity is abnormal. Usually, the intensity drops with temperature in aqueous solutions and on solid surfaces because the number of J-aggregates decreases as they disintegrate into

[24] In accordance with formula (10.11), the small parameter of our theory is $(k_B T/\gamma)^2 \ll 1$. Hence, the prediction in question is more reliable in the case of $n = 1$, where $(k_B T/\gamma)^2 \approx 1/4$, than at $n = 0$, where $(k_B T/\gamma)^2 \approx 3/4$ [73]. Other factors limiting the reliability of prediction for small-extent transitions are electron scattering on the initial state during transient state formation and phonon correlation [70, 73].

[25] See Section 16.6 for dynamic self-organization of electron-vibrational transitions.

constituent molecules.[26] The anomalous temperature dependence of the J-band can probably be observed in polymeric matrices where decomposition of J-aggregates with a rise in temperature is strongly hindered.

15. Brief characteristic of the results obtained with old and new approaches

At first sight, the traditional approach to the solution of the J-band problem has many advantages over the new one. Specifically, it was used to explain the shape of both J- and H-bands (see, for instance, Ref. [25], Section 6) and some other phenomena related to the J-band effect, most of which will be listed in Section 16.3. However, these are ephemeral advantages. The exciton approach makes use of a large number of fitting parameters[27] including some that are difficult (or impossible) to measure directly or calculate (e.g., diagonal disorder, disorder correlations, intermolecular interaction). This markedly reduces the real value of computation results for concrete J- and H-systems, which are obtained in the framework of the exciton model.

Matters stand quite differently with the new approach. It makes use of only one fitting parameter unamenable to direct measurement or calculation: dissipation or dozy chaos energy. The remaining parameters, such as electron binding energy in excited and ground states or environmental reorganization energy, are possible to calculate by modern methods of quantum chemistry. Moreover, the binding energy can be obtained directly in experiment (see, for instance, reviews [307 – 310] and references cited therein) and the nuclear reorganization energy estimated by a simple formula (Section 13). Furthermore, there is a fairly well defined range of dozy chaos energies. This quantity is roughly 1 – 3 times the reorganization energy under conditions usual for the chemical kinetics (see text related to formula (10.33) and Fig. 17) and approximately 0.1 – 0.2 of the reorganization energy under the conditions of the J-band effect (see Figs 17 and 21).

Another indisputable advantage of the new approach is the fact that the theoretical result for the J-band shape has the form (even if complicated) of an analytical formula fully expressed through elementary functions (Section 10.2). It is easy to obtain with a personal computer. At the same time, the old approach requires cumbersome numerical calculations (Section 4.5) using supercomputers, even if the MEBA method is employed (Section 5).

The new approach applied to the theoretical treatment of the known Herz data (Section 13.3) permitted for the first time an explanation of experiments in J-aggregation upon a rise in dye concentration in the solution (these classic experiments (e.g., Refs [42 – 45]) are still of importance [8]). There is thermodynamically reversible equilibrium between monomeric and J-aggregated forms of the dye for each concentration level, as reflected in the existence of the isobestic point (see Figs 2 and 21). It should be emphasized that these classic experiments do not in principle yield to theoretical treatment in the framework of the existing exciton model. Our theoretical interpretation reproduces spectra of both J-aggregates and monomers for various dye concentrations (see Figs 2 and 21). Also, the new theory makes it possible to reproduce the isobestic point and its position with a high degree of accuracy (3 – 4%, cf. Figs 2 and 21). These results clearly demonstrate the indisputable advantage of the new approach.

16. A few remarks

16.1 Experimental assessment of exciton interaction anisotropy in polymethine dye aggregates

Our proposal of the new theory of elementary charge transfer [69 – 73] instead of the traditional exciton approach to the explanation of the J-band is dictated *inter alia* by the specific electron structure of the main chromophore of polymethine dye molecules, namely, its quasilinear polymethine chain (Sections 6 – 8). It can be expected that the distribution of the alternating π-electron charge along the chain in a molecular aggregate should lead to a significantly weaker exciton interaction parallel to the chain compared with its transverse direction.

As mentioned above, molecules in a J-aggregate are organized into a brickwork structure (see Figs 7, 20). It is generally accepted that the unique properties of the J-band (its small width and high intensity) are determined by exciton interaction along the brickwork, i.e., parallel to the quasilinear polymethine chain. But exciton interaction is expected to be minimal just in this direction. That is why the doubts arise on whether or not it might be responsible for the unique properties of the J-band.

The choice between two alternative approaches to explaining the nature of the J-band we make in favor of the one based on the new charge-transfer theory. This approach, unlike the exciton one, permits one to explain not only the properties of the J-band but also other optical bands of polymethine dyes forming J-aggregates [69 – 71, 73] (Section 13). The validity of the exciton approach can be either confirmed or disproved by the direct experimental assessment of anisotropy of exciton interaction in aggregated polymethine dyes. For this purpose, e.g., electron excitation should be induced in a single molecule in the center of a monomolecular film with the brickwork structure, having the form of a sufficiently large circle in order to register anisotropic propagation of excitation at its border.

16.2 On the way to the theory of H-aggregate optical bands

We refused to fall back on the exciton theory for explaining the character of optical bands in J-aggregates, but that does not mean that it cannot be applied at all to the interpretation of optical absorption bands produced by molecular aggregates of polymethine dyes.

Exciton interaction in a molecular aggregate broadens the optical band if it acts efficiently only across the polymethine chain along which the electron transition moment is directed [11]. The small width and high intensity of the J-band are due to the brickwork structure of J-aggregates apparently as thick as two bricks. Such a structure minimizes potential parasitic exciton effects. Indeed, experimental J-aggregates look like long thin rods [109, 171].

On the other hand, exciton effects must be maximally manifested in polymethine dye aggregates with a pack-of-cards structure: their optical absorption band must be very wide and shifted to the short-wave region with respect to the

[26] A drop in temperature stimulates molecular aggregation [163 – 170] (see Section 4.1).

[27] Sometimes, over ten (see, for instance, a recent paper by Didraga et al. [26]).

monomer band. Precisely such effects are reported for H-aggregates [75, 79]. Hence, the necessity to hybridize [70] the new charge-transfer theory [70, 73] and the Frenkel exciton theory [23, 56] in order to develop a theory for optical bands of H-aggregates and theoretically verify the hypothesis for anisotropic exciton interaction in polymethine dye aggregates (Section 16.1). We believe that this problem will be resolved in the near future.

16.3 The theory of the J-band and related problems: extension of the new approach to other topical problems

The new concept of optical transitions in J-aggregates, associated with elementary charge transfer, can be expected to lead to the revision of physical processes in J-aggregates and their nature in the near future. Most of all, this concerns superfluorescence [311, 312, 14–16], nonlinear optical effects [17–19, 238, 241], and pump-probe spectroscopy [313, 314, 53, 67], the theory of which is presently based on the exciton approach. Equally interesting are experimental data on spectral and temperature dynamics of J-aggregates [26–28, 31, 34] that recently received theoretical interpretation in terms of the exciton model [26, 27, 29, 30, 32, 33, 35].

16.4 On the exciton model

Spectra of polymethine dyes at room temperature are poorly resolved (see review [77] and references cited therein) and their shape depends on the interaction of electron transition with the environment, rather than with intramolecular vibrations (Section 1). Interaction between electron transition and the environment is described by the theory of multiphonon processes [76]. This theory is based on the Born–Oppenheimer adiabatic approximation and gives a Gaussian distribution for band shapes at room temperature (Section 1). As shown above, the shape of optical bands produced by monomeric molecules in polymethine dyes as they form J-aggregates is substantially different from the Gaussian one; it is complicated but not structured (see Fig. 1). This fact unambiguously indicates that the solution to the problem of describing optical band shapes in polymethine dyes lies beyond the adiabatic approximation. It was demonstrated in Section 13.2 that the new theory [70, 71], going far beyond the scope of adiabatic approximation, fairly well explains the complicated optical absorption band shape and its marked variations in a series of one and the same dye with a highly variable polymethine chain length. In other words, we have convincingly proved that the Born–Oppenheimer adiabatic approximation cannot be used as a basis for building up the theory of absorption band shape in polymethine dyes and especially their J-aggregates. Meanwhile, this approximation underlies the existing vibron theory or statistical exciton theory of absorption bands of J-aggregates (Sections 3.2.1 and 4.2). Therefore, this sole fact gives no reason to assert the correctness of the exciton approach to the J-band theory and all the results obtained with its help.

This brings us to the end of the discussion of the exciton model. However, a natural question arises: ''Why was it so successfully used in the J-band theory?'' The obvious answer is: it takes account of the static disorder paradigm in electron energies of molecular transitions in J-aggregates.

The point is that the disorder varies substantially during Frenkel exciton movements along a J-aggregate (Sections 3.2.1 and 6). Moreover, the very concept of dynamic and especially static disorder is not comprehensive, for it does not take account of self-consistency between electronic, nuclear, and excitonic motions associated with optical excitation of a 'J-aggregate + environment' system. In other words, the static disorder paradigm is not simply incorrect, it is utterly incorrect. Thus, there are two egregious incorrectnesses in the statistical exciton theory of the J-band: adiabatic approximation, and static disorder. It is not unusual in physical chemistry or chemical physics that two incorrect approximations in one theory mutually compensate for each other and yield a result in agreement with experiment. It should be specially emphasized that the Frenkel exciton concept proper is certainly beyond doubt. However, its application as it stands to the solution of the J-band problem conceals, even if unintentionally, the errors in the Knapp exciton model [58] and all later works relying on it.[28]

16.5 On the new charge-transfer theory

The new theory of elementary charge transfer [70, 71, 73] offers an approximate solution for the description of the extended electron–nuclear(–phonon) state that can be regarded as an alternative to the Born–Oppenheimer adiabatic approximation. In contrast to the latter, our approximation (see, for instance, Ref. [77]) permits describing the electron–nuclear motion in the vicinity of and inside the crossover regions of potential energy surfaces for the initial and final states of the system. The extended electron–phonon state corresponding to the elementary electron transfer (EET) state is described by the wave function of the initial state $\Psi_1 = \Psi_1(\mathbf{r}, q; \mathbf{L}; E_r, \gamma)$ (Section 10.1) that depends on electron–phonon interaction via nuclear reorganization energy E_r and dissipation energy γ. Here, the introduction of dissipative states is somewhat analogous to the introduction of quasi-stationary states in quantum mechanics (see, for instance, Ref. [315]). The quasistationary states ensue from the solution to the time-dependent Schrödinger equation in which the total energy is assumed to have an imaginary part, in addition to the real one. In our EET problem, dissipative states are associated with the standard imaginary addition $i\gamma$ that enters the energy denominator of the Green function of the 'electron + environment' system in the Lippmann–Schwinger equation; they arise from the replacement of infinitesimal quantity γ by any positive or negative number.[29] This procedure implies the existence of a more general dynamic equation than the standard integral Lippmann–Schwinger equation or the equivalent stationary Schrödinger equation. In other words, our description of EET goes

[28] We have demonstrated the irrelevance of the dynamic disorder concept in a special case of the absence of exciton motion (Section 12). It was shown that the Lorentzian shape of an optical absorption band in the framework of the Anderson–Kubo theory of dynamic disorder is significantly different from the shape of J-resonance in the new elementary charge transfer theory where electronic and nuclear motions are self-consistent, by definition, in contrast to the Anderson–Kubo theory. Also worthy of note is the real possibility of posing the problem of self-consistency of the totality of electronic, nuclear, and excitonic motions in a 'polymethine dye aggregate + environment' system. To realize this, a hybrid theory is needed combining the new charge-transfer theory and the Frenkel exciton theory [70]. This issue was mentioned in Section 16.2 in connection with the prospects of building up the theory of H-aggregate optical bands in the near future. The simplest analog of such hybrid theory is the theory of elementary processes of electron transfer from exciton states of molecular aggregates to a local center in the case of strong dissipation [$\gamma > E$, see formula (10.33)] [291, 292, 73].

[29] For certainty, we consider the modulus of this quantity (Section 10.2), bearing in mind the invariance of the result with respect to a change in the sign of γ.

beyond the scope of standard quantum mechanics [71 – 73]. The dynamic equation of the Lippmann – Schwinger type with $0 < |\gamma| < \infty$, postulated by us, suggests that the pure quantum-mechanical state is specified by electron coordinates $\mathbf{r}$, phonon coordinates q, electron transfer distance $L \equiv |\mathbf{L}|$, and electron – phonon interaction possessing a special property [71 – 73]. This property is the manifestation of electron – phonon interaction in the optical band shape not only via the reorganization energy E_r as in the standard multiphonon transition theory [76, 77] but also through the dissipation energy γ.

Roughly speaking, the dissipation energy γ may be regarded as the imaginary part of the 'complex reorganization energy'. Our theory essentially refines the notion of reorganization energy by taking into consideration the disorder (dissipativity) of the environmental nuclear reorganization process in the transient state of the elementary act of electron transfer. The degree of process dissipativity is determined in this context by the relationship between imaginary and real parts of the 'complex reorganization energy' [72, 73].

Quantity γ introduced in the theory [70, 71, 73] performs two functions: it dampens singularity (inherent in the electron-nuclear motion) in the probability of extended transitions, and it determines the small parameter $(k_B T/\gamma)^2 \ll 1$ of the problem (Section 10). The dissipation energy γ resembles the width of energy levels of the electron transient state. However, interpretation of the physical sense of γ in terms of the width of these electron – phonon levels is impracticable for the following reasons [73, 304]. First, quantity γ was defined up to the sign (Section 10.2). Second, the minimal separation between intermediate energy levels equals the vibrational quantum energy $\hbar\omega$, namely, it is significantly smaller than the relatively large 'width' γ itself [see formula (10.7)]. Above all, our formal way of introducing γ is unrelated to time, i.e., we do not consider time-dependent decay and pumping of electron and phonon states separately when accounting for virtual energy exchange between an electron and phonons, but introduce time-independent dissipation in the entire quantum system [72, 73]. Thus, the dissipation energy γ has its own original physical status. In order to distinguish our dissipation from dissipation in other contexts, we call it 'dozy chaos' (Section 10.1). Dozy chaos is absent in the initial and final states and arises in the transient state alone. The physical origin of this dissipation is discussed in Section 16.6.

When dissipation or dozy chaos energy $\gamma = 0$ (Section 10.1), the transferon resonance (Section 11.2) determining the nature of the J-band (Section 13.3) undergoes degeneration into essential singularity of optical absorption (Section 10.2). The character of this singularity viewed as physical reality is related to the directed and absolutely ordered motion of highly inertial nuclei in the medium under the effect of an electron movement from the donor to the acceptor [72, 73] (see also Section 16.6).

Thus, we believe that correct consideration of electron – phonon interaction in the context of the EET problem is possible only if the dissipation (relaxation) process is introduced directly in the pure quantum-mechanical state [71 – 73]. It is easy to understand that such statement of the problem is beyond the EET picture in which relaxation processes are introduced in the density matrix equation in the form of an additional relaxation term (see, for instance, Ref. [271]), i.e., only at the level of description of a physical phenomenon by the mixed (quantum-statistical) state. While relaxation processes at the mixed state level may take place, it is difficult to perceive that they can eliminate the singular (nonphysical) behavior in dynamics of the 'electron + environment' quantum system at the pure state level that develops when the limits of the adiabatic approximation are exceeded. (Such an assumption would mean that the description of the electron – nuclear motion in terms of wave function is devoid of physical sense as a result of exceeding the limits of the adiabatic approximation.) For this reason, in the new charge-transfer theory extending far beyond the framework of the adiabatic approximation, dissipation is introduced in the pure but not mixed state of the 'electron + environment' system [71 – 73].

On the other hand, it is widely believed that the standard theory of multiphonon transitions (see Ref. [76]) makes extensive use of the following methods [70, 71, 73]: the generating polynomial (generating function) method of Krivoglaz and Pekar[30] [251, 252], the operation calculus of Feynman [317] and Lax [318], the density matrix method of Kubo and Toyozawa [319, 320], and the quantum field theory technique (see Ref. [76]). The generating polynomial method is the simplest one and takes into account the main effect of the interaction between an optical electron and vibrational nuclear motion in the environment — that is, the shifts of normal phonon coordinates caused by electron transition. Changes in phonon frequencies and other higher-order effects should be taken into account by the remaining aforementioned methods. The case of extended multiphonon transitions (elementary charge transfer) is much more complicated than that of conventional multiphonon transitions. Evidently, generalization of the multiphonon transition theory to the case of elementary charge transfer in terms of wave function requires further progress in the simplest technique developed by Krivoglaz and Pekar [251, 252] as in Refs [70, 71, 73]. The next principal step in the development of the charge transfer theory [70, 71, 73] will consist in its formulation in terms of the density matrix, based on the modified Kubo – Toyozawa method [319, 320].

16.6 The Born – Oppenheimer adiabatic approximation and Franck – Condon principle. Two alternative mechanisms of electron-vibrational transitions

The fundamental role of the Born – Oppenheimer adiabatic approximation [110] underlying the theories of molecular structure, solid state, and modern quantum chemistry is universally recognized. The motion of a light electron in the stationary state very quickly (adiabatically) adjusts itself to the slow motion of heavy nuclei. The stationary electron charge density distribution creates a potential in which nuclei vibrate about their equilibrium positions. However, the situation is altogether different with electron transitions from one stationary state to another, leading to a change in the electron charge density distribution and creation of a new potential in which nuclei vibrate about their new equilibrium positions. In other words, electron transitions cause equilibrium positions of the nuclei to shift; this process is frequently described as reorganization of nuclear vibrations. Bearing in mind the incommensurability of electron and nucleus masses, the first question is how light electrons make heavy nuclei

[30] The Krivoglaz – Pekar method is similar to computing the thermodynamic quantities by the Darwin – Fowler method [316, 76], known from statistical physics.

leave their equilibrium positions for new ones. The correct answer to this question immediately poses another: How do electrons stop nuclei after they reach new equilibrium positions?

The standard approach to the solution is based on the assumption that electron transition is very quick, while nuclear equilibrium positions are shifted to new ones only slowly. This approach is reflected in the Franck – Condon principle according to which instantaneous electron transition leaves no time for nuclear coordinates and momenta to change. Mathematically, the Franck – Condon principle is derived from the matrix element of electron-vibrational transition in which the adiabatic wave functions of initial and final states are taken as the product of two wave functions depending separately on electron and nuclear coordinates alone. Such an approximation is often called the rough adiabatic approximation. Thus, the interaction operator responsible for electron transition being disregarded, the Franck – Condon principle constitutes the overlap integral of electron-nuclear wave functions of the initial and final states taken in the rough adiabatic approximation. In other words, the Franck – Condon principle completely ignores electronic and nuclear movements in the transient state, or in short transient state dynamics. For small molecules, this approach frequently leads to results that fit the experimental data well.

It is important that the agreement with experiment suggests in this case only weak dependence of the result on transient state dynamics. However, it does not confirm the Franck – Condon picture in which the electron transition and the concomitant displacement of nuclear equilibrium positions are well separated in time. Moreover, it follows from general physical considerations that such a picture would look absurd because of the considerable difference between electron and nucleus masses. It should be expected that the nuclei would not adjust to the new charge distribution resulting from the electron transition; rather they would drive the electron back to its initial state, and the situation would correspond to the zero transition probability. This conclusion holds not only for the rough adiabatic approximation but also for the approximation in the general case when the electron wave function depends on both electronic and nuclear coordinates.

The absurd physical picture resulting from the application of the adiabatic approximation to the description of electron-vibrational transitions may be disregarded in the case of sufficiently small molecules, for which the transition probability predominantly depends on the initial and final states and, as noted above, only weakly on transient state dynamics. In the case of sufficiently large molecules, for which the transition probability essentially depends on transient state dynamics, the solution to the problem lies beyond the adiabatic approximation [70, 71, 73]. Also, this case gives an answer to the question asked above, i.e., how the electron manages to displace nuclei to new equilibrium positions.

The mechanism of electron-vibrational transitions leading to our quantum results in the framework of the regular theory [69, 70, 73] and Heisenberg uncertainty relation [71 – 73] can be described in classical language in the following simplified form. Excitation initiating quantum transition considerably changes electron charge distribution (e.g., in a donor – acceptor system), which may become extended in the direction from the donor to the acceptor. It results in modulation of nuclear vibrational movements with electronic motion. The modulation and atom – atom interactions give rise to chaotic elements in the nuclear motion. This means that the movements of the nuclei cease to be purely vibrational near the equilibrium positions and that it is possible to 'distinguish translational motion of equilibrium positions' in the direction of new positions corresponding to the final state. This is exactly the reason a light electron displaces an ensemble of heavy nuclei from their initial equilibrium positions. As the electron is being localized to the final state, the arising virtual chaos in the transient state causes reverse transformation of the nuclear motion — that is, translational motion turns into a vibrational one again but relative to new equilibrium positions. Due to this, the electron first 'slows down' and then 'stops' nuclei despite their enormous inertia. Thus, the electron succeeds to control nuclear motion by making it chaotic in the transient state. We call this chaos dozy chaos (Section 10.1).

Note that we describe the new mechanism of electron-vibrational transitions using word combinations suggesting free will in an electron. Actually, the case in point is self-organization (dynamic self-organization) of the motion in complex physical systems, perfectly well exemplified by electron-vibrational transitions. Today, similar problems are extensively discussed in quantum information (see reviews [80, 81] and references cited therein) and cybernetic physics (see reviews [321 – 325] and references cited therein). An electron in the transient state exchanges motion and energy with the surrounding nuclei. This is, in fact, the exchange of information about the current motion.

17. Conclusions

This review was designed to fill the gap in the Russian physical literature on a most interesting and important physical phenomenon, namely, the appearance of a narrow intense optical band (J-band) as a result of aggregation of polymethine dyes. The study of this phenomenon has a 70-year history, but its nature has not yet achieved a proper level of comprehension among researchers. This fact accounts for the considerable length of the present review encompassing the entire J-band theory from the Frenkel exciton to charge transfer. The origin of the exciton theory dates to 1931, i.e., 5 years before the J-band was discovered, while the new charge-transfer theory was suggested at the beginning of this century. It is therefore natural that the generally accepted point of view on the nature of the J-band is based on the exciton theory rather than the charge transfer theory.

Unfortunately, the statistical exciton theory of the J-band [58] underlain by the adiabatic approximation and the static disorder paradigm (Section 16.4), as well as all the later studies in its context, is nothing but one of the big hoaxes not infrequent in the history of science and that are seemingly unavoidable. In the past, the authors of the review themselves actively participated in its creation[31] [60 – 65, 212]. In 2001 – 2002, one of them suggested a totally new theory [69 – 71] shown above to be a real alternative to the exciton approach in the J-band theory. This dynamic theory is based on the new concept of charge transfer and goes far beyond the limits of the adiabatic approximation. The theory [69 – 71] has taken only its first steps [72, 73] and

[31] The former position of the authors was rooted in the inertia of traditional concepts and in the absence of an acceptable alternative rather than in the faultless physical foundation of the exciton J-band theory.

will have to confirm in full measure its validity by extending its ideas to other topical physical and chemical problems (e.g., those listed in Section 16.3).

The former approach to interpreting the J-band based on the Frenkel exciton theory implies practical degradation of all characteristic features of the optical spectrum of monomeric molecules in a J-aggregate. The new, opposite approach is based on the charge transfer theory and suggests the development of a characteristic (resonance) feature in the spectra of polymethine dye monomers as a result of their J-aggregation. It explains not only the shape of the J-band but also the shape of optical bands of constituent molecules of J-aggregates.

As shown in this review, the exciton theory of the J-band assumes the band shape of monomeric molecules to be given. This can be accounted for by the absence of a theory of electron-vibrational spectroscopy for such large and extended structures that requires transient state dynamics to be taken into consideration. Nevertheless, quantum transition in these molecules is possible to simulate with the help of the new charge-transfer theory (see above). In other words, this theory is the first step toward the development of theoretical electron-vibrational spectroscopy with due regard for transient state dynamics.

The problem of transient-state quantum dynamics has always been important in chemical physics; today, it has acquired importance in dynamic studies of quantum information systems in physics. K A Valiev concludes his recent review "Quantum computers and quantum computations" [81] with the following words: "... A course in classical mechanics is subdivided into statics and dynamics, while this division is absent in a course on quantum mechanics. It is dominated by statics... It is supposedly expedient to construct a modern course in quantum mechanics such that it consists of two full-fledged volumes dedicated to quantum statics and quantum dynamics. It is believed that such a course on quantum mechanics will make its appearance in the near future." For our part, we believe that quantum dynamics of the transient state of physico-chemical systems will fill a fitting niche in this course.

References

1. Jacak L, Hawrylak P, Wójs A *Quantum Dots* (Berlin: Springer-Verlag, 1998)
2. Stangl J, Holý V, Bauer J *Rev. Mod. Phys.* **76** 725 (2004)
3. Wang M et al. *Chinese Sci. Bull.* **49** 747 (2004)
4. Ostrikov K *Rev. Mod. Phys.* **77** 489 (2005)
5. Kono S et al. *Phys. Rev. B* **72** 155307 (2005)
6. Yuzhakov V I *Usp. Khim.* **61** 1114 (1992) [*Russ. Chem. Rev.* **61** 613 (1992)]
7. Mishra A et al. *Chem. Rev.* **100** 1973 (2000)
8. Shapiro B I *Usp. Khim.* **75** 484 (2006) [*Russ. Chem. Rev.* **75** 433 (2006)]
9. Ginzburg V L *Rev. Mod. Phys.* **76** 981 (2004); *Usp. Fiz. Nauk* **174** 1240 (2004) [*Phys. Usp.* **47** 1155 (2004)]
10. Kobayashi T (Ed.) *J-aggregates* (Singapore: World Scientific, 1996)
11. Kachkovskii A D *Usp. Khim.* **66** 715 (1997) [*Russ. Chem. Rev.* **66** 647 (1997)]
12. Maltsev E I et al. *Appl. Phys. Lett.* **81** 3088 (2002)
13. Kirillov S V, Thesis for Cand. Chem. Sci. Degree (Moscow: Frumkin Institute of Electrochemistry, Russian Acad. of Sci., 2004)
14. De Boer S, Wiersma D A *Chem. Phys. Lett.* **165** 45 (1990)
15. Fidder H, Knoester J, Wiersma D A *Chem. Phys. Lett.* **171** 529 (1990)
16. Kamalov V F, Struganova I A, Yoshihara K *J. Phys. Chem.* **100** 8640 (1996)
17. Bogdanov V L et al. *Pis'ma Zh. Eksp. Teor. Fiz.* **53** 100 (1991) [*JETP Lett.* **53** 105 (1991)]
18. Wang Y *J. Opt. Soc. Am. B* **8** 981 (1991)
19. Markov R V et al. *Phys. Status Solidi B* **221** 529 (2000)
20. von Berlepsch H et al. *J. Phys. Chem. B* **104** 5255 (2000)
21. von Berlepsch H et al. *Langmuir* **16** 5908 (2000)
22. von Berlepsch H et al. *J. Phys. Chem. B* **107** 14176 (2003)
23. Frenkel J *Phys. Rev.* **37** 17, 1276 (1931)
24. Scheblykin I G et al. *Chem. Phys. Lett.* **261** 181 (1996)
25. Basko D M et al. *Chem. Phys. Lett.* **369** 192 (2003)
26. Didraga C et al. *J. Phys. Chem. B* **108** 14976 (2004)
27. Pugžlys A et al. *J. Phys. Chem. B* **110** 20268 (2006)
28. Scheblykin I G et al. *J. Phys. Chem. B* **105** 4636 (2001)
29. Bednarz M, Malyshev V A, Knoester J *Phys. Rev. Lett.* **91** 217401 (2003)
30. Bednarz M, Malyshev V A, Knoester J *J. Chem. Phys.* **120** 3827 (2004)
31. Renge I, Wild U P *J. Phys. Chem. A* **101** 7977 (1997)
32. Heijs D J, Malyshev V A, Knoester J *Phys. Rev. Lett.* **95** 177402 (2005)
33. Heijs D J, Malyshev V A, Knoester J *J. Chem. Phys.* **123** 144507 (2005)
34. Hirschmann R, Friedrich J *J. Chem. Phys.* **91** 7988 (1989)
35. Heijs D J, Malyshev V A, Knoester J *J. Lumin.* **119 – 120** 271 (2006)
36. Fidder H, Knoester J, Wiersma D A *J. Chem. Phys.* **98** 6564 (1993)
37. Durrant J R, Knoester J, Wiersma D A *Chem. Phys. Lett.* **222** 450 (1994)
38. Minoshima K et al. *Chem. Phys. Lett.* **218** 67 (1994)
39. Tilgner A et al. *J. Chem. Phys.* **96** 781 (1992)
40. Shimizu M et al. *Phys. Rev. B* **58** 5032 (1998)
41. Shimizu M, Suto S, Goto T *J. Chem. Phys.* **114** 2775 (2001)
42. Jelley E E *Nature* **138** 1009 (1936)
43. Jelley E E *Nature* **139** 631 (1937)
44. Scheibe G *Angew. Chem.* **49** 563 (1936)
45. Scheibe G *Angew. Chem.* **50** 212 (1937)
46. Tuszyński J A, Jørgensen M F, Möbius D *Phys. Rev. E* **59** 4374 (1999)
47. Scherer P O J, in *J-aggregates* (Ed. T Kobayashi) (Singapore: World Scientific, 1996) p. 95
48. Davydov A S *Teoriya Pogloshcheniya Sveta v Molekulyarnykh Kristallakh* (The Theory of Light Absorption in Molecular Crystals) (Kiev: Izd. AN USSR, 1951) [Translated into English: *Theory of Molecular Excitons* (New York: McGraw-Hill, 1962)]
49. Knox R S *Theory of Excitons* (New York: Academic Press, 1963) [Translated into Russian (Moscow: Mir, 1966)]
50. Davydov A S *Teoriya Molekulyarnykh Eksitonov* (Theory of Molecular Excitons) (Moscow: Nauka, 1968) [Translated into English (New York: Plenum Press, 1971)]
51. Agranovich V M *Teoriya Eksitonov* (The Theory of Excitons) (Moscow: Nauka, 1968)
52. Franck J, Teller E *J. Chem. Phys.* **6** 861 (1938)
53. Knoester J, Spano F C, in *J-aggregates* (Ed. T Kobayashi) (Singapore: World Scientific, 1996) p. 111
54. McRae E G, Kasha M *J. Chem. Phys.* **28** 721 (1958)
55. Kasha M *Rev. Mod. Phys.* **31** 162 (1959)
56. McRae E G, Kasha M, in *Physical Processes in Radiation Biology* (Eds L Augenstein, R Mason, B Rosenberg) (New York: Academic Press, 1964) p. 23
57. Kasha M, Rawls H R, El-Bayoumi M A, in *Molecular Spectroscopy. Proc. of the VIII European Congress, Copenhagen, 14 – 20 August 1965* (London: Clarendon Press, 1965) p. 371
58. Knapp E W *Chem. Phys.* **85** 73 (1984)
59. Knapp E W, Scherer P O J, Fischer S F *Chem. Phys. Lett.* **111** 481 (1984)
60. Bagatur'yants A A, Egorov V V, Makhov D V, Alfimov M V *Dokl. Ross. Akad. Nauk* **337** 615 (1994)
61. Makhov D V, Egorov V V, Bagatur'yants A A, Alfimov M V *Chem. Phys. Lett.* **246** 371 (1995)
62. Makhov D V, Egorov V V, Bagatur'yants A A, Alfimov M V *Zh. Fiz. Khim.* **71** 1805 (1997) [*Russ. J. Phys. Chem.* **71** 1625 (1997)]
63. Makhov D V, Egorov V V, Bagatur'yants A A, Alfimov M V *J. Lumin.* **72 – 74** 439 (1997)

64. Makhov D V, Egorov V V, Bagatur'yants A A, Alfimov M V *Mater. Sci. Eng. C* **5** 311 (1998)
65. Makhov D V, Egorov V V, Bagatur'yants A A, Alfimov M V *J. Chem. Phys.* **110** 3196 (1999)
66. Makhov D V, Thesis for Cand. Phys.-Math. Sci. Degree (Moscow: Semenov Institute of Chemical Physics, Russian Acad. of Sci., 2000)
67. Bakalis L D, Knoester J *J. Phys. Chem. B* **103** 6620 (1999)
68. Fidder H, Terpstra J, Wiersma D A *J. Chem. Phys.* **94** 6895 (1991)
69. Egorov V V *Chem. Phys. Lett.* **336** 284 (2001)
70. Egorov V V *Chem. Phys.* **269** 251 (2001)
71. Egorov V V *J. Chem. Phys.* **116** 3090 (2002); *Virtual J. Biol. Phys. Res.* **3** (4) (2002)
72. Egorov V V *Elektrokhimiya* **39** (1, Spets. Vypusk Posvyashchennyi 70-letiyu so Dnya Rozhdeniya R.R. Dogonadze) 93 (2003) [*Russ. J. Electrochem.* **39** 86 (2003)]
73. Egorov V V, Thesis for Doct. Phys-Math. Sci. Degree (Moscow: Institute of Physical Chemistry, Russian Acad. of Sci., 2004)
74. Brooker L G S et al. *J. Am. Chem. Soc.* **62** 1116 (1940)
75. James T H (Ed.) *The Theory of the Photographic Process* (New York: Macmillan, 1977) [Translated into Russian (Leningrad: Khimiya, 1980)]
76. Perlin Yu E *Usp. Fiz. Nauk* **80** 553 (1963) [*Sov. Phys. Usp.* **6** 542 (1964)]
77. Frank-Kamenetskii M D, Lukashin A V *Usp. Fiz. Nauk* **116** 193 (1975) [*Sov. Phys. Usp.* **18** 391 (1975)]
78. Herz A H *Photogr. Sci. Eng.* **18** 323, 667 (1974)
79. Herz A H *Adv. Coll. Interface Sci.* **8** 237 (1977)
80. Menskiĭ M B *Usp. Fiz. Nauk* **170** 631 (2000) [*Phys. Usp.* **43** 585 (2000)]
81. Valiev K A *Usp. Fiz. Nauk* **175** 3 (2005) [*Phys. Usp.* **48** 1 (2005)]
82. Einstein A, Podolsky B, Rosen N *Phys. Rev.* **47** 777 (1935)
83. Zurek W H *Phys. Today* **44** (10) 36 (1991)
84. Menskiĭ M B *Usp. Fiz. Nauk* **175** 413 (2005) [*Phys. Usp.* **48** 389 (2005)]
85. Schlosshauer M *Rev. Mod. Phys.* **76** 1267 (2004)
86. Zurek W H *Phys. Rev. A* **71** 052105 (2005)
87. McGlynn S P, Azumi T, Kinoshita M *Molecular Spectroscopy of the Triplet State* (Englewood Cliffs, NJ: Prentice-Hall, 1969) [Translated into Russian (Moscow: Mir, 1972)]
88. Landau L D, Lifshitz E M *Teoriya Polya* (The Classical Theory of Fields) (Moscow: Nauka, 1973) [Translated into English (Oxford: Pergamon Press, 1983)]
89. Davydov A S *Kvantovaya Mekhanika* (Quantum Mechanics) (Moscow: Nauka, 1973) [Translated into English (Oxford: Pergamon Press, 1976)]
90. Anderson P W *J. Phys. Soc. Jpn.* **9** 316 (1954)
91. Kubo R *J. Phys. Soc. Jpn.* **9** 935 (1954)
92. Anderson P W, Weiss P R *Rev. Mod. Phys.* **25** 269 (1953)
93. Kubo R, Tomita K *J. Phys. Soc. Jpn.* **9** 888 (1954)
94. Kubo R *Adv. Chem. Phys.* **15** 101 (1969)
95. Kuhn H *Helv. Chim. Acta* **31** 1441 (1948)
96. Kuhn H, Kuhn C, in *J-aggregates* (Ed. T Kobayashi) (Singapore: World Scientific, 1996) p. 1
97. Czikkely V, Försterling H D, Kuhn H *Chem. Phys. Lett.* **6** 11 (1970)
98. Försterling H D, Kuhn H *Moleküle und Molekülanhäufungen. Eine Einführung in die physikalische Chemie* (Heidelberg: Springer-Verlag, 1983)
99. Försterling H D et al., in *Optische Anregung organischer Systeme. 2. Internationales Farbensymposium* (Hrsg. W Foerst) (Weinheim: Verlag Chemie, 1966) p. 55
100. Huber W, Simon G, Kuhn H *Z. Naturforsch.* **17a** 99 (1962)
101. Försterling H D, Kuhn H *Int. J. Quant. Chem.* **2** 413 (1968)
102. Kuhn C *Phys. Rev. B* **40** 7776 (1989)
103. Kuhn H, Kuhn C *Chem. Phys. Lett.* **204** 206 (1993)
104. Kuhn C, Kuhn H *Synth. Met.* **68** 173 (1995)
105. Czikkely V, Försterling H D, Kuhn H *Chem. Phys. Lett.* **6** 207 (1970)
106. Möbius D *Z. Physikal. Chem. NF* **154** 121 (1987)
107. Möbius D, Kuhn H *Isr. J. Chem.* **18** 375 (1979)
108. Kuhn H, in *Interactions between Light and Materials for Photographic Application* (Tokyo: The Society of Photographic Science & Technology of Japan, 1982) p. 245
109. Misawa K et al. *Appl. Phys. Lett.* **63** 577 (1993)
110. Born M, Oppenheimer J R *Ann. Phys.* (Leipzig) **84** 457 (1927)
111. Dushinsky F *Acta Physicochim. URSS* **7** 551 (1937)
112. Misawa K et al. *Chem. Phys. Lett.* **220** 251 (1994)
113. Johnson A E, Kumazaki S, Yoshihara K *Chem. Phys. Lett.* **211** 511 (1993)
114. Kamalov V F et al. *Chem. Phys. Lett.* **226** 132 (1994)
115. Fidder H, Wiersma D A *Phys. Status Solidi B* **188** 285 (1995)
116. Akins D L *J. Phys. Chem.* **90** 1530 (1986)
117. Holstein T *Philos. Mag. B* **37** 49 (1978)
118. Scherer P O J, Fischer S F *Chem. Phys.* **86** 269 (1984)
119. Fidder H, Knoester J, Wiersma D A *J. Chem. Phys.* **95** 7880 (1991)
120. Malyshev V A, Moreno P *Phys. Rev. B* **51** 14587 (1995)
121. Bird G R et al. *Photogr. Sci. Eng.* **12** 196 (1968)
122. Cooper W *Chem. Phys. Lett.* **7** 73 (1970)
123. Kopainsky B, Hallermeier J K, Kaiser W *Chem. Phys. Lett.* **83** 498 (1981)
124. Nüesch F, Grätzel M *Chem. Phys.* **193** 1 (1995)
125. Neria E, Nitzan A *J. Chem. Phys.* **96** 5433 (1992)
126. Van Burgel M, Wiersma D A, Duppen K *J. Chem. Phys.* **102** 20 (1995)
127. Sevian H M, Skinner J L *J. Chem. Phys.* **97** 8 (1992)
128. Köhler J, Jayannavar A M, Reineker P *Z. Phys. B* **75** 451 (1989)
129. Reineker P et al. *Chem. Phys.* **177** 715 (1993)
130. Neidlinger T, Reineker P *J. Lumin.* **60–61** 413 (1994)
131. Barvik I et al. *J. Lumin.* **65** 169 (1995)
132. Cordan A S, Boeglin A J, Villaeys A A *Phys. Rev. A* **47** 5041 (1993)
133. Pschierer H, Friedrich J *Phys. Status Solidi B* **189** 43 (1995)
134. Scherer P O J *Adv. Mater.* **7** 451 (1995)
135. Haken H, Reineker P, in *Excitons, Magnons and Phonons in Molecular Crystals* (Ed. A B Zahlan) (London: Cambridge Univ. Press, 1968) p. 185
136. Haken H, Strobl G *Z. Phys.* **262** 135 (1973)
137. Reineker P *Springer Tracts Mod. Phys.* **94** 111 (1982)
138. Wubs M, Knoester J *Chem. Phys. Lett.* **284** 63 (1998)
139. Burshtein K Ya, Bagatur'yants A A, Alfimov M V *Zh. Fiz. Khim.* **68** 2001 (1994)
140. Burshtein K Ya, Bagatur'yants A A, Alfimov M V *J. Mol. Struct.: THEOCHEM* **314** 311 (1994)
141. Burshtein K Ya, Bagatur'yants A A, Alfimov M V *Izv. Ross. Akad. Nauk Ser. Khim.* (9) 1705 (1995) [*Bull. Russ. Acad. Sci. Div. Chem. Sci.* **44** 1637 (1995)]
142. Burshtein K Ya, Bagatur'yants A A, Alfimov M V *Chem. Phys. Lett.* **239** 195 (1995)
143. Burshtein K Ya, Bagatur'yants A A, Alfimov M V *Izv. Ross. Akad. Nauk Ser. Khim.* (1) 67 (1997) [*Bull. Russ. Acad. Sci. Div. Chem. Sci.* **42** 62 (1997)]
144. Del Bene J, Jaffé H H *J. Chem. Phys.* **48** 1807 (1968)
145. Ohno K *Chem. Phys. Lett.* **64** 560 (1979)
146. Ohno K *Chem. Phys. Lett.* **70** 526 (1980)
147. Eisfeld A, Briggs J Š *Chem. Phys.* **281** 61 (2002)
148. Briggs J S, Herzenberg A *J. Phys. B: At. Mol. Phys.* **3** 1663 (1970)
149. Briggs J S *Z. Phys. Chem. NF* **75** 214 (1971)
150. Briggs J S, Herzenberg A *Mol. Phys.* **21** 865 (1971)
151. Spitz C, Dähne S *Ber. Bunsen. Phys. Chem.* **102** 738 (1998)
152. Jaksch D et al. *Phys. Rev. Lett.* **85** 2208 (2000)
153. Brennen G K, Deutsch I H, Jessen P S *Phys. Rev. A* **61** 062309 (2000)
154. Yuzhakov V I *Usp. Khim.* **48** 2007 (1979)
155. Levshin V L, Baranova E G *Izv. Akad. Nauk SSSR Ser. Fiz.* **20** 424 (1956)
156. Arvan Kh L *Izv. Akad. Nauk SSSR Ser. Fiz.* **20** 443 (1956)
157. Levshin V L, Gorshkov V K *Opt. Spektrosk.* **10** 759 (1961) [*Opt. Spectrosc.* **10** 401 (1961)]
158. Baranova E G et al., in *Fizicheskie Problemy Spektroskopii. Materialy XIII Soveshch., Leningrad, 4–12 Iyulya 1960 g.* (Physical Problems of Spectroscopy. Proc. XIII Meeting, Leningrad, July 4–12, 1960) Vol. 1 (Executive Ed. S E Frish) (Moscow: Izd. AN SSSR, 1962) p. 328
159. Levshin V L, Gorshkov V K, in *Fizicheskie Problemy Spektroskopii. Materialy XIII Soveshch., Leningrad, 4–12 Iyulya 1960 g.* (Physical Problems of Spectroscopy. Proc. XIII Meeting, Leningrad, July 4–12, 1960) Vol. 1 (Executive Ed. S E Frish) (Moscow: Izd. AN SSSR, 1962) p. 325
160. Pant D D, Pant K, Joshi N B *Indian J. Pure Appl. Phys.* **11** 507 (1973)

161. Crozet P, Meyer Y *CR Acad. Sci.* **271** 718 (1970)
162. Drexhage K H *Laser Focus* **9** (3) 35 (1973)
163. Zanker V *Z. Phys. Chem.* **200** 250 (1952)
164. Tumerman L A, Morozov Yu V, Naberukhin Yu I *Biofiz.* **6** 556 (1961)
165. Morozov Yu V, Naberukhin Yu I, Gurskii G V *Opt. Spektrosk.* **12** 599 (1962) [*Opt. Spectrosc.* **12** 332 (1962)]
166. Baranova E G, Levshin V L *Izv. Akad. Nauk SSSR Ser. Fiz.* **27** 554 (1963)
167. Levshin V L, Slavnova T D, Yuzhakov V I *Zh. Prikl. Spektrosk.* **16** 90 (1972) [*J. Appl. Spectrosc.* **16** 69 (1972)]
168. Levshin V L, Slavnova T D, Yuzhakov V I *Vestn. Mosk. Gos. Univ. Ser. 3 Fiz. Astron.* **14** 441 (1973)
169. Levshin V L, Slavnova T D, Yuzhakov V I *Zh. Prikl. Spektrosk.* **24** 985 (1976) [*J. Appl. Spectrosc.* **24** 698 (1976)]
170. Bojarsci C, Obermueller G *Acta Phys. Pol. A* **50** 389 (1976)
171. Daltrozzo E et al. *Photogr. Sci. Eng.* **18** 441 (1974)
172. De Boer S, Vink K J, Wiersma D A *Chem. Phys. Lett.* **137** 99 (1987)
173. Hilson P Y, McKay R B *Trans. Faraday Soc.* **61** 374 (1965)
174. McKay R B *Trans. Faraday Soc.* **61** 1787 (1965)
175. McKay R B, Hilson P Y *Trans. Faraday Soc.* **61** 1800 (1965)
176. Hiroshi H, Chika H, Hatsumi T *Photogr. Sci. Eng.* **21** 83 (1977)
177. Graven B R, Datyner A *J. Soc. Dyers Col.* **79** 515 (1963)
178. Rabinowitch E, Epstein L F *J. Am. Chem. Soc.* **63** 69 (1941)
179. Förster T *Fluoreszenz organischer Verbindungen* (Göttingen: Vandenhoeck & Ruprecht, 1951)
180. Coulson C A, Davies P L *Trans. Faraday Soc.* **48** 777 (1952)
181. Derkacheva L D *Izv. Akad. Nauk SSSR Ser. Fiz.* **20** 410 (1956)
182. Kortüm G *Z. Chem. Phys. B* **34** 255 (1936)
183. Stockmayer W H *Rev. Mod. Phys.* **31** 103 (1959) [Translated into Russian in *Sovremennye Problemy Biofiziki* Vol. 1 (Moscow: IL, 1961) p. 132]
184. Feichtmayer F, Schlag J *Ber. Bunsen. Phys. Chem.* **68** 95 (1964)
185. Avis P, Porter G *J. Chem. Soc. Faraday Trans. II* **70** 1057 (1974)
186. Arvan Kh L, Zaitseva N E *Opt. Spektrosk.* **10** 272 (1961) [*Opt. Spectrosc.* **10** 137 (1961)]
187. Buckingham A D *Adv. Chem. Phys.* **12** 107 (1967)
188. Levshin V L, Slavnova T D *Vestn. Mosk. Gos. Univ. Ser. 3 Fiz. Astron.* **3** (6) 24 (1962)
189. Levshin V L, Karimova A Z *Vestn. Mosk. Gos. Univ. Ser. 3 Fiz. Astron.* **7** (4) 27 (1966)
190. Ignat'eva L A et al. *Opt. Spektrosk.* **13** 396 (1962) [*Opt. Spectrosc.* **13** 219 (1962)]
191. Baranova E G, Levshin V L *Opt. Spektrosk.* **10** 362 (1961) [*Opt. Spectrosc.* **10** 182 (1961)]
192. Rohatgi K K, Singhal G S *J. Phys. Chem.* **70** 1695 (1966)
193. Levshin V L, Nimazov N *Izv. Akad. Nauk SSSR Ser. Fiz.* **34** 599 (1970)
194. Sumi H, Toyozawa Y *J. Phys. Soc. Jpn.* **31** 342 (1971)
195. Klafter J, Jortner J *J. Chem. Phys.* **68** 1513 (1978)
196. Huber D L *Chem. Phys.* **128** 1 (1988)
197. Sumi H *J. Phys. Soc. Jpn.* **32** 616 (1972)
198. Boukahil A, Huber D L *J. Lumin.* **45** 13 (1990)
199. Hoshen J, Jortner J *J. Chem. Phys.* **56** 5550 (1972)
200. Port H, Nissler H, Silbey R *J. Chem. Phys.* **87** 1994 (1987)
201. Schreiber M, Toyozawa Y *J. Phys. Soc. Jpn.* **51** 1528 (1982)
202. Schreiber M, Toyozawa Y *J. Phys. Soc. Jpn.* **51** 1537 (1982)
203. Schreiber M, Toyozawa Y *J. Phys. Soc. Jpn.* **51** 1544 (1982)
204. Argyrakis P et al. *Kratk. Soobshch. Fiz.* (9 – 10) 77 (1997)
205. Argyrakis P et al. *Chem. Phys. Lett.* **268** 372 (1997)
206. Nabetani A et al. *J. Chem. Phys.* **102** 5109 (1995)
207. Tomioka A, Miyano K *Phys. Rev. B* **54** 2963 (1996)
208. Lukashin A V *Opt. Spektrosk.* **30** 877 (1971)
209. Witkowski A, Zgierski M Z *Phys. Status Solidi B* **46** 429 (1971)
210. Knapp E W *J. Chem. Phys.* **81** 643 (1984)
211. Zakirov R R, Kozhushner M A, Khairutdinov R F *Khim. Fiz.* **10** 361 (1991)
212. Makhov D V, Bagatur'yants A A, Alfimov M V *Opt. Spektrosk.* **94** 402 (2003) [*Opt. Spectrosc.* **94** 361 (2003)]
213. Landau L D, Lifshitz E M *Statisticheskaya Fizika* (Statistical Physics) (Moscow: Nauka, 1976) [Translated into English (Oxford: Pergamon Press, 1980)]
214. Agranovich V M *Zh. Eksp. Teor. Fiz.* **37** 430 (1959) [*Sov. Phys. JETP* **10** 307 (1960)]
215. Davydov A S *Usp. Fiz. Nauk* **82** 393 (1964) [*Sov. Phys. Usp.* **7** 145 (1964)]
216. Philpott M R *Adv. Chem. Phys.* **23** 227 (1973)
217. Davydov A S *Teoriya Tverdogo Tela* (The Theory of Solids) (Moscow: Nauka, 1976)
218. Broude V L, Rashba E I, Sheka E F *Spektroskopiya Molekulyarnykh Eksitonov* (Spectroscopy of Molecular Excitons) (Moscow: Energoizdat, 1981) [Translated into English (Berlin: Springer-Verlag, 1985)]
219. Anderson P W *Phys. Rev.* **109** 1492 (1958)
220. Mott N F, Twouse W D *Adv. Phys.* **10** 107 (1961)
221. Borland R E *Proc. R. Soc. London Ser. A* **274** 529 (1963)
222. Berezinskii V L *Zh. Eksp. Teor. Fiz.* **65** 1251 (1973) [*Sov. Phys. JETP* **38** 620 (1974)]
223. Mott N, Davis E *Electronic Processes in Non-Crystalline Materials* (Oxford: Clarendon Press, 1979) [Translated into Russian (Moscow: Mir, 1982)]
224. Abrahams E et al. *Phys. Rev. Lett.* **42** 673 (1979)
225. Kramer B, MacKinnon A *Rep. Prog. Phys.* **56** 1469 (1993)
226. Ziman J M *J. Phys. C: Solid State Phys.* **2** 1230 (1969)
227. Korringa J *J. Phys. Chem. Solids* **7** 252 (1958)
228. Beeby J L *Proc. R. Soc. London Ser. A* **279** 82 (1964)
229. Beeby J L *Phys. Rev.* **135** A130 (1964)
230. Elliott R J, Krumhansl J A, Leath P L *Rev. Mod. Phys.* **46** 465 (1974)
231. Velický B, Kirkpatrick S, Ehrenreich H *Phys. Rev.* **175** 747 (1968)
232. Soven P *Phys. Rev.* **156** 809 (1967)
233. Taylor D W *Phys. Rev.* **156** 1017 (1967)
234. Onodera Y, Toyozawa Y *J. Phys. Soc. Jpn.* **24** 341 (1968)
235. Brouers F *J. Phys. C: Solid State Phys.* **4** 773 (1971)
236. Malyshev V A *Opt. Spektrosk.* **71** 873 (1991) [*Opt. Spectrosc.* **71** 505 (1991)]
237. Malyshev V A *J. Lumin.* **55** 225 (1993)
238. Knoester J *J. Chem. Phys.* **99** 8466 (1993)
239. Malyshev V A, Rodríguez A, Domínguez-Adame F *Phys. Rev. B* **60** 14140 (1999)
240. Moll J et al. *J. Chem. Phys.* **102** 6362 (1995)
241. Mukamel S *Principles of Nonlinear Optical Spectroscopy* (New York: Oxford Univ. Press, 1995)
242. Dähne S *Science* **199** 1163 (1978)
243. Landau L D *Phys. Z. Sowjetunion* **1** 88; **2** 46 (1932)
244. Zener C *Proc. R. Soc. London Ser. A* **137** 696 (1932)
245. Marcus R A *J. Chem. Phys.* **24** 966, 979 (1956); **26** 867, 872 (1957)
246. Levich V G, Dogonadze R R *Dokl. Akad. Nauk SSSR* **124** 123 (1959); **133** 158 (1960)
247. Marcus R A *Annu. Rev. Phys. Chem.* **15** 155 (1964)
248. Dogonadze R R, Kuznetsov A M "Kinetika khimicheskikh reaktsii v polyarnykh rastvoritelyakh" ("Kinetics of chemical reactions in polar solvents") *Itogi Nauki i Tekhniki. Fizicheskaya Khimiya, Kinetika* (Advances in Science and Technology. Physical Chemistry, Kinetics) Vol. 2 (Moscow: VINITI, 1973)
249. Pekar S I *Zh. Eksp. Teor. Fiz.* **22** 641 (1952)
250. Pekar S I *Usp. Fiz. Nauk* **50** 197 (1953)
251. Krivoglaz M A, Pekar S I *Tr. Inst. Fiz. Akad. Nauk USSR* **4** 37 (1953)
252. Krivoglaz M A *Zh. Eksp. Teor. Fiz.* **25** 191 (1953)
253. Glasstone S, Laidler K J, Eyring H *The Theory of Rate Processes* (New York, 1941) [Translated into Russian (Moscow: IL, 1948)]
254. Zusman L D *Chem. Phys.* **49** 295 (1980)
255. Krishtalik L I *Usp. Khim.* **34** 1931 (1965) [*Russ. Chem. Rev.* **34** 785 (1965)]
256. Ovchinnikov A A, Ovchinnikova M Ya *Zh. Eksp. Teor. Fiz.* **56** 1278 (1969) [*Sov. Phys. JETP* **29** 688 (1969)]
257. German E D et al. *Elektrokhim.* **6** 350 (1970)
258. Dogonadze R R, Kuznetsov A M *Zh. Vsesoyuzn. Khim. Obshch. im. D.I. Mendeleeva* **19** 242 (1974)
259. Jortner J *J. Chem. Phys.* **64** 4860 (1976)
260. Chernavskaya N M, Chernavskii D S *Tunnel'nyi Transport Elektronov v Fotosinteze* (Tunnel Transport of Electrons in Photosynthesis) (Moscow: Izd. MGU, 1977)
261. Dogonadze R R, Kuznetsov A M "Kinetika geterogennykh khimicheskikh reaktsii v rastvorakh" ("Kinetics of heterogeneous

chemical reactions in solutions'') *Itogi Nauki i Tekhniki. Kinetika i Kataliz* (Advances in Science and Technology. Kinetics and Catalysis) Vol. 5 (Moscow: VINITI, 1978)
262. Ivanov G K, Kozhushner M A *Fiz. Tverd. Tela* **20** 9 (1978)
263. Ulstrup J *Charge Transfer Processes in Condensed Media* (Berlin: Springer-Verlag, 1979)
264. Benderskii V A, Ovchinnikov A A, in *Fizicheskaya Khimiya. Sovremennye Problemy* (Physical Chemistry. Modern Problems) (Ed. Ya M Kolotyrkin) (Moscow: Khimiya, 1980) p. 202
265. Aleksandrov I V, Smedarchina Z K *Khim. Fiz.* **1** 346 (1982)
266. Ivanov G K, Kozhushner M A *Khim. Fiz.* **1** 1039 (1982)
267. Ovchinnikov A A, Ovchinnikova M Ya, in *Advances in Quantum Chemistry* Vol. 16 (Ed. P O Louwdin) (New York: Academic Press, 1982) p. 161
268. Sutin N *Prog. Inorg. Chem.* **30** 441 (1983)
269. Frauenfelder H, Wolynes P G *Science* **229** 337 (1985)
270. Marcus R A, Sutin N *Biochim. Biophys. Acta* (*BBA*) — *Rev. Bioenerg.* **811** 265 (1985)
271. Gol'danskii V I, Trakhtenberg L I, Flerov V N *Tunnel'nye Yavleniya v Khimicheskoi Fizike* (Tunnel Effects in Chemical Physics) (Moscow: Nauka, 1986)
272. Egorov V V *Khim. Fiz.* **7** 1466 (1988) [*Sov. J. Chem. Phys.* **7** 2629 (1991)]
273. Purcell K F, Blaive B, in *Photoinduced Electron Transfer* Pt. A (Eds M A Fox, M Chanon) (Amsterdam: Elsevier, 1988) p. 123
274. Wasielewski M R, in *Photoinduced Electron Transfer* Pt. A (Eds M A Fox, M Chanon) (Amsterdam: Elsevier, 1988) p. 161
275. Calef D F, in *Photoinduced Electron Transfer* Pt. A (Eds M A Fox, M Chanon) (Amsterdam: Elsevier, 1988) p. 362
276. Egorov V V, in *Fiziko-khimicheskie Protsessy v Preobrazovatelyakh Energii* (Physical and Chemical Processes in Energy Convertors) (Executive Ed. N N Kudryavtsev) (Moscow: MFTI, 1989) p. 4
277. Egorov V V *Zh. Fiz. Khim.* **64** 2305 (1990) [*Russ. J. Phys. Chem.* **64** 1245 (1990)]
278. Kuznetsov A M, Ulstrup J *Chem. Phys.* **157** 25 (1991)
279. Kuznetsov A M *J. Phys. Chem.* **96** 3337 (1992)
280. Basilevsky M V, Chudinov G E *Chem. Phys.* **165** 213 (1992)
281. Moser C C et al. *Nature* **355** 796 (1992)
282. Egorov V V *Zh. Fiz. Khim.* **68** 250 (1994) [*Russ. J. Phys. Chem.* **68** 221 (1994)]
283. Rossky P J, Simon J D *Nature* **370** 263 (1994)
284. Kuznetsov A M *Charge Transfer in Physics, Chemistry, and Biology* (New York: Gordon and Breach, 1995)
285. Kharkats Yu I, Kuznetsov A M, Ulstrup J *J. Phys. Chem.* **99** 13545 (1995)
286. Egorov V V *Thin Solid Films* **284–285** 932 (1996); **299** 190 (1997)
287. Egorov V V *J. Lumin.* **72–74** 871 (1997)
288. Basilevsky M V, Vener M V *J. Mol. Struct.: THEOCHEM* **398–399** 81 (1997)
289. Egorov V V *J. Mol. Struct.: THEOCHEM* **398–399** 121 (1997)
290. Medvedev E S, Stuchebrukhov A A *J. Chem. Phys.* **107** 3821 (1997)
291. Egorov V V *Mater. Sci. Eng. C* **5** 321 (1998)
292. Egorov V V *J. Lumin.* **76–77** 544 (1998)
293. Kuznetsov A M, Medvedev I G *J. Electroanal. Chem.* **502** 15 (2001)
294. Medvedev E S, Stuchebrukhov A A *Chem. Phys.* **296** 181 (2004)
295. Dufey F *Phys. Rev. A* **68** 034501 (2003)
296. Di Giacomo F, Nikitin E E *Usp. Fiz. Nauk* **175** 545 (2005) [*Phys. Usp.* **48** 515 (2005)]
297. Egorov V V, in *Tezisy Dokl. Vtoroi Vsesoyuzn. Konf. po Kvantovoi Khimii Tverdogo Tela* (*Lielupe, LatvSSR, 8–11 Oktyabrya 1985 g.*) [Proc. of the Second All-Union Conf. in Quantum Chemistry of Solid State (Lielupe, LatvSSR, October 8–11, 1985)] (Riga: Latviiskii Gos. Univ. im. P. Stuchki, 1985) p. 141
298. Fermi E *Ricerca Sci., Ser. II* **7** (1–2) 13 (1936)
299. Demkov Yu N, Ostrovskii V N *Metod Potentsialov Nulevogo Radiusa v Atomnoi Fizike* (Method of Zero-Radius Potential in Atomic Physics) (Leningrad: Izd. LGU, 1975)
300. Naito K, Miura A *J. Am. Chem. Soc.* **115** 5185 (1993)
301. Brönsted J N, Pedersen K *Z. Phys. Chem.* **108** 185 (1924)
302. Brönsted J N *Chem. Rev.* **5** (3) 231 (1928)
303. Shapiro I O, in *Fizicheskaya Khimiya. Sovremennye Problemy* (Physical Chemistry. Modern Problems) (Ed. Ya M Kolotyrkin) (Moscow: Khimiya, 1987) p. 128
304. Egorov V V, Thesis for Doct. Phys.-Math. Sci. Degree. Abstract (Moscow: Institute of Physical Chemistry, Russian Acad. of Sci., 2004)
305. Egorov V V *Byull. VAK* (4) 27 (2005)
306. Toyabe T, Master's Thesis (Tokyo: Department of Physics, Univ. of Tokyo, 1966)
307. Gurevich Yu Ya, Pleskov Yu V *Usp. Khim.* **52** 563 (1983) [*Russ. Chem. Rev.* **52** 318 (1983)]
308. Shapiro B I *Usp. Nauchn. Fotografii* **24** 69 (1986)
309. Shapiro B I *Usp. Khim.* **63** 243 (1994) [*Russ. Chem. Rev.* **63** 231 (1994)]
310. Lenhard J R, Hein B R *J. Phys. Chem.* **100** 17287 (1996)
311. Kuhn H *J. Chem. Phys.* **53** 101 (1970)
312. Grad J, Hernandez G, Mukamel S *Phys. Rev. A* **37** 3835 (1988)
313. Juzeliūnas G *Z. Phys. D* **8** 379 (1988)
314. Juzeliūnas G, Reineker P *J. Chem. Phys.* **107** 9801 (1997); **109** 6916 (1998)
315. Baz' A I, Zel'dovichYa B, Perelomov A M *Rasseyanie, Reaktsii i Raspady v Nerelyativistskoi Kvantovoi Mekhanike* (Scattering, Reactions, and Decays in Nonrelativistic Quantum Mechanics) 2nd ed. (Moscow: Nauka, 1971)
316. Schrödinger E *Statistical Thermodynamics* (Cambridge: Univ. Press, 1946) [Translated into Russian (Moscow: IL, 1948)]
317. Feynman R P *Phys. Rev.* **84** 108 (1951)
318. Lax M *J. Chem. Phys.* **20** 1752 (1952)
319. Kubo R *Phys. Rev.* **86** 929 (1952)
320. Kubo R, Toyozawa Y *Prog. Theor. Phys.* **13** 160 (1955)
321. Kadomtsev B B *Usp. Fiz. Nauk* **164** 449 (1994) [*Phys. Usp.* **37** 425 (1994)]
322. Kadomtsev B B *Dinamika i Informatsiya* (Dynamics and Information) 2nd ed. (Moscow: Red. Zh. 'Uspekhi Fizicheskikh Nauk', 1999)
323. Kilin S Ya *Usp. Fiz. Nauk* **169** 507 (1999) [*Phys. Usp.* **42** 435 (1999)]
324. Kholevo A S *Vvedenie v Kvantovuyu Teoriyu Informatsii* (Introduction to the Modern Quantum Information Theory) (Sovremennaya Matematicheskaya Fizika. Problemy i Metody, Vyp. 5) (Modern Mathematical Physics. Problems and Methods, Issue 5) (Moscow: Izd. MTsNMO, 2002)
325. Fradkov A L *Usp. Fiz. Nauk* **175** 113 (2005) [*Phys. Usp.* **48** 103 (2005)]